CHEMICAL REVIEWS

Review

pubs.acs.org/CR

Mechanical Properties of Organic Semiconductors for Stretchable, Highly Flexible, and Mechanically Robust Electronics

Samuel E. Root, Suchol Savagatrup, Adam D. Printz, Daniel Rodriquez, and Darren J. Lipomi*

Department of NanoEngineering, University of California, San Diego, 9500 Gilman Drive, Mail Code 0448, La Jolla, California 92093-0448, United States

ABSTRACT: Mechanical deformability underpins many of the advantages of organic semiconductors. The mechanical properties of these materials are, however, diverse, and the molecular characteristics that permit charge transport can render the materials stiff and brittle. This review is a comprehensive description of the molecular and morphological parameters that govern the mechanical properties of organic semiconductors. Particular attention is paid to ways in which mechanical deformability and electronic performance can coexist. The review begins with a discussion of flexible and stretchable devices of all types, and in particular the unique characteristics of organic semiconductors. It then discusses the mechanical properties most relevant to deformable devices. In particular, it describes how low modulus, good adhesion, and absolute extensibility prior to fracture enable robust performance, along with mechanical "imperceptibility" if worn on the skin. A description of techniques of metrology precedes a discussion of the mechanical properties of three classes of organic semiconductors: π-conjugated polymers, small molecules, and composites. The discussion of each class of materials focuses on molecular structure and how this structure (and postdeposition processing) influences the solid-state packing structure and thus the mechanical properties. The review concludes with applications of organic semiconductor devices in which every component is intrinsically stretchable or highly flexible.

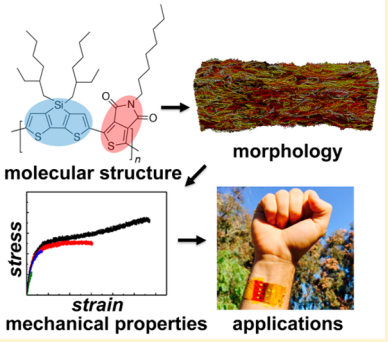

CONTENTS

Received: January 3, 2017
Published: March 25, 2017

DOI: 10.1021/acs.chemrev.7b00003
Chem. Rev. 2017, 117, 6467−6499

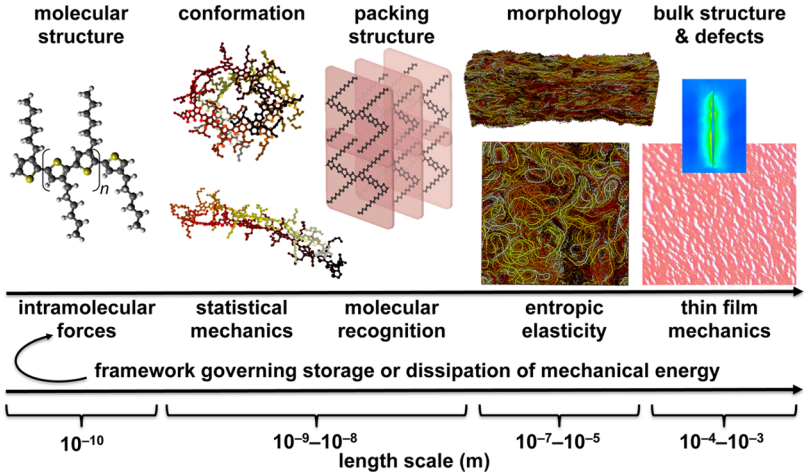

Figure 1. Length scales and framework governing for storage or dissipation of mechanical energy. Embodied in the molecular structure are the restoring forces of covalent bonds, but also the intramolecular forces manifested in electrostatic interactions between distal units and dihedral potential energies between adjacent ones. The conformation of molecules in solution influences the structure and mechanical properties of the film upon the process of solidification, and is in turn predicted by statistical thermodynamics. The packing structure is determined by sterics, electrostatic interactions, and molecular recognition. This structure produces the overall morphology of the solid film. Amorphous chains within the bulk store elastic energy entropically. Finally, the deformability of the bulk structure is determined in large part by defects. The effective mechanical properties of a thin film can be treated using thin-film mechanics. (Drawing illustrating "packing structure" reproduced with permission from ref 31. Copyright 2010, American Chemical Society.)

1. INTRODUCTION

Developments in semiconductor technology have left few aspects of modern life untouched.[1] These developments have been driven by the concerted efforts of chemists, physicists, and engineers over the last 50 years. The fruit of this labor is reflected in an exponential rate of progress, which was identified by Intel's Gordon Moore in 1965.[1,2] Moore predicted that the density of transistors on an integrated circuit would double approximately every two years. The technologies that have enabled this periodic doubling underpins several other exponential improvements, for example, the capacity of memory circuits, the resolution of digital imaging, and the overall cost-per-function of semiconductor devices. The outcome in all cases is an increase in electronic performance. One can imagine, however, analogous trends describing the evolution of other physical parameters of importance for semiconducting devices, not just performance and efficiency derived from miniaturization. One such parameter could be mechanical compliance.[3−5] Development of electronic materials and devices with the goal of deformability, for example, would permit the fabrication of robust devices for portable electronics,[6,7] the production of flexible solar modules[8] and displays[7,9,10] using roll-to-roll printing methodologies,[11,12] and the property of "mechanical invisibility"[13] for wearable[3,14] and implantable[15,16] applications. The research done on rigid semiconductor systems is,[17,18] of course, a prerequisite for deformable electronics to achieve a useful level of function, but mechanical resilience or toughness would be the goal.[19]

One class of materials that since its inception has been associated with flexible, printed electronics is organic semiconductors.[20] In fact, deformability is the characteristic that underpins most touted advantages of organic electronic materials, especially if they are to be manufactured by roll-to-roll printing.[21−23] While it might be natural to assume that the carbon framework common to all organic molecules would afford some level of softness (by analogy to biological materials) the diversity of structures of organic semiconductors embodies a rich mechanical behavior that is only sometimes best described as "plastic" (in the sense of "deformable").[5] Even semiconducting polymers, whose repeating structures evoke comparisons to engineering plastics, do not exhibit high strength and toughness characteristic of, for example, high molecular weight polyethylene or nylon.[24−27] The requirement that π-conjugated organics still transport charge with efficiency that is comparable to structurally simpler inorganic semiconductors seems to necessitate rigidity in the molecular backbone[28] and assembly into ordered aggregates in the solid state.[29−31] Moreover, the presence of side chains, required for processing from solution, nearly always reduces the cohesion of these materials by reducing strong van der Waals forces that would exist between unsubstituted main chains.[32−34] Mechanical performance is also limited by synthetic procedures. That is, the synthesis of semiconducting polymers often leads to degrees of polymerization that can be both more broadly distributed and significantly smaller than those obtained for commodity polymers and engineering plastics. Low degrees of polymerization are a consequence of the poor solubility of π-conjugated systems with increased molecular weight. Additionally, there are the practical difficulties of combining AA and BB monomers in a ratio of exactly 1:1 (as required by the Carothers equation to achieve high molecular weight) when performing polycondensation reactions at a small scale.[35] Solid samples comprising short polymer chains and high dispersity exhibit reduced densities of entanglements, which limit the cohesion[26] and extensibility.[36]

While it may seem from this discussion that organic semiconductors could never have the excellent thermomechanical properties characteristic of engineering plastics (which are, after all, optimized for some combination of toughness, strength, extensibility, high-temperature operation, and other parameters),

DOI: 10.1021/acs.chemrev.7b00003
Chem. Rev. 2017, 117, 6467−6499

there is a reason to be optimistic. That is, in most thin-film devices, the active layer is not responsible for bearing the load. The substrate and encapsulant[37] are usually 1 or more orders of magnitude thicker than the active material[38] and are responsible for providing the strength to keep the device intact. Thus, properties that describe the ability of a material to store or dissipate mechanical energy (resilience and toughness) take on less importance for organic semiconductors than for engineering plastics. Instead, the properties that seem to be of increased importance in thin-film organic semiconductors are low tensile modulus in the elastic regime (to minimize interfacial stresses upon deformation and to permit mechanical imperceptibility when worn on the skin[13]) and absolute extensibility prior to fracture. (We note, however, that intentional fracture of organic semiconductors is one possible route toward producing stretchable devices.[39]) In many cases, consideration of the strain in the active materials is more important than consideration of the stress, because deformation of the active material is driven by deformation of the substrate. Because of the mismatch in thickness between the substrate-encapsulant and the active material, the force needed to deform the ultrathin active layer is vanishingly small. Toughness and cohesive fracture energy take on increased importance in twisting and shear deformations (and deformations that act to delaminate the device stack)[27,40,41] and during thermal cycling, when unequal coefficients of thermal expansion place stress on the layers. In such scenarios, metrics related to the energy density absorbed during the course of deformation should of course be maximized to the extent possible.[42]

This review takes the position that despite the apparent mutual incompatibility of charge transport and mechanical deformability in organic electronic materials, the chemistry of these materials nevertheless provides several routes to achieving mechanical softness combined with state-of-the-art electronic properties. Such approaches include tailoring of the chemical structure (e.g., the lengths and composition of the side chains and rigidity of the backbones) and tuning properties familiar to the polymer engineering community (e.g., molecular weight, polydispersity, and cross-linking).[43] Quite often, the mechanical properties of organic semiconductors are determined not only by molecular structure but also by the ways in which the molecules pack in the solid state.[28,30,31] The solid-state packing structure is determined by the phase behavior of the molecules and the conditions of deposition and processing post deposition.[44−47] Moreover, organic semiconductors accommodate mechanical energy by a range of mechanisms across many length scales, from sub-T_g bond rotations to the breakage of covalent bonds. Figure 1 illustrates the molecular mechanisms by which strain is accommodated across various length scales and strain regimes.

This paper is a comprehensive review of the literature related to the mechanical properties of organic semiconductors. The focus is on the molecular and morphological determinants of these properties, the relevant physics of polymeric solids, theoretical and computational approaches to predicting these properties, techniques for metrology, examples of materials that have been synthesized that exhibit especially high deformability, and applications in devices. Progress in this field can benefit from what is known about the mechanical properties of commodity polymers and engineering plastics; however, the necessity to retain optoelectronic properties in organic semiconductors substantially constricts the available options for designing new materials. For example, rigid molecular chains and highly aggregated morphologies, which are conducive to charge transport, tend to make materials stiff and brittle.[31]

In examining the literature, we found that work related to determining the mechanical properties of π-conjugated materials went through three distinct phases. The first phase (1980s) coincided with the advent of conductive polymers, during which time it first seemed possible to combine metal-like conductivity with the processability of plastics.[48−51] The second phase (1990s to 2000s) saw a lull in interest in the thermomechanical properties of organic semiconductors, possibly because of the development of the organic thin-film transistor,[52] light-emitting device,[53] and solar cell.[54−56] Synthesizing new materials, understanding their charge-transport physics, and producing optimized devices required significant resources, which in general were not allocated toward understanding the mechanical properties. The third phase (2010s to the present) was characterized by a reaction to activity in the field of soft electronics based on metals and inorganic semiconductors. Inorganic materials can be rendered stretchable using specialized device layouts, i.e., wavy interconnects and topographic features.[17,18,57−60] These strain-relief structures permit the use of metallic films, semiconductor nanoribbons, and whole integrated circuits, which though not quite deformable by themselves (especially under tensile deformation), can be rendered stretchable and highly flexible using the appropriate layout.[10,61] This work suggested to the community interested in organic semiconductors that it no longer had a monopoly on deformability. Moreover, the success of these devices highlighted the inferiority of organic semiconductors with respect to both charge transport (the mobility of silicon is 2−3 orders of magnitude higher than even the best organic semiconductors[62]) and lifetime (organics are susceptible to degradation when unencapsulated[63]).[64] These results spurred activity on increasing the mechanical deformability of organic semiconductors and in pursuing areas in which organics retained their advantages against competition from conventional electronic materials.

1.1. Deformable Organic Electronics as a Subset of All Deformable Electronics

Stretchable and ultraflexible electronics originated in the late 1990s and early 2000s and are primarily attributed to the work of Wagner and Suo.[18,57,58,65−68] Early systems of materials included films of metals and other materials on thin flexible foils[18] and elastomers. Such thin films could accommodate strain by intentional fracture[58,68] or mechanical buckling.[57] Exploiting these routes of deformation was facilitated by the development of the theory of "film-on-foil" mechanics.[18,66] This vein of research was later substantially developed by the work of Rogers and co-workers,[60] who developed device layouts using fractal,[69] interconnecting structures,[3,70] and topographically patterned island-bridge approaches[8] to direct strain away from the active components of devices. This work produced a number of impressive demonstrations, including an electronic eye camera,[71,72] implantable devices for in vivo electrophysiological mapping of the heart[73] and brain,[15] and myriad examples in energy[8] and healthcare.[3,15,73−76] An effort in parallel by Someya and co-workers used organic active materials and stretchable composite interconnects[77] whose goal was also largely to direct strain away from the active components[78−82] (though the same authors were also among the first to study the effect of mechanical strain on the charge-transport properties of organic semiconductors[83]). Bauer and co-workers[4,84] have also made significant contributions to this field, especially in the area of

DOI: 10.1021/acs.chemrev.7b00003
Chem. Rev. 2017, 117, 6467−6499

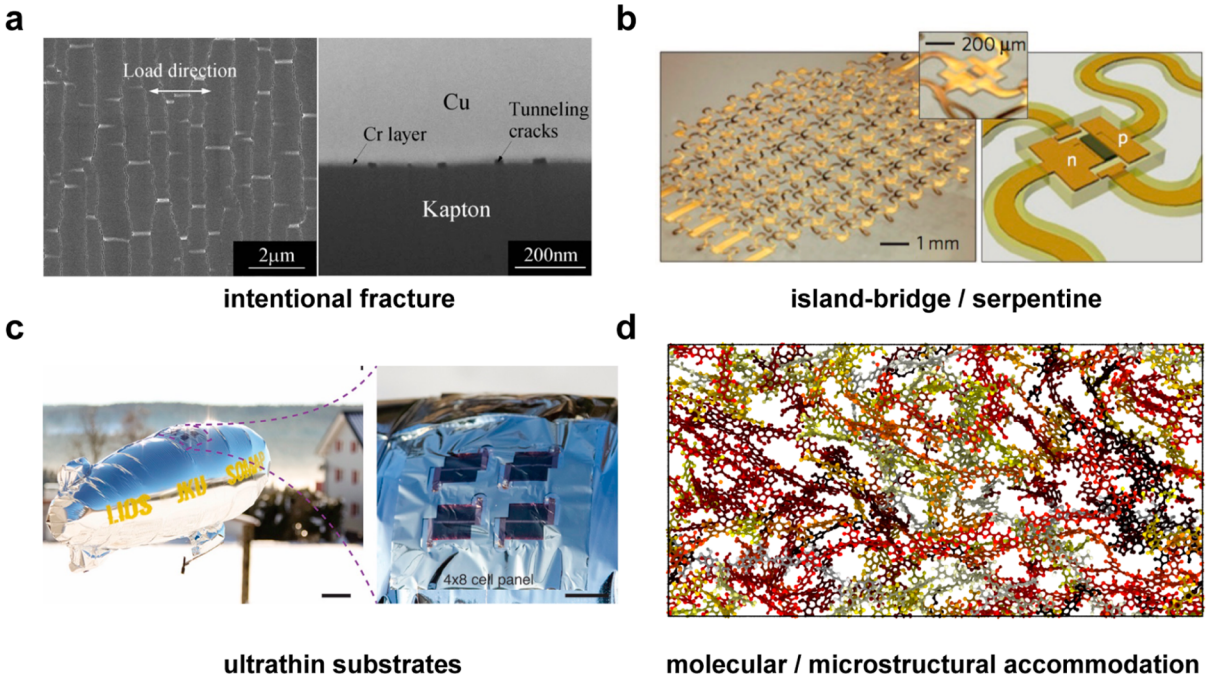

Figure 2. Approaches taken to impart stretchability or extraordinary flexibility to electronic devices. (a) Intentional fracture can produce percolated conductive pathways that open and close with strain. Reproduced with permission from ref 90. Copyright 2007, American Institute of Physics. (b) Wavy, fractal, and island-bridge type geometries have been used extensively for stretchable devices based on inorganic thin films. Reproduced with permission from ref 10. Copyright 2010, Nature Publishing Group. (c) Ultrathin substrates can be used for lightweight, flexible, and low-cost electronics. Reproduced with permission from ref 88. Copyright 2015, Nature Publishing Group. (d) Intrinsically or molecularly stretchable materials use the materials themselves to accommodate strain. Reproduced with permission from ref 25. Copyright 2015, American Chemical Society.

stretchable batteries,[85] soft actuators,[86,87] solar cells,[38,88] and metrology.[89] Figure 2 illustrates the approaches taken by members of the community to permit semiconductor devices to accommodate strain.

An alternative approach to these composite systems, in which the conductors or semiconductors are dispersed in or on top of a matrix, is one in which the active material itself accommodates the strain.[5,9] Such an approach would simplify patterning, as all materials could be printed in the same layer without relief structures. The ability to avoid patterning interconnects in complex serpentine patterns, which occupy a large footprint, could also increase the density of the active components. In this approach, which might be selected when digital patterning and low cost are more important considerations than complex function or high-performance operation, organic materials are a logical option. In addition to facile replication by screen,[91] gravure,[92] or slot-die printing,[93] rapid tailorability in circuit design can be accomplished by digital inkjet printing.[94] The advantages of low cost and rapid fabrication are complimented by several other characteristics unique to organics: tailorability by synthesis,[95] tunable color[96] and bandgap,[97] oxide-free interfaces for biological integration,[98,99] low-cost disposal or recycling,[100] and the potential for self-repair[101,102] and biodegradability.[103]

The challenges associated with organics for ultracompliant applications include, significantly, that the molecular and microstructural characteristics needed for charge transport, namely rigid, π-conjugated polymer chains and highly ordered aggregates in the solid state, also tend to render such materials stiff and brittle. This apparent trade-off is not a fundamental rule, however, and can be negotiated. The simple fact that electronic performance and brittleness or elastic modulus are not directly correlated (Figure 3) admits to several conceivable strategies to combine charge transport and deformability. These strategies (to

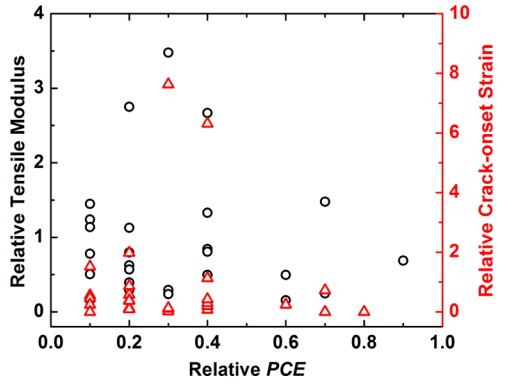

Figure 3. Plot of relative tensile modulus (black circles) and crack-onset strain (red triangles) for a library of semiconducting polymers described in ref 108 vs relative power conversion efficiency (PCE) of a bulk heterojunction consisting of the polymer mixed with $PC_{61}BM$. The lack of correlation suggests that it should be possible to coengineer mechanical deformability with electronic performance.

be covered in detail in this review) include the use of plasticizers,[34,104] various processing techniques (for example, to improve the entanglement density),[30,105] and the use of flexible side chains and unconjugated linkers in the main chain.[102,106,107] It is first, however, necessary to understand the relevant mechanical properties of existing organic semiconductors, and how they are similar to or different from those of other organic solids, using a combination of experimental and theoretical techniques. Success in understanding the molecular and microstructural determinants of both charge transport and mechanical properties would bring the field closer to achieving electronics with truly "plastic", i.e., deformable, character. Such an outcome would have two major consequences. The first is that

DOI: 10.1021/acs.chemrev.7b00003
Chem. Rev. 2017, 117, 6467−6499

it would permit devices that are destined for commercialization to be more mechanically robust. The second is that it would permit a new class of electronic materials and devices that exhibited extraordinary deformability for devices like electronic skin and wearable and implantable health monitors.

2. THERMAL AND MECHANICAL PROPERTIES AND HOW TO MEASURE THEM

In considering which mechanical properties are desirable for deformable applications of organic electronics, we find that the terminology in this field is not always used consistently.[19] The field sometimes refers to qualities such as "stiffness," "compliance," "hardness," "resilience," "toughness," "ductility," and "elasticity" in ways that differ from the precise meanings used in the mechanics community, whose lexicon is well established. On the other hand, the descriptor "flexible" is so inclusive in that it does not distinguish qualities afforded by the dimensions of the material from qualities afforded by the material itself. That is, any material can be made flexible if it is sufficiently thin.[18] The descriptor "stretchable" is imprecise because it does not convey whether the deformation is elastic (reversible) or plastic (irreversible), and does not define the range over which it exhibits one or the other behavior. In this review, we use "flexible" to mean any form of any device that can be bent to radii of curvature smaller than 1 cm, regardless of the thickness of the substrate, and "stretchable" to mean a device or material that can be elongated by approximately 5% or more, regardless of whether the deformation is elastic or plastic. The rarity of the term "deformable" in this field has preserved its generality, and we use it liberally throughout this review in its colloquial sense. A material or device that is "deformable" is thus taken to be an order of magnitude more flexible and stretchable than a typical silicon wafer with a thickness of ~200 μm. The adjective "extensible" will be used to mean "having a high strain at fracture" (in a pull test) or "having a high crack-onset strain" (if the film is measured on an elastomer).

The mechanical properties of organic solids most relevant to deformable devices include the elastic modulus (usually obtained as the tensile or Young's modulus),[109] elastic range and yield point,[110] toughness,[111] and strain to fracture[31] (Figure 4). These properties are determined not only by the structure of individual molecules, but how these molecules pack in the solid state.[30] Measuring the mechanical properties of thin films poses particular challenges because (1) it is difficult to handle thin films for a conventional pull test[112,113] and (2) pilot-scale synthetic procedures usually do not produce enough material for more than a few films. These challenges have been met by the development of "film-on-elastomer" methods for approximating the range of behavior to tensile strain.[110] These "film-on-elastomer" methods provide the benefits of simplicity to perform and applicability to a range of materials, but require multiple techniques to reconstruct the stress–strain behavior.[110] There are other methods, which may require specialized equipment, however, that obtain these data directly. For example, a method resembling a conventional pull test using a thin film supported by water can obtain a stress–strain curve in a single step (Figure 5).[114] For measurements of cohesion and adhesion using stresses applied perpendicular to the plane of the films, double-cantilever beam and four-point bending experiments have proven to be valuable.[25−27,40,41,115−117] Comparisons of the results between methods do not always yield the same values, but these discrepancies often produce insights, and the results of one measurement may be more relevant than the results of another to a particular application. The section will conclude with a discussion of which mechanical properties are desirable for deformable applications.

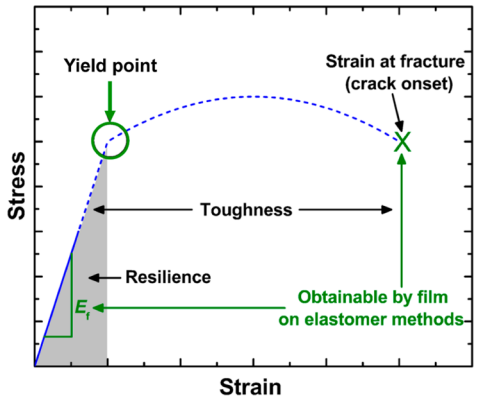

Figure 4. Hypothetical stress–strain curve showing the critical features. The stress is an intensive property equal to the force per unit area normal to the load. The strain is the engineering strain, $(l-l_0)/l_0$, where l is the deformed length and l_0 is the length at equilibrium. The elastic modulus of a film, E_i, is the slope of the curve in the linear, elastic regime. The area under the curve in this region is the resilience, which has units of energy per volume. The yield point represents the stress and strain at which the material undergoes irreversible deformation. The strain at fracture represents mechanical bifurcation of the specimen. The area under the entire curve is called the toughness and has units of energy per volume. Quantities labeled in green can be obtained using film-on-elastomer methods, that is, the modulus by buckling, the yield point by onset of buckling, and the strain at fracture by the crack-onset strain. Reproduced with permission from ref 110. Copyright 2015, American Chemical Society.

2.1. Glass Transition Temperature

The glass transition temperature (T_g) is a second-order phase transition that ultimately describes the thermally activated reorganization of chains in the amorphous domains of a polymer specimen.[119] A plot of density vs temperature exhibits a change in slope in the vicinity of T_g (Figure 6).[35] Similarly, a plot of heat flow vs temperature measured by differential scanning calorimetry (DSC) reveals an increase in heat capacity. Below T_g, a polymer is said to be glassy; above the T_g, it is rubbery. In a purely amorphous sample (e.g., atactic polystyrene), the material flows readily above its T_g. A semicrystalline sample above its T_g, but below the temperature at which its crystalline domains melt (T_m), exists as a solid at ordinary time scales and is said to be in its elastomeric state. The position of the T_g of a polymer relative to its operating temperature is thus an important predictor of the mechanical properties of a polymer. The T_g also influences the morphological stability of the solid state of the polymer, which can be problematic if the morphology that is most conducive to device performance is not the most thermodynamically stable one.[119] Devices based on composite systems, e.g., bulk heterojunction solar cells, can phase separate with deleterious consequences if operated above their T_g.[119] The requirement that a bulk heterojunction solar cell have a high T_g for morphological stability and a low T_g for mechanical stability is another competing criterion. For an account of the role of T_g in the operation and stability of organic photovoltaic devices, see the comprehensive review by Müller.[119]

Despite its importance, the glass transition of many organic semiconductors is not easily determined. The change in heat capacity in the vicinity of T_g for organic semiconductors is often

DOI: 10.1021/acs.chemrev.7b00003
Chem. Rev. 2017, 117, 6467–6499

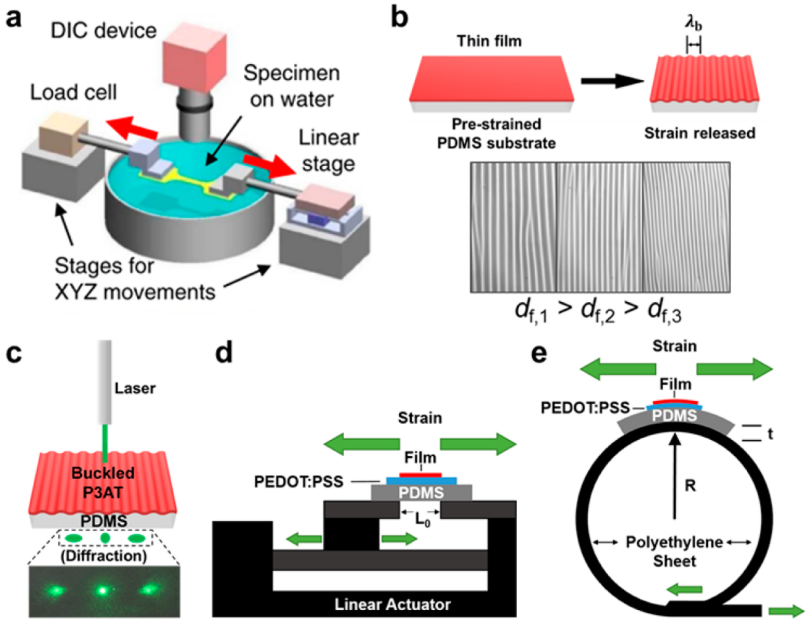

Figure 5. Tools for measuring the mechanical properties of organic thin films. (a) The film-on-water method. Reproduced with permission from ref 111. Copyright 2015, Nature Publishing Group. (b) Schematic diagram of surface wrinkling used to determine the tensile modulus of films. The thickness of the film (d_f) and the modulus determines the buckling wavelength. (c) Buckling wavelength can be determined by the spacing of the diffraction pattern for measurements of modulus or in the technique of buckle-onset to determine the yield point. Reproduced with permission from ref 110. Copyright 2016, American Chemical Society. (d) A linear actuator or (e) bending experiment can be used to determine the crack-onset strain at the high- and low-strain regimes. Reproduced with permission from ref 118. Copyright 2016, American Chemical Society.

too weak to detect by DSC.[106,120−125] Other techniques, such as dynamic mechanical analysis (DMA)[126] or variable-temperature ellipsometry (which has been applied to polyolefins[127,128] as well as conjugated polymers[129]), are often required. The glass transition can also be predicted computationally, as atomistic and coarse-grained molecular dynamics (MD) simulations have been used to obtain values that are in good agreement with experiment.[130]

2.2. Elastic Modulus, Poisson Ratio, and Elastic Range

Several bulk mechanical properties can influence the mechanical robustness of organic semiconductor films for deformable applications (Figure 4). The elastic moduli quantify the ability of a material to store mechanical energy reversibly. They can be expressed in three common forms depending on the mode of deformation: the tensile modulus (E), the shear modulus (G), and the bulk modulus (K). For isotropic solids, these quantities can be interconverted. In thin films, the easiest to measure and perhaps the most relevant property is the tensile (Young's) modulus, E. This quantity refers to the force required per unit cross sectional area normal to the load (stress, σ) to deform the material a fraction of its initial length (strain, ε) reversibly under uniaxial deformation. The shear modulus describes the response of a material to shear stress and is defined as the ratio of shear stress to shear strain. The bulk modulus describes the volume change of a material undergoing an infinitesimal change under uniform (i.e., hydrostatic) pressure. For isotropic, homogeneous materials, the elastic moduli along with the Poisson ratio (ν), which describes the negative fractional deformation of a material along the two axes perpendicular to the strained axis, are sufficient to fully describe the elastic behavior of a material. That is, a material stretched axially by 1% with concomitant reduction of the transverse dimension by 0.5% has a Poisson ratio of 0.5. The tensile modulus is expressed in units of force per cross-sectional area (N m^{-2} or Pa). A typical value of E for polycarbonate is ∼1 GPa; for silicone rubber it is ∼1 MPa. Values for the common semiconducting polymer regioregular poly(3-hexylthiophene) (P3HT) range from 0.1−1 GPa, depending on the sample and, given its T_g near room temperature of 12 °C, the temperature at which the measurement was taken. The elastic moduli and Poisson ratio are valid only for small strains within the elastic regime of the material or less than approximately 10%. The area under the curve for the linear portion of the stress strain curve is called the modulus of resilience (U_r), and represents the total amount of energy per unit volume (e.g., J m^{-3}) storable by the solid before the onset of plastic deformation.

The tensile modulus is highly relevant for deformable applications because it can be tuned to minimize interfacial stresses (among other layers in the device or between the device and another surface, i.e., the skin) and it is closely related to molecular structure and solid-state packing structure. The modulus is often correlated to other mechanical properties and even to optoelectronic properties. The molecular mechanisms responsible for storing mechanical energy in the elastic regime depend on the phase of the solid. For crystalline solids and the crystalline phases of semicrystalline solids, displacement of the molecules from their equilibrium positions in the lattice produces a restoring force. For van der Waals solids, the restoring force can be described by a Lennard-Jones or similar potential. For glassy phases below T_g, elastic deformation is mediated by van der Waals forces, but also by deformation of covalent bonds. For semicrystalline polymeric phases above T_g, in which the polymer chains are unfrozen, chains are aligned along the axis of tensile deformation; this reduction in degrees of freedom produces a restoring force, as polymer chains tend toward increasing their configurational entropy. Elastomers thus behave as "entropic springs," in which changes in internal energy are negligible, and changes in entropy dominate.

DOI: 10.1021/acs.chemrev.7b00003
Chem. Rev. 2017, 117, 6467−6499

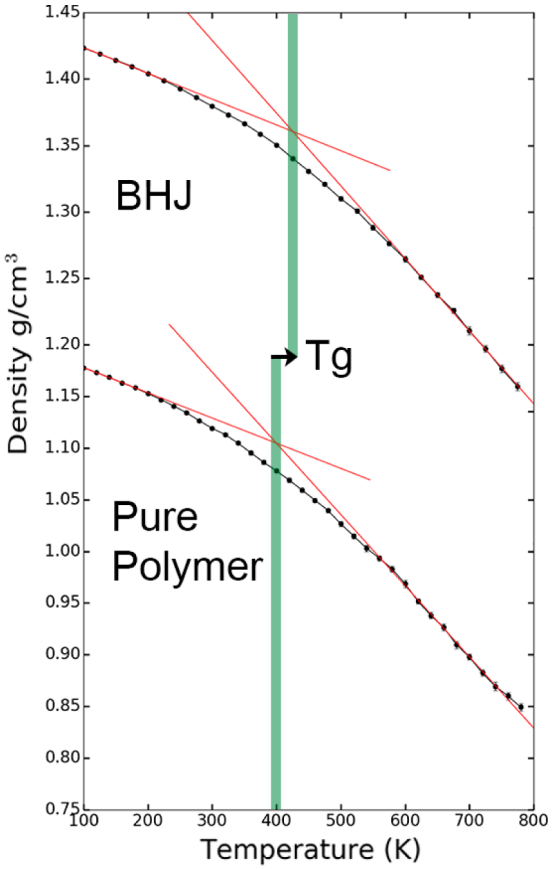

Figure 6. Theoretical prediction of glass transition temperature (T_g) for the semiconducting polymer PTB7 based on molecular dynamics simulations. The density is estimated by the intersection of the linear fits to the glassy (low T) and rubbery (high T) regions. The plot also shows the increase in T_g upon mixing with PCBM, which behaves as an antiplasticizer, in a bulk heterojunction (BHJ) film. Reproduced with permission from ref 105. Copyright 2016, Royal Society of Chemistry.

The tensile modulus can be measured using several different techniques, and in many cases the technique chosen depends on the amount of material available and the forms into which it can be processed. If enough material is available for a conventional pull test, a typical specimen can be cast into the appropriate size and shape (e.g., dog-bone), and its force−displacement curve can be measured and transformed into its stress−strain curve using the dimensions of the sample.[24,36] In practice, this method is limited to simple polymeric structures like the poly(3-alkylthiophene)s (P3ATs), whose synthetic procedures comprising only a few steps can produce quantities of material large enough (e.g., > 100 mg) for a bulk measurement. Designer materials, i.e., low-bandgap polymers exhibiting the alternating donor−acceptor motif,[95] are synthesized at laboratory scale in only modest quantities. The quantities of materials available at the laboratory scale are limited in the case of conventional reactions by low concentrations and in the case of microwave-assisted reactions by small reaction vessels. Moreover, vastly greater quantities of material are required for conventional mechanical tests, which require a bulk sample, than for a charge-transport measurement,[131,132] which requires a thin film (∼10 μg, excluding a 10-fold greater fraction of wasted material if the film is produced by spin coating). Given the importance of mechanical properties in determining the lifetime and stability of organic devices, there has thus been a drive toward obtaining properties directly from thin films.

Pull testing of bulk samples of organic electronic materials was used extensively in early work using materials such as poly(acetylene)[48,49] and unsubstituted polyaromatic[50] species synthesized by simple routes, such as oxidative polymerization. An early test of regiorandom P3ATs synthesized in this way revealed a striking decrease in tensile modulus with increasing length of the alkyl side chain,[33] which is a common effect observed among P3ATs and other conjugated polymers.[34,133,134] More recently, block copolymers of P3HT and poly(ethylene) have been synthesized and determined by conventional pull testing to exhibit decreasing tensile modulus with increasing fraction of the insulating component, but also extraordinary ductility and toughness.[24] The effect of molecular weight on the mechanical properties of P3HT has also been measured on bulk samples (Figure 7a);[36] greatly increased ductility and toughness with molecular weight (though similar tensile modulus) measurements pointed to the importance of entanglements, even in semirigid polymers such as P3HT. Direct tensile testing of bulk samples of low-bandgap polymers or semiconducting small molecule films has not been reported.

Techniques used to determine the tensile moduli of thin films circumvent the need to produce large amounts of material and also the need to manipulate fragile, freestanding films.[112] Moreover, the mechanical properties of thin films often differ from those of bulk samples of the same material,[135] and thus direct measurements on thin films may produce results that are more in line with the properties exhibited by the materials in working devices. Techniques that have been developed include direct pull testing of thin films on water,[111,114] nanoindentation,[136−138] and the buckling-based method.[112] Kim and coworkers have pioneered the use of a water-based pull test, in which a film is coated on a flat substrate and then gently floated onto the surface of water (Figure 7b).[111,114] A highly sensitive load cell coupled to a linear actuator is used to obtain a plot of force vs displacement. Critical to this method is ensuring that the contacts do not tear the delicate thin film; slabs of poly(dimethylsiloxane) (PDMS), which adhere to top surfaces of the termini of the floating thin films by van der Waals forces, are used in place of a clamp and thus minimize mechanical damage. The water-based technique has been used to measure the stress−strain behavior of P3HT as a function of regioregularity[114] (the films become more deformable with increasing regiorandomness, though the charge-carrier mobility decreases) and also of all-polymer active layers for intrinsically stretchable solar cells.[111] As the film is not bonded to a solid substrate in the water-based method, the results may thus be influenced by concentration of strain in thin areas and defects within the thin film.[139] The force required to stretch the sample will thus be lowered, as will the stress, which is calculated on the assumption that the cross section of the sample is mathematically uniform. For example, the water-based method produced values of tensile moduli that were 3−6 times lower than values produced by the buckling method (described below). In a recent study that compared the results of the two methods,[139] the differences in moduli were attributed to the combined effects of inhomogeneities in film thickness, void space in the films behaving differently under tension and compression, and differences in strain rate. Nevertheless, the advantage of the water-based technique is that it provides the full stress−strain behavior (not just the tensile modulus), it is simple to perform, and it provides convenient comparisons between materials.

DOI: 10.1021/acs.chemrev.7b00003
Chem. Rev. 2017, 117, 6467−6499

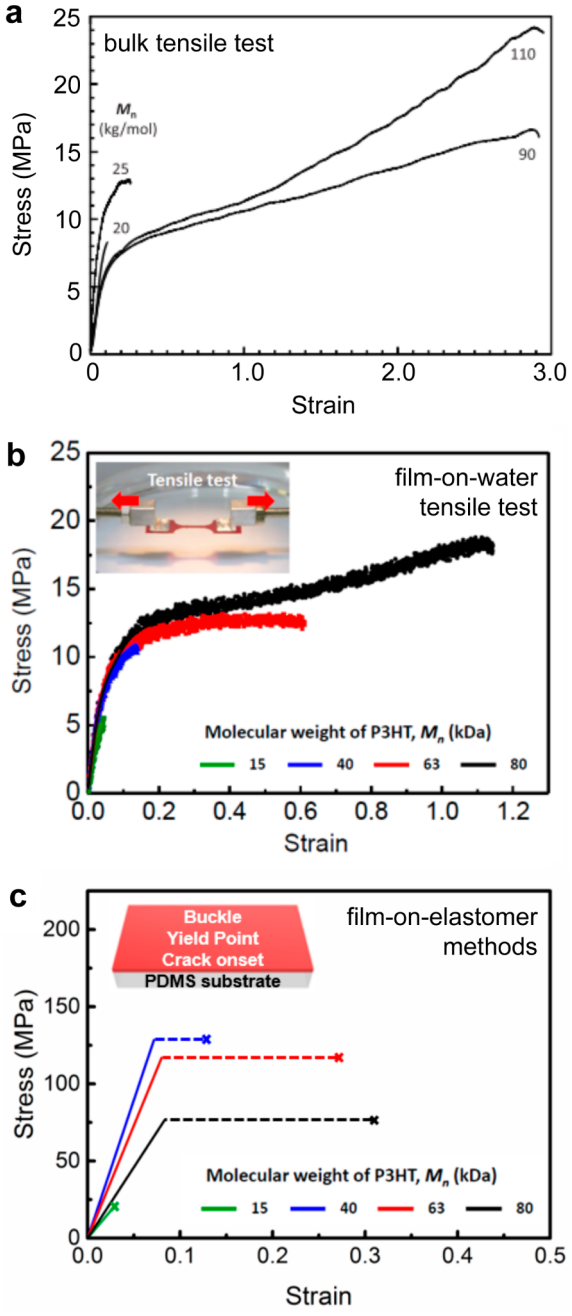

Figure 7. Stress−strain curves for P3HT obtained by three different metrology techniques. (a) Bulk tensile test of P3HT samples with different molecular weights. Reproduced with permission from ref 36. Copyright 2013, Elsevier. (b) Tensile test obtained using the film-on-water technique. (c) Stress−strain behavior reconstructed using film-on-elastomer techniques: the buckling technique, determination of yield point by the onset of buckling, and crack-onset strain. Reproduced with permission from ref 139. Copyright 2017, American Chemical Society.

The buckling technique uses the wavelength of the sinusoidal wrinkles that form in a thin film when it is compressed on a compliant substrate and has been implemented successfully to measure the tensile moduli of a variety of organic thin films, including several examples of semiconducting polymers and small molecules.[112,113] The buckling phenomenon was described for metal films on PDMS substrates by Whitesides and Hutchinson,[140] and the mechanics were adapted into a metrology technique for measuring the elastic properties of thin films by Stafford and co-workers.[113] The method was extended to organic semiconductors by Khang and co-workers[109] and then used extensively by O'Connor and co-workers,[30,31,141] along with our group,[34,104,134,142] for a variety of materials.[42] The technique has been reviewed before by Stafford and co-workers,[112] and a description of it was included in an earlier review by our group in the context of the mechanical stability of organic solar cells,[42] so here we will focus on the practical issues related to measurement of tensile modulus for organic semiconductors.

Briefly, the buckling wavelength increases with the stiffness (modulus and thickness) of the thin film, and thus the modulus (E_f) can be obtained by plotting the buckling wavelength (λ) vs film thickness (d_f); E_f increases with the cube of the slope, λ/d_f, according to eq 1.[113]

$$E_f = 3E_s\left(\frac{1-\nu_f^2}{1-\nu_s^2}\right)\left(\frac{\lambda}{2\pi d_f}\right)^3 \quad (1)$$

Accurate values of the modulus of the PDMS substrate (E_s) and the Poisson ratios of the film (ν_f) and the substrate (ν_s) are needed for the determination of E_f. There is a practical difficulty in casting films directly on the elastomeric substrate, typically PDMS, because it swells when in contact with organic solvents. This challenge can be overcome by first casting the film on a passivated glass or Si/SiO_2 substrate, and transferring the films by kinetic (rapid) transfer[143] using PDMS as a carrier substrate. It is often best to cure the PDMS (Sylgard 184 cured at the normal ratio of 10:1 base:cross-linker) for 36 h at room temperature, so that the bulk structure is solid, but that the top surface is still somewhat tacky. If the film is too strongly adhered to the original substrate to remove using fast transfer, transfer can be facilitated by using immersion in water. If direct transfer fails, it may be necessary to form a bilayer film using a second material with a known tensile modulus ($E_{f,2}$) and thickness ($d_{f,2}$). The modulus of the film (E_f) can then be related to the modulus of the bilayer film (E_{eff}) using eq 2.

$$E_{eff} = \frac{1 + m^2n^4 + 2mn(2n^2 + 3n + 2)}{(1+n)^3(1+mn)}E_f; \quad \text{where } m = \frac{E_{f,2}}{E_f},\ n = \frac{d_{f,2}}{d_f} \quad (2)$$

The small compressive strain is typically generated by prestraining the PDMS and then releasing the strain once the thin film has been transferred. The buckling wavelength should be measured immediately (within 1 h) after the film is transferred to the PDMS and compressed, so that time-dependent relaxation of the PDMS, thin film, or both, does not affect the result.

The advantage of the buckling technique is that it does not require specialized equipment for measuring mechanical properties; all that is required is a microscope and a technique for measuring the thickness of thin films, such as stylus profilometry, atomic force microscopy, or ellipsometry. While it is necessary to know the tensile modulus of the PDMS substrate, this quantity can be measured using a conventional pull tester available to most laboratories (or in principle simply by suspending weights from a sample and measuring the displacement). Moreover, the buckling-based measurement provides a measure of the tensile modulus that is not subject to the influence of defects. The buckling wavelength is usually measured at multiple locations using image analysis, and reported results are usually averages. A disadvantage of the technique (unlike water-supported pull

DOI: 10.1021/acs.chemrev.7b00003
Chem. Rev. 2017, 117, 6467−6499

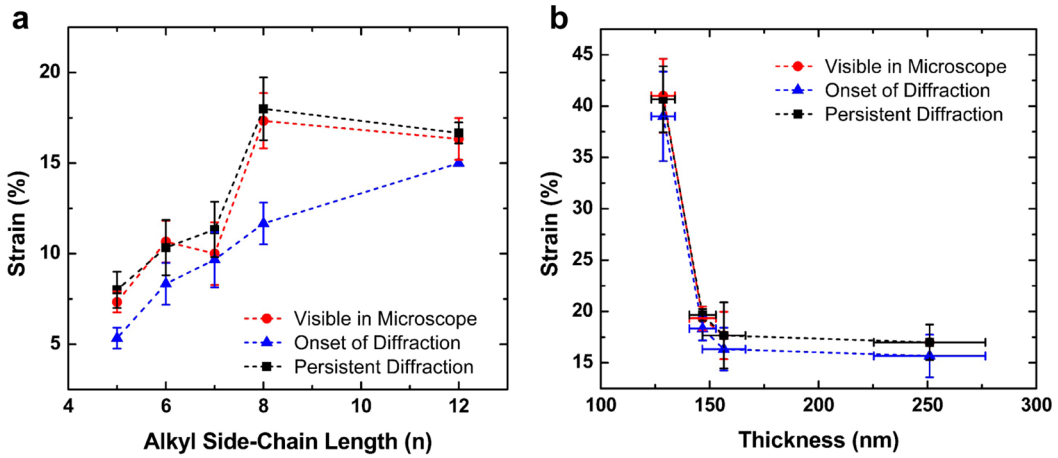

Figure 8. Yield point as determined by onset of buckling. (a) Strain at the yield point vs alkyl side-chain length for P3ATs. The three plots refer to the onset of diffraction, persistent diffraction, and the strains at which the buckles were visible by optical microscopy. The onset of diffraction occurs at smaller strains because the buckles form and then recede because of the viscoelasticity of the polymer films and the PDMS substrate. (b) Strain at the yield point vs thickness for poly(3-dodecylthiophene). The yield point of the material exhibits a strong dependence on thickness, with films thinner than approximately 140 nm exhibiting a greater elastic limit. Reproduced with permission from ref 110. Copyright 2015, American Chemical Society.

testing or nanoindentation) is that it measures only a single mechanical property. The buckling technique is thus one of three techniques that can be used in concert to approximate the key features of the stress−strain curve (Figure 7c), which also include determination of yield point by onset of buckling (Section 2.3) and crack-onset strain (Section 2.4).

In the development of the buckling-based method, Stafford and co-workers showed that the tensile modulus of plasticized polystyrene as measured by nanoindentation was in good agreement with the buckling-based method.[113] Nanoindentation is one of the standard measurement techniques for thin films and has been successfully used to measure the hardness and tensile modulus of thin films of ceramics and metals. Typically, the material properties are calculated from the shape of the curve of the load vs depth of penetration and indenter type. Significant challenges arise when the method is applied to materials with submicron thickness. Such measurements are complicated by effects of the substrate, along with viscoelastic behavior, which produces a dependence of the mechanical properties on the rate of the displacement of the indenter tip. In order to eliminate the effect of the underlying substrate on the measurement of the tensile modulus, one strategy is to use films thicker than 1 μm. For example, Venkatanarayanan et al. measured the tensile modulus of two conjugated polymers, poly(*p*-phenylenevinylene) (PPV) and polyacetylene (PA), using nanoindentation on films thicker than 3 μm and observed good agreement to the values they obtained by molecular dynamics simulations.[144]

2.3. Yield and Ductility

The elastic behavior of a solid material terminates with either brittle fracture or plastic yield. At the yield point, the energy stored during elastic deformation (i.e., the modulus of resilience, U_r) is converted to plastic deformation. That is, this energy overcomes the barrier imposed by intermolecular forces and entropic effects in the elastic regime and the molecules adopt a new configuration at mechanical equilibrium. For van der Waals solids, yield corresponds to molecules sliding past each other, and is facilitated by a low glass transition, for example, by the presence of side chains. In semicrystalline semiconducting polymers whose structure permits interdigitation between the side chains in the crystallites, there are strong intermolecular forces along all axes in the lattice, and these materials tend to exhibit brittle behavior as opposed to plastic deformation.[31]

The yield point in conjugated polymers has practical consequences.[110] The lower limit of this quantity, generally expressed as a strain, defines the elastic range, up to which a material can be expected to be deformed many times over its lifetime with little change in performance.[145] In applications requiring repeated deformation (e.g., devices integrated with the moving parts of the body or of machines), it is thus desirable to operate within the elastic range. For applications that require only one-time bonding to curved surfaces (e.g., windshields, lenses, and architectural elements),[9,146] permanent plastic deformation may be acceptable.[147] Whether or not the effects of plastic deformation are deleterious depend on the ways in which the deformed microstructure influences optical absorption[148] or charge transport.[149] During tensile loading, polymer chains tend to align along the axis of strain; this alignment corresponds to increased tensile strength along the strained axis and birefringence in semiconducting polymers. O'Connor and co-workers have used this approach to generate organic photovoltaic devices based on a stretched P3HT:fullerene active layer. This device behaves essentially as a polarization-dependent photodetector.[148] Strain alignment also produces anisotropy in elastic modulus[150] and charge transport.[151] Generally, measurements of field-effect mobility have been highest along the strained axis for stretched samples of P3ATs.[151,152] The extent of chain alignment in strained films of P3HT has been measured experimentally by O'Connor et al.[151] and has been predicted computationally using coarse-grained molecular dynamics;[130] the results of both of these techniques have excellent agreement. Mechanical strain can also produce changes in texture, as has been observed in P3HT, in which molecules partially reorient with their π-stacking axes perpendicular to the substrate. Gargi et al. demonstrated that this reorientation increased the mobility in samples of biaxially strained P3HT, which exhibited highly face-on stacking, relative to samples that were unstrained, which comprised a blend of face-on and edge-on stacking.[149]

The yield point can be measured using a variety of techniques. In a pull test, the yield point occurs just after the end of the linear portion of the stress−strain curve. Using film-on-elastomer techniques, the yield point can be estimated by the onset of

DOI: 10.1021/acs.chemrev.7b00003
Chem. Rev. 2017, 117, 6467−6499

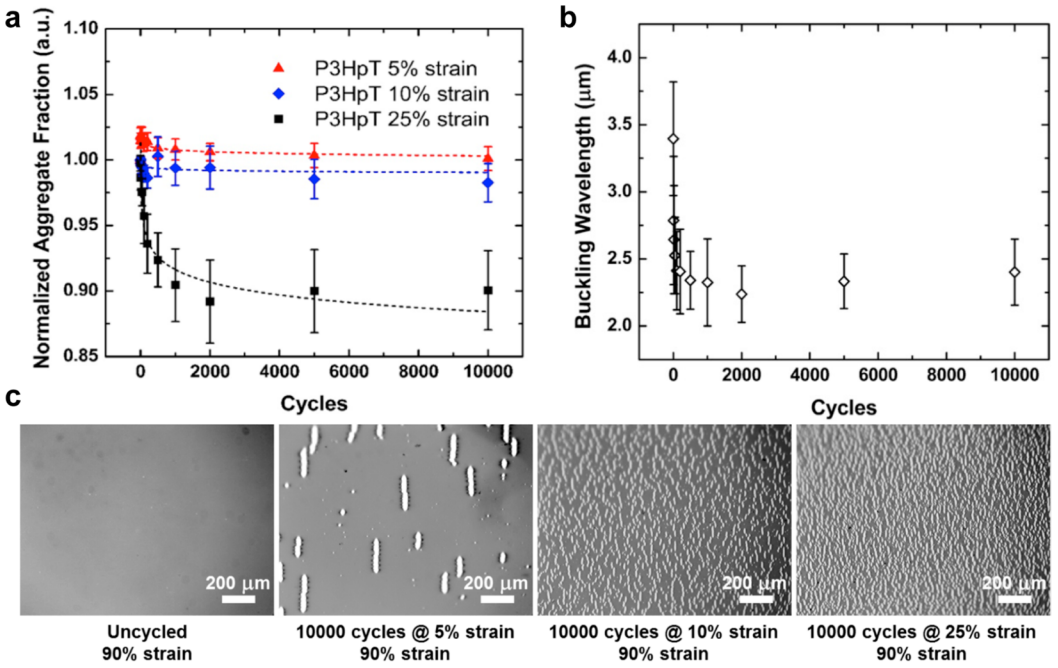

Figure 9. Fatigue in poly(3-heptylthiophene) (P3HpT). (a) Normalized fraction of H-aggregates as a function of number of cycles of strain to 5, 10, and 25%. The greatest change is observed for a strain above the yield point, or 25%. (b) The buckling wavelength decreases significantly as a function of cycles of strain, which is indicative of a tensile modulus that decreases with cyclic loading. (c) Micrographs showing the density of cracks as a function of maximum strain before fatigue (left image), and after 10 000 cycles of 5, 10, and 25% strain. Reproduced with permission from ref 161. Copyright 2016, Elsevier.

buckling.[110] In this experiment, a thin film on an elastomeric substrate is cyclically strained by incrementally increasing amounts, e.g., 0% → 1% → 0% → 2%, etc. At the first appearance of buckles upon returning the film to 0% strain, it can be assumed that the yield point has been surpassed. The appearance of buckles can be determined by inspection using optical microscopy for stiff and highly absorbing materials (i.e., easy-to-see films). In the case of transparent or hard-to-see films, the onset of buckling can be inferred from the production of a diffraction pattern when passing a laser beam through the sample (Figure 5c). Printz et al. found a dependence of the yield point on the length of the alkyl side chain, namely that the elastic limit increases with increasing length of the side chain.[110] Interestingly, the yield point also increased with decreasing thickness, as observed in films of poly(3-dodecylthiophene) (P3DDT, Figure 8b).

2.4. Moduli of Resilience and Toughness

The deformation of a sample is characterized by two energy densities: modulus of resilience (U_r) and modulus of toughness (U_t). The modulus of resilience is the total energy stored by the sample within the elastic regime and is calculated as the area under the linear portion of the stress−strain curve. The modulus of toughness is the total energy absorbed by the sample at the point of fracture and is the total area under the stress−strain curve from 0% strain to the point of fracture. The toughness increases with the product of strength and extensibility, and generally increases with increasing intermolecular forces and with molecular weight. The absolute extensibility prior to fracture, however, may not be the most important predictor of the ability of encapsulated devices to survive extreme deformation. Rather, the substrate and encapsulant, rather than the active layer, bear the load. For extreme deformations, it may be sufficient for a material to be neither strong nor tough, assuming the active materials are at least as deformable as, and have good adhesion to, the substrates and encapsulants.[37]

2.5. Crack-Onset and Fracture

Once the mechanical energy density absorbed by a specimen exceeds its modulus of toughness, its bulk structure fractures. The molecular mechanisms responsible for fracture of organic structures depend on the molecular weight and phase of the solid sample. For small molecular semiconductors,[118] fracture occurs when the van der Waals forces between molecules are overcome. For crystalline solids, the van der Waals cohesive pressure is theoretically greater than 10^8 Pa (>1000 atm),[153] and thus it is likely that fracture initiates at boundaries between crystallites. In samples of semicrystalline polymers, scission of covalent bonds and pulling out of chains can both be active:[154] chain scission[155] is favored with high T_g and density of entanglements (which scales with molecular weight) and pullout is favored with low T_g and low molecular weight.[156,157]

Catastrophic decohesion of a sample is generally measured by the strain at failure in a bulk tensile test—i.e., when the sample bifurcates. For thin films, the strain at fracture can be measured using the water-supported tensile test, or indirectly by measuring the strain at which the first crack appears when the film is bonded to an elastomer (the crack-onset strain). The water-based method generally produces a smaller value for fracture strain than the crack-onset strain.[139] The origin of the discrepancy is that thin films have inhomogeneities in thickness that can be a significant fraction of the thickness of the film. Concentration of strain at thin areas and defects produce cracking at smaller strains than would be expected for a mathematically smooth film. This argument is analogous to the one given for the lower tensile moduli obtained using the water-based method. This effect is counterbalanced somewhat by the fact that the fracture strain in the water-based method represents complete bifurcation of the

DOI: 10.1021/acs.chemrev.7b00003
Chem. Rev. 2017, 117, 6467−6499

sample, whereas the crack-onset strain where the film is bonded to an elastomer represents only the first appearance of a crack as visible by optical microscopy.

While it might seem that fracture would mean the demise of a device based on organic semiconductors, fracture is not always catastrophic. The extent to which fracture is deleterious to performance depends on the extent of the cracks and the direction of charge-transport in the device. For example, in organic solar cells and light-emitting devices, charge-transport is perpendicular to the plane of the device; for field-effect transistors, it is in-plane. Thus, cracking in devices with perpendicular charge transport is not necessarily catastrophic, as cracked devices can in principle behave as multiple devices connected in parallel.[158] Short-circuiting of the electrodes through the active layer, however, will eventually lead to complete failure of such devices. In devices operating using lateral, in-plane transport, operation will continue if there is a percolated pathway between electrodes.[159] Intentional fracture has long been a method for introducing stretchability into metallic thin films,[58,68,160] and such an approach has also proven effective in organic field-effect transistors.[39]

2.6. Cyclic Loading and Fatigue

A device in outdoor or on-body environments will be subjected to cyclic deformations.[3,145] The ultimate effects of cyclic loading in engineering materials are deleterious.[160] That is, strain hardening produced by the accumulation of dislocations within crystalline grains harden and embrittle metallic samples,[160] and chain scission embrittles plastics. Like engineering plastics, semiconducting polymers also undergo fatigue, as Printz et al. showed for poly(3-heptylthiophene) (P3HpT, Figure 9).[161] When cyclically strained 10 000 cycles above the yield point, P3HpT exhibited a loss in tensile modulus (as deduced by a decrease in buckling wavelength) and increase in brittleness (as deduced by an increase in the linear density of cracks at a given applied strain). Interestingly, fatigued films of P3HpT exhibited a correlation between tensile modulus and brittleness that was opposite to what was expected for other conjugated polymers, including P3ATs with increasing length of the alkyl chain (for which stiffness increases with brittleness).[161] For fatigued films, low tensile modulus correlated with brittleness. Moreover, analysis of the UV−vis spectra by the weakly interacting H-aggregate model showed deaggregation of the polymer chains by a reduction in the vibronic absorptions characteristic of $\pi-\pi$ stacking. Thus, cyclic loading and fatigue have dually detrimental effects: by degrading the microstructure in a way that is deleterious to charge transport but also increasing the susceptibility to mechanical failure.[161]

2.7. Adhesive and Cohesive Fracture Energy

The Dauskardt laboratory has described extensively the adhesive and cohesive energies of organic semiconductors and devices.[25−27,40,41,115−117] Films with poor adhesion[115] or cohesion are susceptible to delamination, which results in catastrophic failure of devices. Adhesion and cohesion depend on chemical bonding, van der Waals interactions, and chain entanglements. Methods for probing the adhesion and cohesion of thin films include the four-point bending technique (FPB, Figure 10a) and the double-cantilever beam technique (DCB, Figure 10b). Briefly, FPB is most appropriate for measuring the interfacial adhesion between layers, although it can be used to measure layer cohesion as well. It involves placing (or sandwiching) a thin film between two beams and applying a load using bending pins with inner and outer symmetry. The thin film/beam sandwich has a

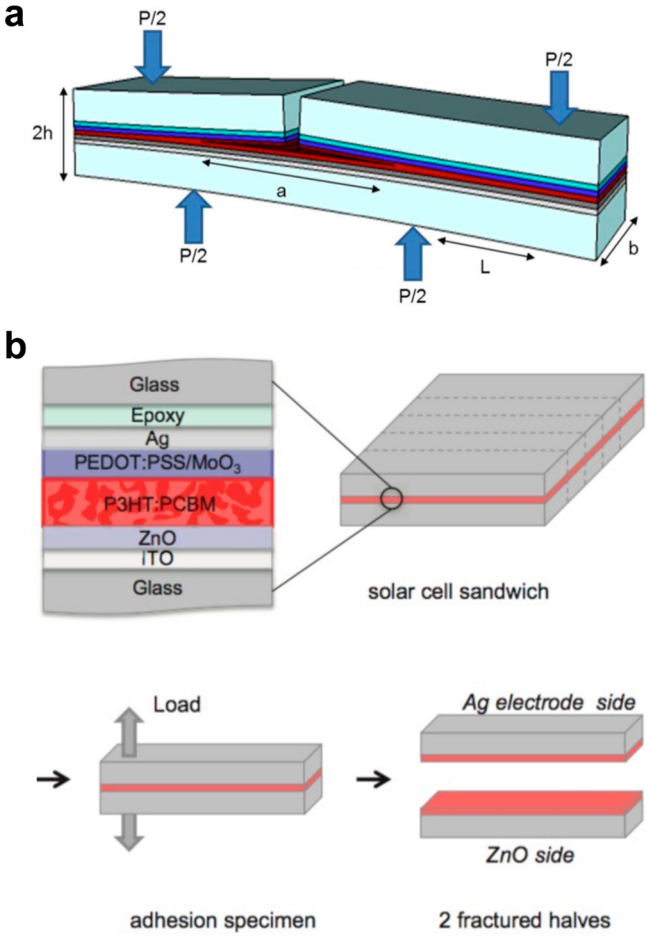

Figure 10. Schematic drawings of the (a) four-point bend and (b) double cantilever beam tests. Reproduced with permission from refs 25 and 115. Copyright 2015 and 2013, Elsevier and American Chemical Society, respectively.

starter notch equidistant from the pins on the side under tension. To prevent the fracture from propagating from the notch through the film and to the other beam, a small area of material known to have poor adhesion is sometimes added to direct the fracture to the interface of interest.

The experimental setup for DCB is a thin film or films sandwiched between two beams; at one end of the beams, a load is applied normal to the surfaces. This technique can be utilized to probe either adhesive or cohesive failure. The cohesive fracture energy determined by DCB can be considered to be essentially the same as toughness in the case of a homogeneous thin film sandwiched between two essentially rigid beams. However, in the case where additional layers are sandwiched between the beams, these layers can plastically deform ahead of the fracture path; this scenario results in a measured fracture energy greater than the film toughness. Typical values for the cohesive energy obtained using the DCB and FPB tests for organic electronics are typically less than 5 J m^{-2}, with PEDOT:PSS measured to be 2.5 J m^{-2},[116] although very high molecular weight P3HT (100 kDa) blended with PCBM has been measured as high as 17 J m^{-2}.[26]

2.8. Viscoelasticity

All polymers, especially those above or near their glass transition temperatures, are at least partially viscoelastic, and thus exhibit mechanical behavior that depends on time. A viscoelastic solid is

DOI: 10.1021/acs.chemrev.7b00003
Chem. Rev. 2017, 117, 6467−6499

solid-like at short time scales and small deformations, and fluid-like at long time scales and large deformations. Viscoelastic properties of polymeric materials can be characterized using dynamic mechanical analysis (DMA).[154] This technique measures the complex dynamic modulus (composed of the storage and loss modulus) by monitoring the ratio of an oscillating stress and strain—either tensile, compressive, flexural, or shear—in a deformed sample as a function of frequency and temperature (<0.5% strain). DMA is typically performed on free-standing films and has been used to study only a few conjugated polymers, which include P3ATs,[162−166] polytriarylamine,[167] and poly(diphenylacetylene)[168] derivatives.

Chen and Ni performed some of the earliest work aimed at corrleating the structure and viscoelastic properties of regiorandom P3ATs. The authors performed temperature-dependent DMA on a series of bulk samples of regiorandom P3ATs with varying side-chain lengths (P3BT, P3OT, and P3DDT). Three characteristic thermal transitions were observed: a γ-transition associated with methylene linkages in side chains (<−150 °C), a β-transition associated with side chains, and an α-transition (T_g) associated with dihedral twists of the thiophene backbone. The β-transition was observed to increase with length of the side chain, while the α-transition exhibited the opposite trend. In going from P3BT to P3OT the T_g decreased to below room temperature, enabling P3OT and P3DDT to undergo viscoelastic stress relaxation under ambient conditions.[162] van der Leur et al. investigated the frequency dependence of the α relaxation mode for a series of P3ATs (P3HT, P3OT, and P3DDT), and observed a 15−20 °C increase in the glass transition when increasing the frequency from 0.1 to 10 Hz.[166] More recently, Smith et al. have used DMA to measure the room-temperature storage and loss modulus of a series of P3ATs containing randomly incorporated unsubstituted thiophene rings along the backbone. In all cases, at room temperature the storage modulus was observed to be on the order of 10 times larger than the loss modulus indicating that the response was predominately elastic.[164]

A particularly striking example of a soft, viscoelastic conjugated polymer was a poly(diphenylacetylene) derivative reported by Jin et al. that was shown to exhibit gum-like mechanical behavior at room temperature. The authors found that the addition of long alkyl side chains to the off-axis phenyl units resulted in fluorescent materials that exhibited significant viscoelastic relaxation at room temperature. Room temperature DMA revealed placement of the side chain at the meta position of the phenyl unit led to a much softer and stickier materials than the para position. Unfortunately, the diphenyl acetylene backbone has poor charge-transport characteristics, so these materials would principally be of use for their fluorescence properties.[168]

2.9. Which Properties Are Desirable?

For an engineering plastic, the desired mechanical behavior is straightforward to specify. For example, automotive plastic in a dashboard must survive high temperatures in the summer, while plastic used in machinery must have high mechanical strength and temperature stability. Semiconducting polymers, however, exist as a thin film and are not expected to bear significant mechanical loads. (These polymers would not be able to do so anyhow because their electronic function requires them to be very thin.) For materials expected to endure only tensile modes of deformation (e.g., stretching and bending), it is sufficient in most cases for a material to have a low tensile modulus and high crack-onset strain. Each material in a multimaterial stack will have different tensile moduli, and the magnitude of these differences will determine the interlayer stresses, which contribute to delamination. As deformation of the substrate (and encapsulant) will dictate the deformation in the active materials due to the much greater thicknesses of the substrate, the simplest route to minimizing interfacial stresses is to lower the modulus of the active material. For stretchable substrates (e.g., PDMS or thermoplastic polyurethane, $E \leq 1$ MPa), the typical modulus of an organic semiconductor would have to be lowered by several orders of magnitude to achieve the elastic response of the elastomeric substrate. For skin-wearable devices, the concept of "mechanical invisibility", imperceptibility of the device by the wearer requires low stiffness, or a combination of low modulus and low thickness, and an elastic range that is commensurate with that of skin. Depending on the region on the body and the axis along which it is stretched, human skin exhibits an extensibility of ca. 30%. In all cases, the extensibility (i.e., the crack-onset strain) of the active material should be equal to or greater than that of the substrate, unless cracking itself is used as a means to impart stretchability.

In modes of deformation characterized by bending and stretching, it is the absolute extensibility prior to fracture, rather than the energy absorbed over this range, that will determine the failure of devices. It may, for example, be acceptable to have an organic semiconductor with properties resembling those of a hydrogel:[169] low modulus, large extensibility, and either low or high toughness. Modes of deformation that generate significant shear (i.e., twisting) or forces normal to the plane of the active layer, in effect require the active layer to behave as glue, and thus toughness and cohesive energy play a critical role.

Adhesion is a parameter that depends on the characteristics of both the active material and the adjacent layers.[40,115] It is critical in all forms of deformation, as strong bonding between adjacent layers can mitigate unequal elastic moduli and hold the device stack together. For obvious reasons, it increases the stability of devices in twisting and shear modes of deformation. For example, DuPont et al. found that interpenetration of PEDOT:PSS electrodes into P3HT:PCBM active layers shifts the plane in which the device stack was most likely to fracture from the interface between PEDOT:PSS and the active layer to the bulk of the active layer (Figure 11a).[115] Adhesion also plays a role in the fracture behavior within thin films under tensile and bending deformations. It is well-known that adhesion layers act to distribute strain and mitigate cracking. Lu et al. showed that copper films on polyimide substrates could be stretched to 50% with an adhesion layer of chromium.[90] The same concept applies in organic thin films.[34] For example, PEDOT:PSS similarly behaves as an adhesion promoter for P3AT:PCBM films on PDMS.[147] Encapsulation layers also play a significant role in reducing the occurrence of cracks. For example, Sawyer et al. was able to increase the crack-onset strain of both PEDOT:PSS and P3HpT:PCBM by a factor of 3 simply by encapsulating the stack in an overlayer of thermoplastic polyurethane (Figure 11b).[37]

3. THEORETICAL MODELS

Experimental characterization techniques have been complemented by a variety of theoretical treatments to provide a more detailed understanding of the thermal and mechanical properties of organic semiconductors. These methods range in sophistication from back-of-the-envelope calculations using semi-empirical bond-connectivity indices[155] to large-scale molecular dynamics simulations (both atomistic[25] and coarse-grained[170])

DOI: 10.1021/acs.chemrev.7b00003
Chem. Rev. 2017, 117, 6467−6499

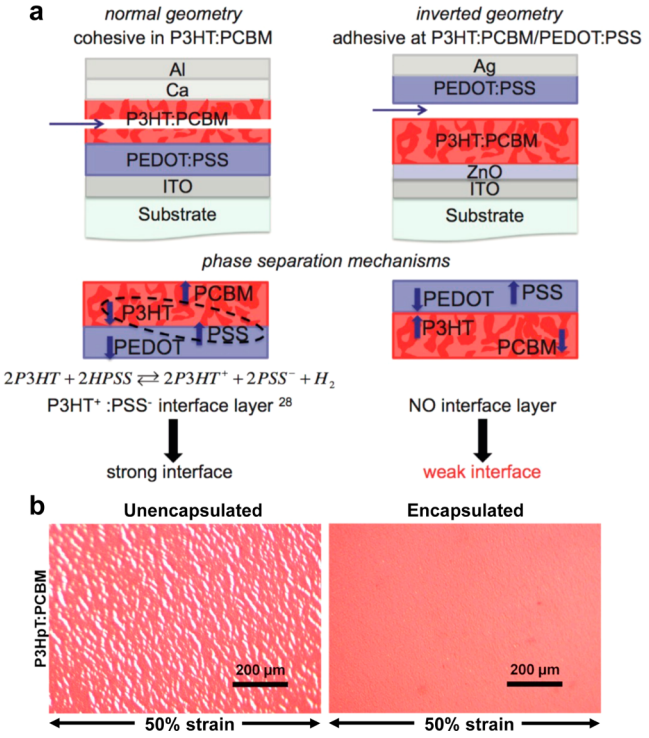

Figure 11. Influence of interfaces on the mechanical behavior of polymer films. (a) Interpenetration of P3HT:PCBM into PEDOT:PSS. Reproduced with permission from ref 115. Copyright 2013, Elsevier. (b) Effect of encapsulation on the cracking behavior of P3HpT:PCBM films. Reproduced with permission from ref 37. Copyright 2016, Elsevier.

and sophisticated finite-element models for device-scale deformation and fracture phenomena.[170] Insights obtained from computation have the potential to augment the understanding of experimental findings. Computational resources available at the time of this writing[171] can simulate solid-state structures with good resemblance to experimental thin films, and are now able to make experimentally testable predictions. It can be expected that computation will play an increasing role in developing experimentally testable hypotheses and co-optimizing the mechanical and optoelectronic properties of organic semiconductors.

3.1. Semi-Empirical Approaches Using Connectivity Indices

A simple model for estimating the mechanical properties of polymeric materials, using structure−property relationships, has been developed by Seitz.[155] These predictions are based on five molecular properties: the molecular weight, van der Waals volume, the length and number of rotational bonds in the repeat unit, and the glass transition temperature of the polymer. While originally developed for amorphous polymers, the method was applied successfully (though unmodified) to semicrystalline semiconducting polymers.[109] Despite the ability to predict the tensile moduli of simple polymers such as P3ATs, significant problems in predicting the properties of polymers with complex molecular structures limit the transferability of the method.[134] Details of the implementation of this method can be found in previous publications.[34,109,155] Such simple methods are useful for quick predictions on paper, which may save researchers time in the laboratory, but are only practical for relatively simple molecular structures. For more sophisticated polymers, computation is required.

3.2. Molecular Dynamics Simulations of P3ATs

Molecular dynamics (MD) simulations use the numerical solution of Newton's equations of motion to model interactions between organic molecules based on semiempirical atomistic force fields. Such simulations have been successfully used to predict the mechanical properties of conjugated polymers and composites. For polymeric systems, due to the difference in time

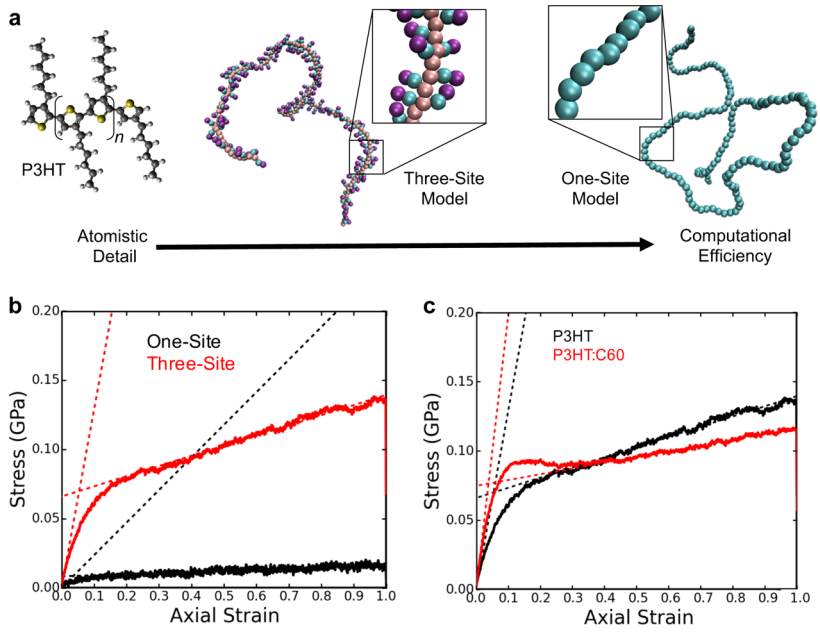

Figure 12. Coarse-grained molecular dynamics simulations of poly(3-hexylthiophene) (P3HT). (a) Schematic diagram showing the competition between atomistic detail and computational efficiency when one decreases the resolution. (b) Calculated stress−strain behavior of P3HT using one-site and three-site coarse-grained models. The three-site model reproduced the experimental value of the tensile modulus. (c) Calculated stress−strain behavior of P3HT and P3HT:C_{60} bulk heterojunction. The model correctly predicts the stiffening effect of the fullerene on the polymer. Reproduced with permission from ref 130. Copyright 2016, American Chemical Society.

DOI: 10.1021/acs.chemrev.7b00003
Chem. Rev. 2017, 117, 6467−6499

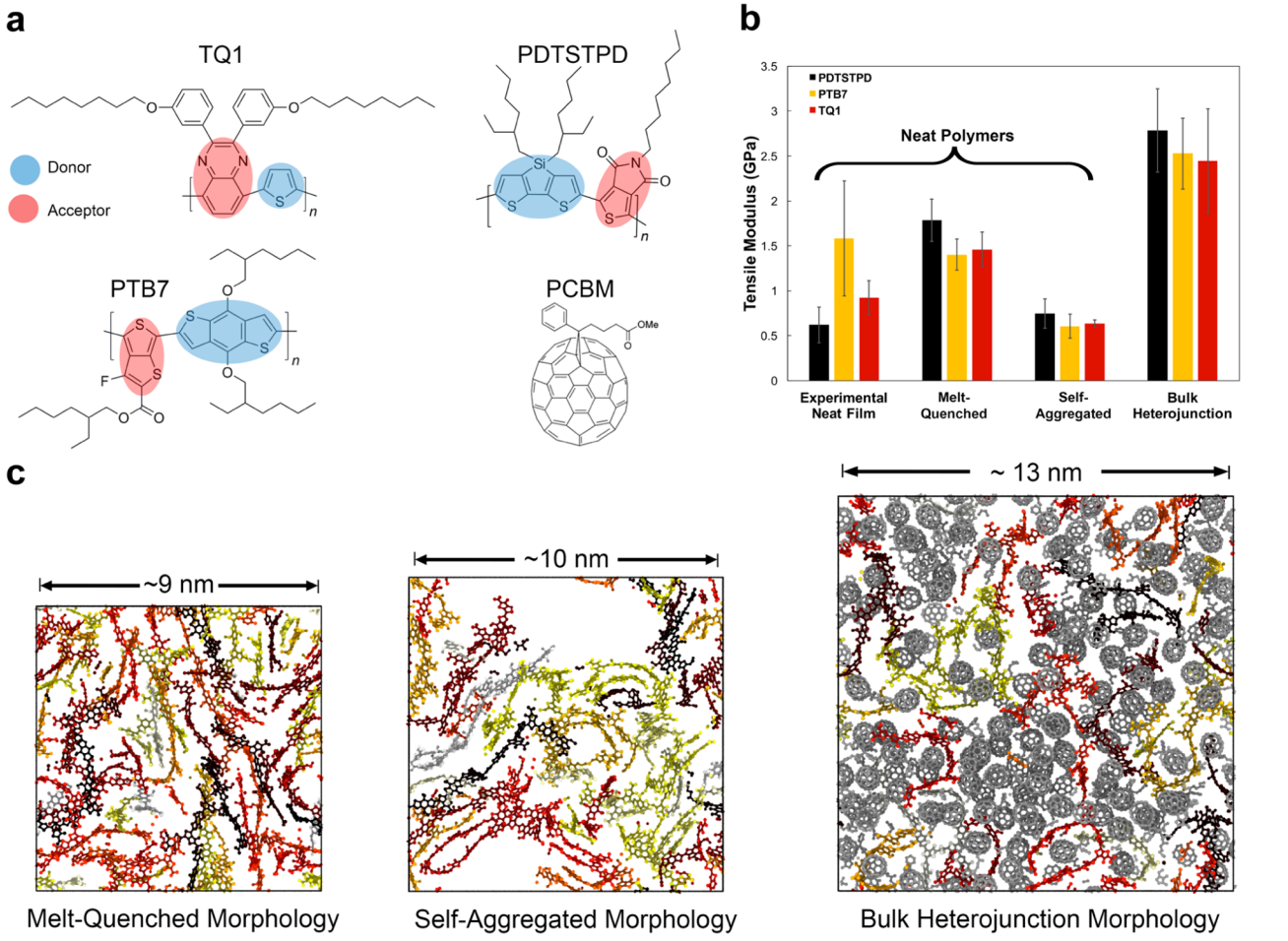

Figure 13. Atomistic molecular dynamics approaches to predicting the mechanical behavior of donor−acceptor polymers and bulk heterojunction films. (a) Molecular structures of the materials simulated. (b) Tensile moduli of the three conjugated polymers grouped by the way in which the solid films were prepared. The bulk heterojunction of the polymers mixed with PCBM is also shown. (c) Visualization of the melt-quenched, self-aggregated and bulk heterojunction morphologies. Reproduced with permission from ref 105. Copyright 2016, Royal Society of Chemistry.

scales between fast dynamic modes (e.g., vibrations of covalent bonds) and slow modes (e.g., reptation of chains), simulations using coarse-grained (CG) models are often used for the sake of computational efficiency. In a CG model, groups of covalently bonded atoms are mapped into representative CG beads.[172] The resolution of the model decreases when these beads are used to represent greater numbers of atoms. The resolution can range from a united-atom treatment, where all hydrogen atoms are grouped into the atom to which they are bonded,[173] to extremely coarse models in which several monomers are mapped to a single coarse-grained bead.[174] Coarse-graining thus represents a compromise between atomistic detail and computational efficiency. For example, P3HT could be simulated using a fully atomistic model (Figure 12, left), a three-site model (middle), or a single-site model (right). A CG procedure allows for the simulation of larger systems and longer time steps than can be achieved using atomistic models.

Tummala et al. described the first use of MD simulations to predict the mechanical properties of P3HT and its blends with fullerenes.[25] In one study, the authors used atomistic models to predict the effects of molecular weight and entanglement on the uniaxial tensile response.[170] They have additionally simulated the effect of various fullerene-based electron acceptors on the mechanical properties of the composite film.[25] The authors found that degrees of polymerization of at least 50 were required to obtain elastic behavior. To predict the solid-state structure of larger systems comprising longer polymer chains, two CG models have been proposed: the one-site model of Lee et al.[175] and the three-site model of Huang et al.[176,177] We compared the abilities of these two models to predict the glass-transition temperature, density, and tensile modulus of P3HT and its blend with C_{60}.[130] The three-site model gave values close to the experimentally determined values for these quantities, whereas the one-site model overestimated the density and underestimated the tensile modulus. An important observation that arose from this study was that there were a significantly lower number of calculated interior kinks per chain,[178] proportional to the density of entanglements, in the P3HT:C_{60} blend films (2.4 kinks per chain) compared to films of the neat polymer (7.0). This observation is consistent with increased brittleness that is always observed in bulk heterojunction films compared to films of pure polymers. One limitation of the CG approach is its limited transferability. When the three-site model was extended to attempt to predict the tensile modulus of P3ATs with longer side chains, the absolute values were overestimated when compared to experiment. This lack of transferability is possibly due to the inadequacy of representing the thiophene ring as a symmetrical CG bead and implies that, at this level of resolution, predictive models for materials with even minor changes to the molecular structure require parametrization from atomistic

DOI: 10.1021/acs.chemrev.7b00003
Chem. Rev. 2017, 117, 6467−6499

simulations. Nevertheless, it seems that CG models are adequate to predict a wide range of thermomechanical properties of the P3ATs with degrees of polymerization of 150 or more. Potential future work in this area includes simulating the effect of substrate interactions and including a realistic polydispersity in the simulations.

3.3. Molecular Dynamics Simulations of Low-Bandgap Polymers

Atomistic MD simulations have been applied to low-bandgap polymers exhibiting the donor−acceptor (DA) motif. Using the quantum mechanically informed force fields computed by Jackson et al., our group recently simulated the mechanical properties of PDTSTPD, PTB7, and TQ1 (Figure 13a).[105,179] These materials were chosen to represent a range of solid-state packing structures adopted by DA polymers, from the semicrystalline PDTSTPD, to PTB7, which exhibits local order, and TQ1, which is amorphous. Perhaps the most striking finding of this study was the importance of the ways in which a film solidifies from solution or from the melt influence the mechanical properties (Figure 13b). For example, we have shown that glassy morphologies of the low-bandgap polymers PDTSTPD, PTB7, and TQ1 can be prepared in two ways (Figure 13c).[105] In the first way, an equilibrated melt is quenched rapidly, to generate a thermodynamically favored glass (melt-quenched morphology). In the second way, implicitly solvated polymer molecules are permitted to self-aggregate prior to deposition (self-aggregated morphology). This process, which is intended to mimic casting from a poor solvent, generates a kinetically trapped structure. Compared to the melt-quenched morphology, the self-aggregated morphology contains a greater fraction of void space (∼10% greater) and a significant reduction in the fraction of entanglements.[105] These two structural features are predicted to decrease the elastic modulus and extensibility.

4. MECHANICAL PROPERTIES OF CONJUGATED POLYMERS

This section is the first of three (4−6) that focus on particular classes of organic semiconductors. In this section, we examine the most attractive from a mechanical stability standpoint: conjugated polymers. Important differences between conjugated polymers and engineering plastics, e.g., polyolefins, suggest that lessons learned from many years of research in the polymer research community to increase the elasticity and toughness of materials are not directly applicable to organic semiconductors, in part because of the requirement that elastic and tough conjugated polymers must retain charge transport properties. Significant work has been done in the last three years to elucidate the effects of molecular structure on the bulk properties in the categories of molecular parameters covered in this section.

4.1. Molecular Weight

Along with molecular structure, the most important molecular parameter used to improve the mechanical performance of commodity polymers and engineering plastics is molecular weight. The molecular weight of a polymer is most commonly described by one of two measures, the number-average molecular weight (M_n) and the weight-average molecular weight (M_w). The M_n is a conventional average. It is obtained by summing the molecular weights of every molecule in the system and dividing by the number of molecules. It can be an inaccurate predictor of the mechanical properties of a polymeric sample, however, because one or more fractions with a given molecular weight may comprise the bulk of the weight of the entire sample. (For example, a system comprising a single chain with a molecular weight of 1000 kDa, and ten unreacted monomers.) The M_w, on the other hand, is biased toward the fraction of the sample with the greatest molecular weight and is thus a more accurate predictor of the mechanical properties of the system. The two molecular weights are calculated using the equations below:

$$M_n = \frac{\sum M_i N_i}{\sum N_i}$$

$$M_w = \frac{\sum M_i^2 N_i}{\sum M_i N_i}$$

In these equations, i is the degree of polymerization, and thus M_i and N_i are the weight and number of molecules with degree of polymerization i. As M_w is always greater than M_n, the ratio of M_w/M_n is greater than 1, and this quantity is termed the dispersity ($Đ$), which reflects the narrowness of the distribution in molecular weight for a given sample.

The principal effect of the molecular weight on the mechanical properties is to increase its strength and toughness by increasing the density and quality of entanglements. The effects of molecular weight on the mechanical properties have been characterized most thoroughly for P3HT (see Figure 7). These properties have been assayed by traditional pull testing of bulk samples[36] but also on thin films using the film-on-water and film-on-elastomer techniques.[139] Pull testing of bulk samples revealed similar moduli for samples from 20 to 110 kDa, though the high molecular weight samples (90 and 110 kDa) exhibited very high extensibilities (nearly 300%) prior to fracture, with the greatest toughness for the 110 kDa sample.[36] A similar trend was observed for films tested while suspended on water. In that case, the modulus increased with molecular weight, but saturated at approximately 40 kDa, while the maximum extensibility increased (>100%) for 80 kDa, the highest molecular weight tested.[139] Results from pull testing mirrored the key features of those obtained using film-on-elastomer methods. However, the compressive mode of deformation used in the buckling technique produced values of moduli that were 3−6 times greater than those obtained using pull testing. Microstructurally, low molecular weight is correlated with the presence of highly ordered needle-like aggregates, which in principle could stiffen the films. However, the opposite effect is usually observed, and some high-molecular-weight samples exhibit significant aggregation characteristic of extensive π-stacking.[139]

We close this section with a caveat on measuring molecular weights. Because of the ubiquity of the equipment and experimental simplicity, it is common practice to measure M_n and M_w using size-exclusion (gel-permeation) chromatography (SEC or GPC), which uses a column filled with porous beads. The molecules with the largest hydrodynamic volumes bypass a large fraction of the pores, and thus have the smallest retention time (i.e., they elute first). Conversely, molecules with the smallest hydrodynamic volumes have the longest integrated pathways through the pores, and elute later. The apparatus is calibrated using polystyrene samples of molecular weights that are well-known (i.e., by light scattering). As SEC/GPC provides a measure of the hydrodynamic volume, not the molecular weight, the technique is subject to inaccuracies when the solution-phase conformations of the polymers under study are significantly different from those of the standards. This procedure overestimates the molecular weight of conjugated polymers by a factor of approximately 2,[180] because these

DOI: 10.1021/acs.chemrev.7b00003
Chem. Rev. 2017, 117, 6467−6499

structures adopt an extended conformation in solution, i.e., when the molecular weights of rigid conjugated polymers are compared to standards that adopt ideal random coils in solution. Heeney and co-workers found that the molecular weights of P3HT are overestimated by a factor of 1.67 when the results of SEC/GPC are compared with those of NMR or matrix-assisted laser desorption ionization time-of-flight secondary ion mass spectrometry (MALDI-TOF-SIMS).[181] Since P3HT is expected to be more flexible than most donor−acceptor polymers (which contain fused rings and significantly higher barriers to rotation), the factor by which the molecular weight determined by SEC/GPC is greater than the actual molecular weight is expected to be greater than 1.67.

4.2. Entanglements

The excluded volume of long polymer chains gives rise to a structure in the solid and melt phase in which the molecules can be highly entangled, as chains can slide past, but not through, each other. Consequently, the motion of an individual polymer chain consists of reptation through a tube-like region along the chain contour called a primitive path.[182,183] Interior kinks are defined as nodes along the primitive path that represent the limit to which the contour can be reduced to a minimum length without violating the topological constraint of excluded volume of the chains.[178] The density of entanglements is proportional to the number of interior kinks per chain and can be quantified in MD simulations using the Z1 algorithm of Kröger and co-workers.[184,185] This quantity thus increases with degree of polymerization, and it manifests physically in the rheological properties of polymer melts and solutions and in the mechanical properties of solid films. A polymeric solid with a highly entangled microstructure exhibits high viscosity, tensile strength, toughness, and extensibility. A metric that describes the likelihood that a polymeric sample will exhibit entanglements is termed the entanglement molecular weight, which is believed to have a value of ∼10 kDa for P3HT in principle, though ∼20 kDa as typically measured by GPC. The density of entanglements is also affected by blending, and a MD study by our laboratory showed that BHJ films of P3HT:PCBM are significantly less entangled than pure P3HT.[130] This finding is consistent with increased brittleness of the BHJ relative to the pure polymer. Polymers such as donor−acceptor materials, which have substantially greater radii of gyration than P3HT with a similar contour length, also exhibit entanglements (Figure 14), the density of which depends strongly on the way in which the solid film was formed. For example, MD simulations predict that a thermodynamic glass prepared by quenching an equilibrated melt structure will exhibit a significantly greater density of entanglements than a solid structure prepared by depositing preaggregated polymer chains from solution (i.e., from a poor solvent).[105] These simulated results in particular suggest prescriptions for increasing the entanglement density, and hence the mechanical stability, through the judicious choice of solvents and thermal treatments.

4.3. Side-Chain Length, Branching, and Attachment Density

The unsubstituted π-conjugated main chain of a semiconducting polymer is generally insoluble. To render semiconducting polymers soluble, alkyl side chains are usually attached. Side chains afford solubility by reducing strong van der Waals forces between the main chains, and also permit greater entropic freedom of the polymer structure in the solution phase.[186] These side chains also have a strong effect on the thermomechanical properties.[32] In general, the effect of increasing lengths of side

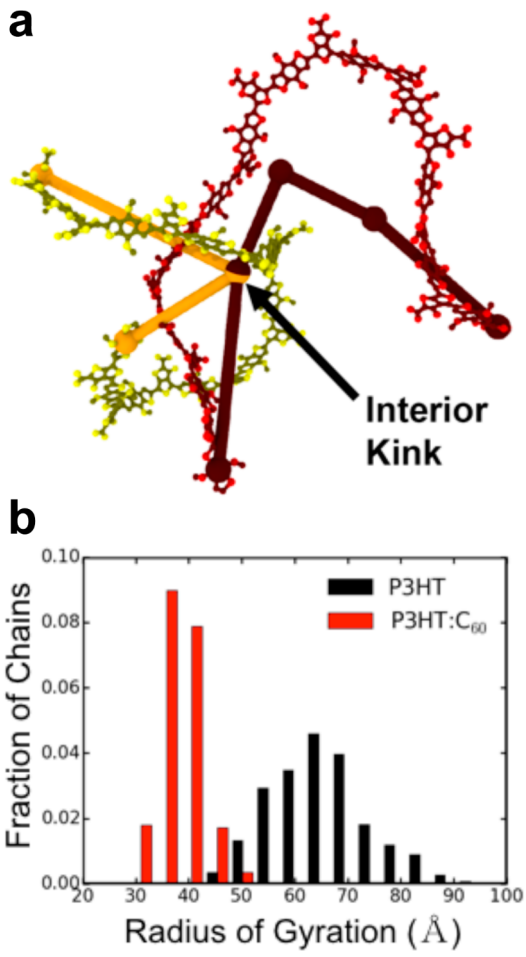

Figure 14. Entanglements and radius of gyration. (a) Graphical representation of interior kinks as the intersection of the primitive paths for two polymer chains. Reproduced with permission from ref 105. Copyright 2017, Royal Society of Chemistry (b) Fraction of polymer chains as a function of radius of gyration for both pure P3HT and the P3HT:C_{60} bulk heterojunction. Reproduced with permission from ref 130. Copyright 2016, American Chemical Society.

chains is to decrease the tensile modulus and increase the crack-onset strain for materials with a common backbone structure and similar molecular weights. This effect was observed strikingly in both regiorandom[33] and regioregular[34] P3ATs, as the tensile modulus was found to decrease significantly from poly(3-butylthiophene) to poly(3-dodecylthiophene), the material with the longest side chain tested.[133] The decrease in tensile modulus, and increase in extensibility, mirrored a similar trend in glass transition temperature, which decreases with increasing length of the side chain.[133] The intuitive rationale for the decrease in glass transition temperature and increase in softness is similar to its effect on solubility: longer side chains decrease the van der Waals energy between the main chains and, in the case of mechanical deformation, reduce the density of load-bearing carbon−carbon bonds along the strained axis.[32]

For regioregular P3ATs, the largest reduction in stiffness and increase in extensibility with increasing length of the side chain occurs between P3HT and P3HpT, where Hp = heptyl (see Figure 6a).[134] This behavior is reflected in the glass transition temperature. In particular, the T_g of P3HT is ca. 12 °C, while that of P3HpT is ca. − 5 °C, significantly below room temperature.[133] Given this extensibility, P3HpT:PCBM has been used in the

DOI: 10.1021/acs.chemrev.7b00003
Chem. Rev. 2017, 117, 6467−6499

active layer in the first solar cell in which each polymeric component is an elastomer,[37] i.e., an "all-rubber solar cell", and P3OT has been used in biaxially stretchable solar cells that can be bonded to hemispherical surfaces without cracking or wrinkling.[147] Copolymers that exhibit side chains of mixed lengths have also been examined for their mechanical properties. Savagatrup and Printz et al. measured the tensile moduli of block and statistical copolymers of poly(3-hexylthiophene) and poly(3-octylthiophene), along with physical blends of these materials.[134] This approach produced compromises, as opposed to the "best of both worlds", between mechanical deformability and optoelectronic properties. Recently Smith et al. reported a detailed study of a series of rr-P3ATs with randomly incorporated unsubstituted thiophene units.[164] The authors found that 1:1 random copolymer containing P3DDT and PT led to a co-optimization of the electrical and mechanical properties. Compared to the P3DDT homopolymer, there was approximately a 5-fold increase in both the conductivity and mobility. This improvement in electrical performance was accompanied by a 760% increase in toughness.[164] This study clearly demonstrated the importance of side chain length, and grafting density on the bulk material properties.

The effects of side chains on the mechanical properties of semiconducting polymers with molecular structures that are significantly more complex than P3AT have also been studied. With these materials too, one finds a strong role of side chains. Roth and Savagatrup et al. measured the tensile modulus and crack-onset strains of a library of over 50 low-bandgap polymers,[108] whose photovoltaic properties were described by the Krebs laboratory[187] (Figure 15). A trend in the data was increased deformability for polymer structures bearing branched side chains, as opposed to linear ones. An interesting historical note is that the softening effect of the side chains in comb-like polymers included for processability was regarded as catastrophic for materials intended for structural applications.[32] In the case of deformable organic semiconductors, however, we argue that increased compliance and extensibility produced by side chains is desirable.

4.4. Regioregularity

In the early 1990s, McCullough[188,189] and Rieke[190] independently published methods leading to the regioregular synthesis of P3ATs (rr-P3ATs, in which the monomers are all coupled with the same head-to-tail configuration such that all of the side chains point in the same direction). Given a large improvement in conductivity, mobility, and performance in solar cells of rr-P3ATs compared to regiorandom material (rra-P3AT), there has been limited interest in materials exhibiting less-than-high regioregularity. The principle way in which regiorandom couplings reduce the abilities of these materials to transport charge is to twist the backbone out of planarity and thus increase the bandgap and decrease the mobility. Increased flexibility of the chains also prevents crystallization, i.e., rra-P3HTs are amorphous,[141] and also has a softening effect on the solid films. Kim and co-workers recently published a study in which the regioregularity of P3HT was varied from 64% to 98%.[114] They observed a monotonic increase in both the degree of crystallinity, from 0% to 48.4%, and hole mobility, from 4.84×10^{-8} to 1.81×10^{-1} $cm^2\ V^{-1}\ s^{-1}$.[114] These increases in crystallinity and mobility were coupled with a decrease in the extensability from 5.3% to 0.6% and an increase in the tensile modulus from 13 to 287 MPa, indicating that as regioregularity

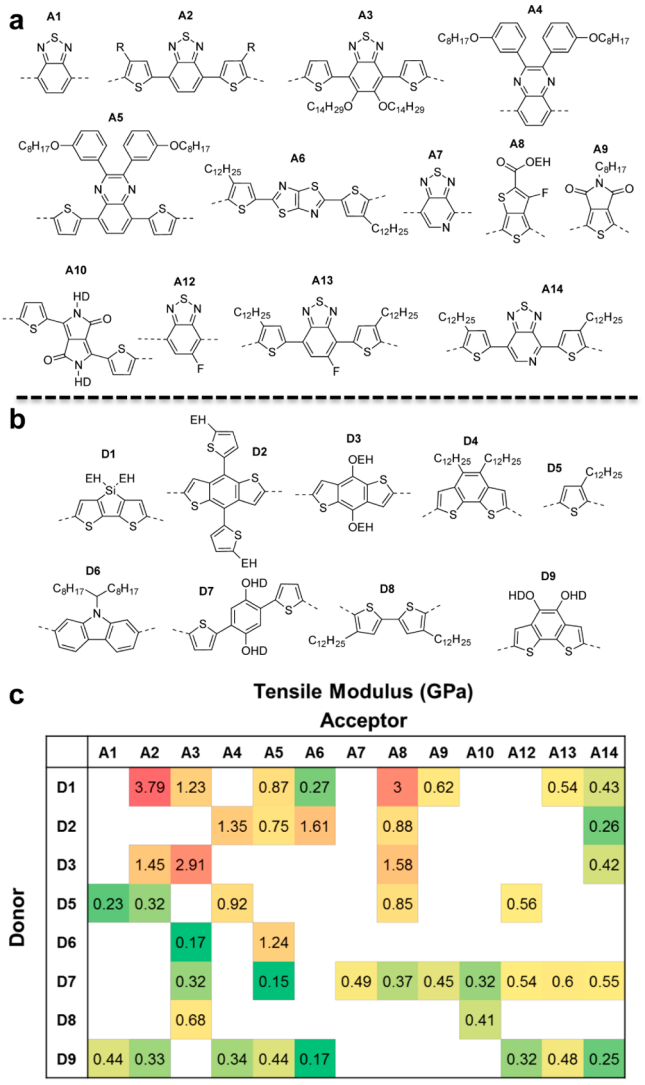

Figure 15. Structures of acceptor (a) and donor (b) units, and mechanical properties (c), of a library of low-bandgap polymers. Reproduced with permission from ref 108. Copyright 2016, American Chemical Society.

increased and ordering improved, the films became less soft and more brittle.[114]

4.5. Main-Chain Rigidity: Fused Rings, Isolated Rings, and Aliphatic Spacers

One would expect based on intuition that the deformability of the solid film would be a manifestation of the flexibility of the individual polymer chains. This intuition has been supported in a few studies, but the conclusions are not easily generalizable. In one of the first contributions to the field of intrinsically stretchable organic semiconductors, Müller et al. synthesized a block copolymer of polyethylene and P3HT. Films of these materials exhibited still-unmatched extensibilities (up to 600%), and retained charge-carrier mobilities of up to 2×10^{-2} $cm^2\ V^{-1}\ s^{-1}$ with as great as 90 wt % of the insulating fraction.[24] For polymers in which every atom in the backbone is conjugated, much less is known. The deformability of PBTTT, which contains the fused thienothiophene (TT) unit, is substantially less than that of P3HT, as noted by O'Connor et al.,[31] but a direct comparison of the effect of the rigidity of the backbone is problematic because the space provided by the unsubstituted TT

DOI: 10.1021/acs.chemrev.7b00003
Chem. Rev. 2017, 117, 6467−6499

unit permits intercalation of the side chains of PBTTT, which also increases the stiffness and brittleness (Figure 16a). In an

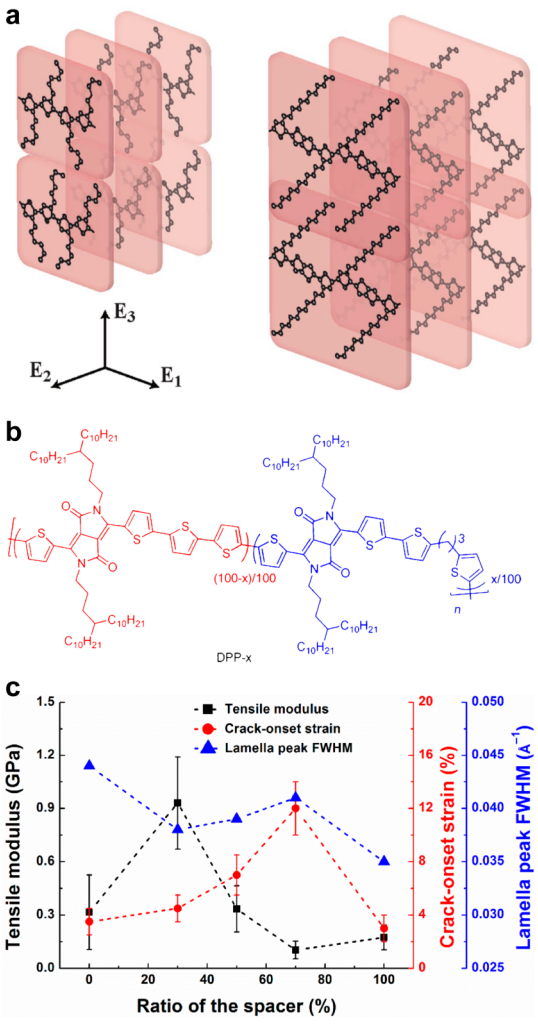

Figure 16. Effect of interdigitation of side chains on the mechanical properties of conjugated polymers. (a) The noninterdigitated structure of P3HT (left) and the interdigitated structure of PBTTT (right). Reproduced with permission from ref 31. Copyright 2010, American Chemical Society. (b) The structure of polymers bearing flexible conjugation-break spacers. (c) Tensile modulus, crack-onset strain, and lamellar full width at half-maximum (fwhm) vs ratio of the conjugation break spacer. Reproduced with permission from ref 28. Copyright 2016, Wiley-VCH Verlag, GmbH & Co. KGaA.

early measurement involving low-bandgap polymers comprising the DPP unit, Lipomi et al. observed that the incorporation of the TT unit produced a somewhat (~25%) lower modulus than the bithiophene (2T)-containing polymer.[158] In a large-scale screening of a combinatorial library of low-bandgap polymers, it was again observed that structures comprising fused rings were stiffer and more fragile than similar compounds with isolated rings.[108] While this effect is intuitive and provides a foundation for future work in this area, it should be noted that other parameters, e.g., molecular weight, were not rigorously controlled. In a more controlled study, Lu et al. reported a detailed characterization of a series of DPP-based polymers containing tetrathienoacene units.[191] They found that the addition of an extra unsubstituted thiophene spacer along the conjugated backbone improved the ductility (in comparison to a control without the spacer), enabling the film to accommodate up to 40% strain without cracking. The improved ability to accommodate strain while retaining good charge-transport characteristics was attributed to an increased propensity for edge-on backbone configurations compared to the control which exhibited a bimodal distribution of orientations among the crystallites.[191]

Recently, Mei and co-workers introduced the concept of conjugation-break spacers (CBSs) to increase the flexibility of DPP-based low-bandgap polymers. A series of polymers starting with the fully rigid DPP-0 and the fully flexible DPP-100 containing aliphatic propylene groups in every repeat unit (Figure 16b).[192] The hypothesis was that such flexible units would increase the entropy of the melt phase compared to fully conjugated analogues, and thus decrease the melting temperature (T_m).[192] Because of the rigidity of most conjugated polymers, they tend to decompose at a lower temperature than that at which they melt. The high melting temperatures of conjugated polymers precludes possible benefits of melt processing, e.g., highly crystalline samples crystallized from the melt, injection molding, hot embossing, and extrusion-based printing. Savagatrup et al. hypothesized that the melt-processable films containing the flexible CBS units would have increased deformability.[28] What was found instead (Figure 16c) was that the fully flexible DPP-100, which contains an aliphatic spacer within every monomer residue, formed the stiffest, most brittle solid! This finding was rationalized by comparison to GIXS data, which showed that the DPP-100 had the smallest lamellar spacing (and thus possibly interdigitation the strongest secondary interactions between the main chains) and the greatest lamellar order (smallest full-width at half-maximum, fwhm). This study highlights the dual roles of the main chain, as it simultaneously determines the flexibility of the isolated molecules, which is easy to predict, and also the solid-state packing structure, which is not.[28]

The concept of a conjugation-break spacer has also been explored by the Bao laboratory.[106] Aliphatic spacers along the axis of the conjugated backbone were first employed to improve the solution processability of isoindigo based conjugated polymers without compromising device performance.[106] This concept was further expanded upon through the synthesis of a series of DPP-based polymers with a variety of conjugation-break spacers containing different molecular structures.[102] The hypothesis was that the addition of chemical moieties with the ability to form dynamic noncovalent cross-linking sites would help dissipate mechanical energy due to tensile loading and potentially enable self-healing properties. The authors found that the incorporation of a 2,6-pyridine dicarboxamide unit as the conjugation-break spacer along the backbone (10 mol %) led to the best improvement in extensibility without a significant sacrifice in the charge transport properties. Additionally, this material was reported to exhibit healing characteristics when a damaged film was exposed to high temperature and solvent vapor.[102]

4.6. Small-Molecule Additives

One commonly used strategy in polymer engineering to increase the deformability of the solid is the use of plasticizers. These compounds are small molecules, e.g., phthalates, that suppress the T_g by increasing the free volume, along with the compliance and extensibility. Semiconducting polymers are frequently processed with small molecule additives, especially in solar cells. These compounds, which have included 1,8-dithiooc-

DOI: 10.1021/acs.chemrev.7b00003
Chem. Rev. 2017, 117, 6467−6499

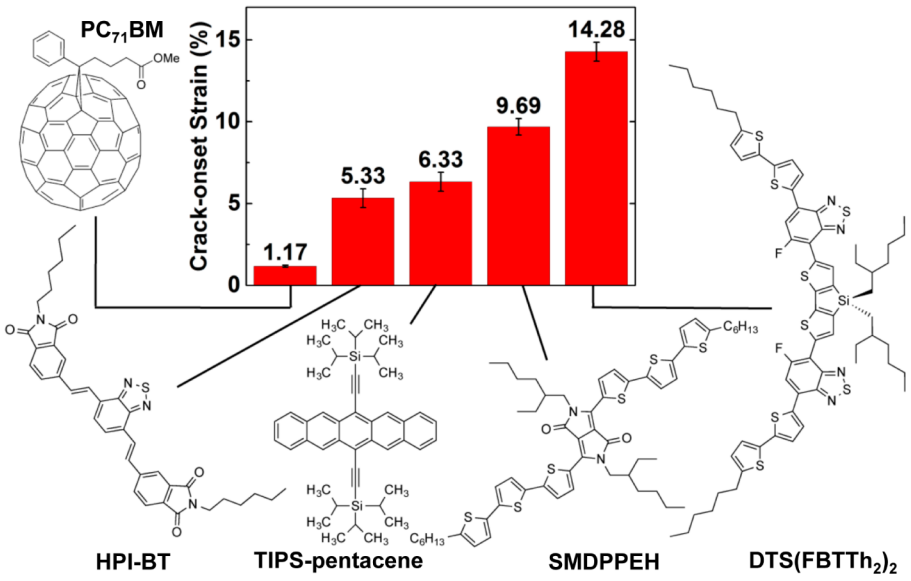

Figure 17. Crack-onset strains of several solution-processable semiconducting small molecules. Reproduced with permission from ref 118. Copyright 2016, American Chemical Society.

tane[193] and diiodooctane,[20] and low-molecular-weight PDMS,[194] have various effects that under favorable circumstances promote the formation of an ideal donor−acceptor morphology between the conjugated polymer and electron acceptor, typically a methanofullerene. Several of these compounds have also been found to have a plasticizing effect on bulk heterojunction films of P3HT:$PC_{61}BM$.[34] It is unclear, however, if the plasticizing effect is because of the effect of the additive on the morphology, or because additive remaining in the film behaves as a conventional plasticizer. It is possible that both mechanisms are operative. We will return to the effects of plasticizers, namely the strong effect of Capstone (formerly Zonyl) fluorosurfactant on the deformability of PEDOT:PSS,[104] and of polystyrene additives on bulk heterojunctions consisting only of semiconducting small molecules.[118]

4.7. Special Case: PEDOT:PSS

The conductive polyelectrolyte complex known as poly(3,4-ethylenedioxythiophene):poly(styrenesulfonate) (PEDOT:PSS) is ubiquitous in organic electronics.[98,99,195−199] This material consists of long chains of PSS^- complexed with shorter chains of $PEDOT^+$[200] and in neat form exhibits stiff, brittle behavior characteristic of PSS.[104] Several stretchable composite materials have been generated using PEDOT:PSS as the conductive phase and an elastomeric component as the stretchable matrix.[201,202] While the mechanical properties of neat PEDOT:PSS are unfavorable,[104] it is only moderately conductive in its native state (<1 S cm^{-1}) and is thus nearly always processed with a high-boiling, polar additive, such as dimethyl sulfoxide (DMSO). This solvent has the effect of encouraging the growth of conductive PEDOT grains;[203] increased percolation improves the conductivity of the film (>1000 S cm^{-1}). PEDOT:PSS is coated as a commercial suspension in water, and thus cannot be printed on hydrophobic substrates. In order to decrease the surface tension, PEDOT:PSS is often mixed with a fluorosurfactant of the general form $CF_3(CF_2)_n(CH_2CH_2O)_mH$ (called Capstone by DuPont, formerly called Zonyl), which in small weight fractions (≥0.1%) permits wetting on hydrophopic substrates.[204,205] These additives, DMSO and Capstone, are ubiquitous in the solution processing of PEDOT:PSS and also have effects on the mechanical properties. In particular, DMSO has a small stiffening and embrittling effect, which is overwhelmed by the strong plasticizing effect of the fluorosurfactant.[104] This additive, in concentrations between 1% and 10%, has the effect of decreasing the tensile modulus by a factor of 100, and the extensibility by a factor of 10.[104]

5. MECHANICAL PROPERTIES OF SMALL-MOLECULE SEMICONDUCTORS

This section focuses on molecular semiconductors, which have purported advantages of high purity, monodispersity, and high crystallinity. The absence of entanglements and other morphological features of polymers that confer mechanical benefits have suggested that solid films of molecular materials could not be deformed significantly. Recent work, however, suggests that, while the energy required to deform or fracture these materials is lower than that of polymers, the range over which these materials can be deformed is quite high (>10% for some materials) but only if the molecules contain solubilizing pendant groups.[118] The role of the substrate and encapsulant to bear mechanical loads partially reduces the requirement that the active materials themselves be strong or tough. The small amount of energy required to deform or fracture films of small-molecule semiconductors relative to polymers thus does not imply that small molecules cannot be used for deformable applications. This section discusses the molecular mechanisms by which van der Waals solids, such as these, accommodate mechanical energy.

5.1. Unsubstituted Acenes

The semiconducting cores of small-molecular semiconductors tend to comprise multiple fused rings. An early calculation of the tensile modulus of naphthalene and anthracene produced values of 8.1 and 8.4 GPa.[206] Tahk et al. measured the mechanical properties of a vapor deposited thin film of pentacene using the buckling technique.[109] While the film cracked extensively under the small compressive strains (<4%) required for the measurement, the authors were nevertheless able to extract a value for tensile modulus of 16 GPa, one of the highest values ever measured for an organic semiconductor. Pendant groups, installed on conjugated cores for solubility, increase the free

DOI: 10.1021/acs.chemrev.7b00003
Chem. Rev. 2017, 117, 6467−6499

volume in solid films and permit greater deformability. The modulus of TIPS-pentacene is thus reduced to 3.0 GPa, as measured by the buckling technique.[118] Cun et al. used a combination of STM and density functional theory (DFT) calculations to determine a modulus of *N,N′*-dihexadecylquinacridone, whose conjugated core is isosteric with pentacene, of 0.92 GPa.[207] It thus seems from these measurements that the newest generation of low-bandgap small-molecule semiconductors (which all bear pendant groups) would have significant deformability.

5.2. Solution-Processable Small Molecules

Our research group recently measured the mechanical properties (modulus and crack-onset strain) for several high-performance small-molecule organic semiconductors (Figure 17).[118] These materials were the electron donors SMDPPEH and DTS(FBTTh$_2$)$_2$ and the electron acceptors HPI-BT and PC$_{71}$BM. We also measured the mechanical properties of the donor:acceptor blends and determined the effect of additives (diiodooctane and polystyrene) on the properties of BHJ films of DTS(FBTTh$_2$)$_2$:PC$_{71}$BM. For all small-molecule films except PC$_{71}$BM, we found surprisingly low tensile moduli (<3 GPa) and high crack onset strains (>5%, and as high as 14.28% for DTS(FBTTh$_2$)$_2$).[118] We attributed the ability of these materials to accommodate such large plastic deformations to molecules sliding past each other in the solid films, facilitated by the presence of alkyl pendant groups. Blending the two donor materials with PC$_{71}$BM had the effect of increasing the modulus and lowering the crack-onset strain, which was also observed in polymer:fullerene BHJ films. While blending of the two donor materials with HPI-BT produced compliant (<1 GPa) and ductile (7−12% strain) films, they were not efficient (*PCE* < 1%), though there are potentially many alternative nonfullerene acceptors. The deformability of DTS(FBTTh$_2$)$_2$:PC$_{71}$BM films could be increased somewhat to a maximum of 4.67% strain with a corresponding modulus of 12.5 GPa using diiodocotane and polystyrene with a molecular weight of 900 kDa.[118] While the extensibility of DTS(FBTTh$_2$)$_2$ is promising for some applications, more work is required to understand the molecular mechanisms for the accommodation of strain without cracking.

5.3. Fullerenes and Soluble Fullerenes

By far the most common electron-transporting materials in organic electronics are fullerenes. These materials have the advantage of high electron mobilities and solubilities when appropriately derivatized, as in the methanofullerene PC$_{61}$BM. In solar cells, soluble fullerenes often adopt a ternary morphology with conjugated polymers—comprising fullerene-rich, polymer-rich, and mixed phases—that are beneficial for charge separation.[44,47,208,209] Unfortunately, solid films of pure methanofullerenes such as PC$_{61}$BM and PC$_{71}$BM have high moduli and crack at low strains.[142] For example, pure films of PC$_{61}$BM were measured to have a tensile modulus of 25.6 GPa, and a crack-onset strain of 3.5%.[142] Owing to its oblong shape and the fact that it exists as a mixture of isomers, films of PC$_{71}$BM are more deformable (modulus of 5.39 GPa and crack-onset strain of 5.25%).[142] Given the observation that some disorder may actually be beneficial for lowering the modulus and increasing the extensibility, we tested the hypothesis that blending PC$_{61}$BM with PC$_{71}$BM would produce films with increased deformability compared to pure films of either material. This outcome would be beneficial for an additional reason in that "technical grades" of methanofullerenes, which are incompletely separated (but otherwise pure) blends of the two materials, are less processed than the pure fullerenes and therefore have a lower embodied energy and reduced cost.[142] Indeed, the maximum extensibility (14.7%) was achieved for a 1:1 mixture, and the lowest modulus (5.13 GPa) was achieved for a technical grade comprising 93.5% PC$_{71}$BM and the remainder PC$_{61}$BM.[142] We attributed the increased deformability of the blends to void space created by inefficient packing of dissimilar molecules. While the mechanical properties of films of pure fullerenes and their derivatives are not favorable, blending can recover some deformability.

6. COMPOSITE SYSTEMS

This section describes the mechanical properties of blends of polymers, and of polymers with small molecules. The importance of composite films is exemplified by the bulk heterojunction, e.g., blends of conjugated polymers with methanofullerenes, used in organic solar cells.[210,211] Composite structures introduce additional challenges and constraints to the goal of maximizing the deformability of the active layers without sacrificing electronic performance. Some small molecules behave as plasticizers in a polymeric matrix; others behave as antiplasticizers. In fact, the stiffening and embrittling effects of fillers can have multiple origins. The details of molecular recognition (i.e., whether or not a small molecule intercalates in a regular way between the side chains of a polymer[117,212,213]) also have an effect on the mechanical properties of the bulk structure.[214] This section describes the molecular and microstructural bases for the mechanical properties of composite films compared to those of the pure components. To avoid repetition, interested readers are referred to the discussion of composite systems comprising two small molecules in section 5.2.

6.1. Polymer:Fullerene (Bulk Heterojunction) Composites

One of the most well-known classes of organic electronic devices is the organic solar cell (OSC).[215] The active layer of an OSC comprises an electron-donating material and an electron-accepting material. In the vast majority of devices, the donor is a semiconducting polymer and the acceptor is a methanofullerene (e.g., PC$_{61}$BM), which can be present in amounts as great as 80%, by weight.[216] The mechanical properties of the methanofullerene thus have a strong effect on the deformability of the composite film, called the bulk heterojunction (BHJ).[34,109] The current model for the solid structure of the BHJ for many systems of polymers and fullerenes (exemplified by P3AT:PCBM) comprises three phases: an ordered polymer phase, a fullerene-rich phase, and a mixed phase.[45] Methanofullerenes in general behave as antiplasticizers for conjugated polymers.[142] That is, they increase the glass transition temperature of the blend, increase the elastic modulus, and decrease the crack-onset strain.[133,142]

The effect on the mechanical behavior can be predicted using a simple composite theory first applied to the bulk heterojunction by Khang and co-workers.[109] This theory requires knowledge of the mechanical properties of the filler itself, in this case, the methanofullerene. As we have seen in section 5.3, the mechanical properties of pure methanofullerenes vary on the basis of the size and shape of the fullerene, e.g., films of PC$_{71}$BM are more deformable than PC$_{61}$BM, and also by the extent of separation between fullerenes of different sizes and shapes. That is, deformability is maximized with some intermediate combination of PC$_{71}$BM and PC$_{61}$BM, which can be obtained naturally in an incompletely separated sample, so-called "technical grade" material.[142] The mechanical properties of the pure films thus

DOI: 10.1021/acs.chemrev.7b00003
Chem. Rev. 2017, 117, 6467−6499

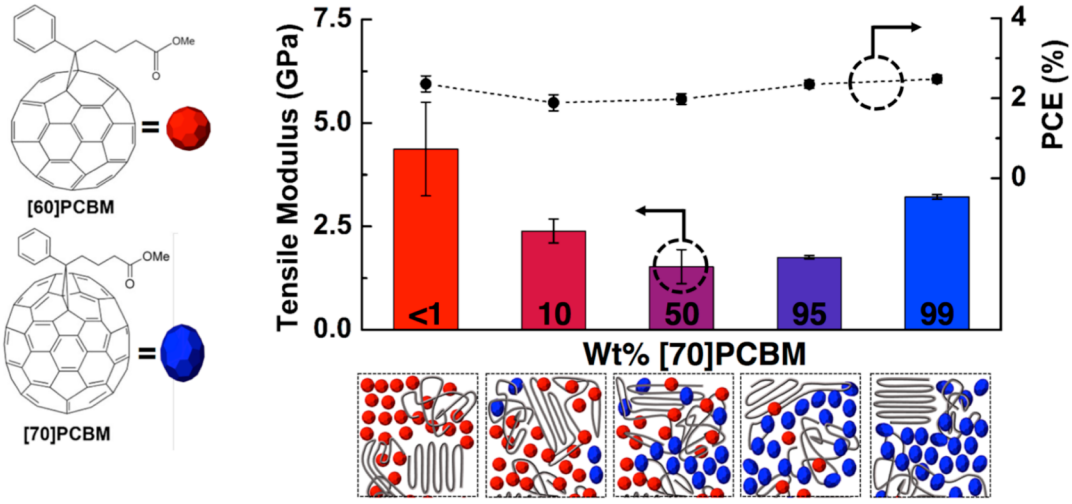

Figure 18. Tensile modulus and power conversion efficiency of P3HT:PCBM blends with different weight fractions of $PC_{71}BM$. Reproduced with permission from ref 142. Copyright 2015, American Chemical Society.

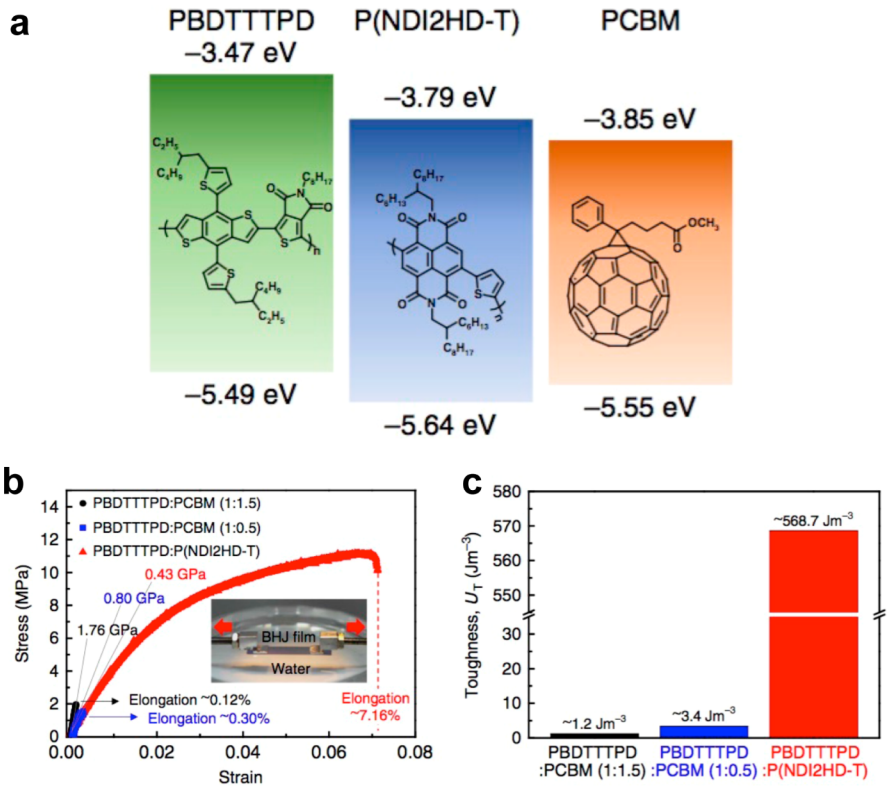

Figure 19. All-polymer stretchable solar cells. (a) Chemical structures of PBDTTTPD, P(NDI2HD-T), and $PC_{61}BM$, along with the positions of their frontier molecular orbitals. (b) Stress–strain behavior of the bulk heterojunction composites obtained by the film-on-water method. The all-polymer blend had the lowest modulus and the greatest extensibility. (c) Toughness of the bulk heterojunction blends, again, greatest for the all-polymer blend. Reproduced with permission from ref 111. Copyright 2015, Nature Publishing Group.

influence the mechanical properties of the BHJ and even the microstructure of the polymeric phase. Analysis of the UV–vis spectra of P3HT with different blends of methanofullerenes, ranging from pure $PC_{61}BM$ to pure $PC_{71}BM$, showed that technical grades of $PC_{71}BM$ (which were 6.5% $PC_{61}BM$) had a favorable combination of deformability and power conversion efficiency (PCE). Interestingly, analysis of the UV–vis spectra of these BHJ films using the weakly interacting H-aggregate model revealed that the order in the polymer phase was correlated with order in the fullerene phase (Figure 18).[142] It is possible that reduced order in the polymer phase allowed recruiting of polymer chains from the polymer crystallites into the disordered mixed phase because of the partial miscibility of the fullerene and amorphous polymer. Increased deformability for BHJs comprising incompletely separated fullerenes may thus arise from two effects: inefficiently packed fullerene in the fullerene-rich phases and reduced aggregation of the polymer phases. The net effect of the fullerenes on the mechanical properties of the BHJ is still nonetheless deleterious, and these effects amount to one of the reasons that the research community is seeking nonfullerene

DOI: 10.1021/acs.chemrev.7b00003
Chem. Rev. 2017, 117, 6467–6499

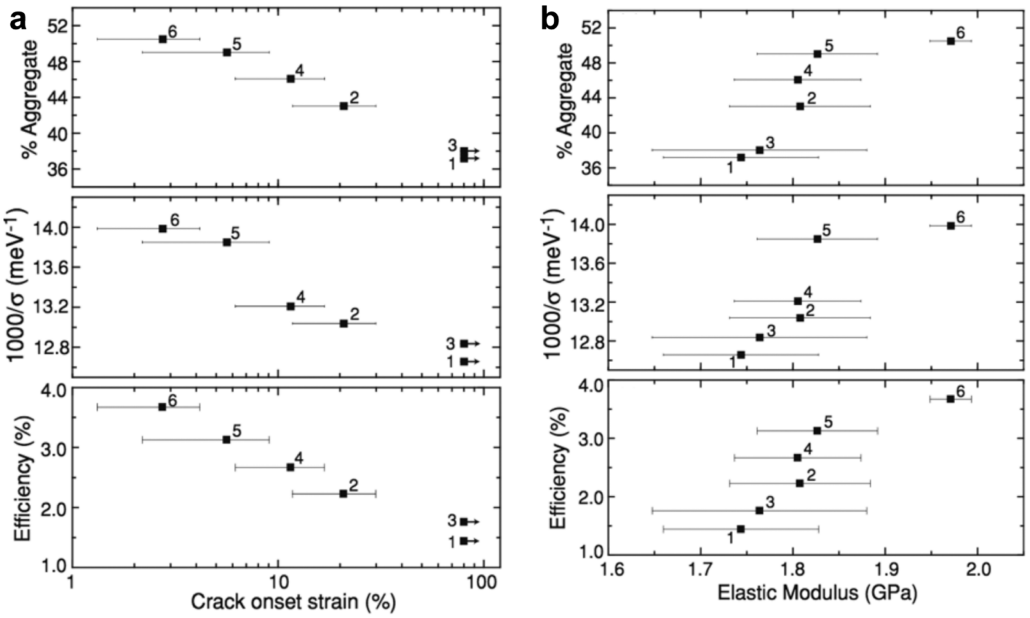

Figure 20. Correlations between mechanical properties, photovoltaic efficiency, and solid-state ordering. Percent aggregate, order parameter ($100/\sigma$, where σ is the Gaussian line width), and efficiency vs extensibility (left) and elastic modulus (right) for P3HT:$PC_{61}BM$ blends processed using a combination of spin-coating speed and concentration to produce BHJ films with different degrees of ordering of the polymer phase. Reproduced with permission from ref 30. Copyright 2013, Wiley-VCH Verlag GmbH & Co. KGaA.

acceptors (NFAs),[217] some of which have achieved performance equal to that of fullerenes in solar cells.[218] As of this writing, the mechanical properties of polymer:NFA BHJs have not been explored extensively.

6.2. Polymer:Polymer Composites

The favorability of the mechanical properties of polymeric materials derive from their high degrees of polymerization, which facilitates coordination of many van der Waals interactions along adjacent molecules, along with entanglements. It is thus reasonable that using an all-polymer blend would lead to a significantly more deformable semiconducting composite, i.e., for solar cells, than one in which one of the components was a small molecule. The Kim group recently described the mechanical properties of a blend of PBDTTTPD (donor) and P(NDI2HD-T) (acceptor) for an intrinsically stretchable solar cell, and measured the mechanical properties of the blend using the film-on-water method.[111] The all-polymer active layer exhibited a maximum extensibility of 7.2% and tensile modulus of 0.43 GPa, compared to 0.12% and 1.76 GPa for the PBDTTTPD:$PC_{61}BM$ film (Figure 19).[111] Moreover, the blend containing $PC_{61}BM$ exhibited high brittleness.

Blends of polymers have also been investigated as a means to improve the extensibility of organic semiconductors for transistor applications. The O'Connor group recently reported a new composite design strategy in which a brittle high performance donor−acceptor polymer (PCDTPT) was blended with a more ductile semiconducting polymer (P3HT) to improve extensibility without sacrificing the charge-transport characteristics.[219] When supported by an elastomeric substrate, the composite was shown to reversibly orient and relax under large tensile strains up to 75% and up to 100 strain cycles. When subsequently transferred to a rigid test bed, the film was shown to exhibit high charge-carrier mobility in both unstrained and strained states. The high mobility was attributed to vertical phase segregation of PCDTPT toward the interface with the gate dielectric.[219]

7. EFFECT OF MICROSTRUCTURE AND MORPHOLOGY

The solid-state packing structure has a large influence on the mechanical properties of an organic semiconductor. The microstructure and morphology is, in turn, strongly influenced by the processing conditions, e.g., solvent used, kinetics of solidification, and postdeposition treatment. In many cases, the molecular structure plays a subordinate role to the solid-state microstructure. Indeed, the ease with which the mechanical properties can be manipulated by the conditions of processing suggests that in some cases, the most important role of the molecular structure is to influence self-aggregation in solution and packing in the solid state. Results of MD simulations from which one can derive similar conclusions are discussed in section 3.3.

7.1. Correlation of Mechanical Properties with Aggregation

Spectroscopic and micrographic tools have been used to correlate solid structure to mechanical properties. For example, O'Connor and co-workers have used the weakly interacting H-aggregate model, originally developed by Spano and co-workers,[29] to correlate the order present in P3HT and P3HT:PCBM films to the stiffness and ductility (Figure 20).[30] In particular, when the UV−vis spectra are deconvoluted into signals originating from vibronic transitions of aggregated material and amorphous material, spectra with the greatest aggregated fraction are associated with the stiffest and least extensible films. The aggregated fraction, and hence the mechanical properties, can be controlled using the rate of solvent evaporation. Our group employed the weakly interacting H-aggregate model in our studies on the effects of mixed ratios of side chains in P3ATs,[134] the purity of the fullerene component,[142] cyclic loading and fatigue,[161] and the role of interdigitation of side chains and intercalation of small molecules.[214]

While the electronic properties of the most deformable films generated by manipulating the processing conditions were generally inferior to those of the stiffer films,[30] Awartani et al. was

DOI: 10.1021/acs.chemrev.7b00003
Chem. Rev. 2017, 117, 6467−6499

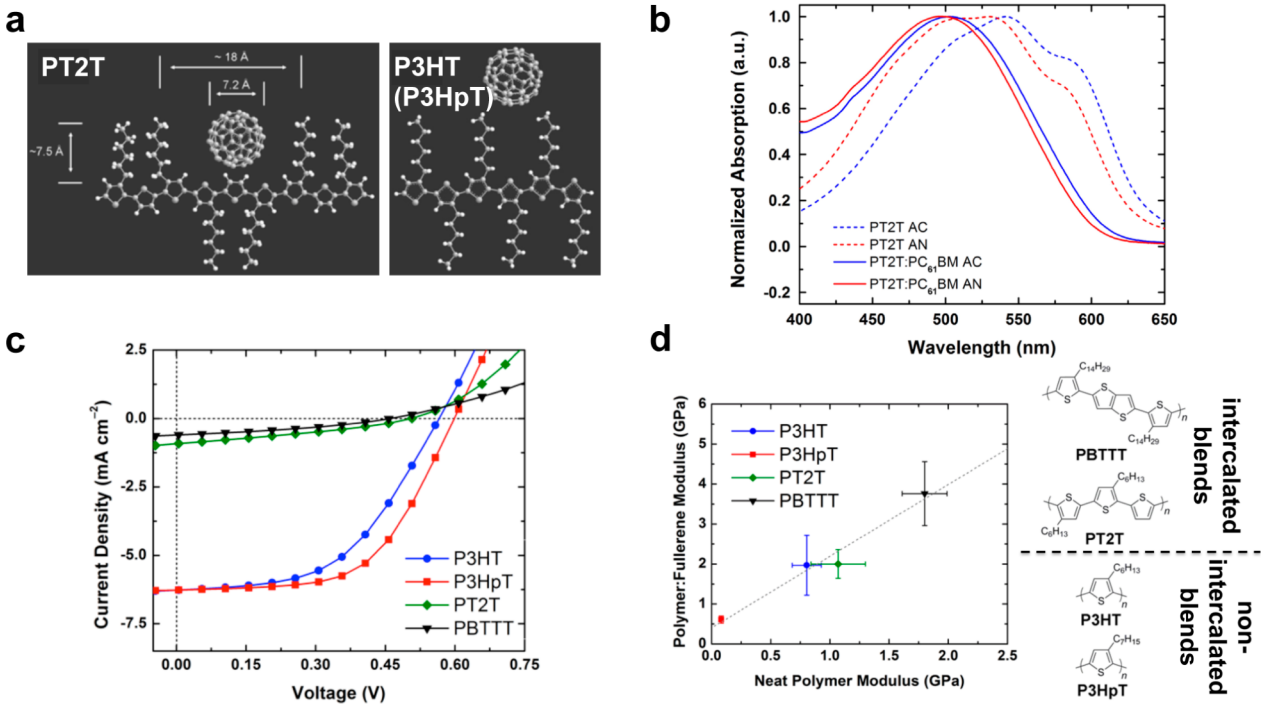

Figure 21. Effects of intercalation on the mechanical properties of semiconducting polymers. (a) Structures of the poly(terthiophene) PT2T and P3HT showing intercalation and nonintercalation. Reproduced with permission from ref 224. Copyright 2007, Wiley-VCH Verlag, GmbH & Co. KGaA. (b) UV−vis spectra of pure PT2T as-cast and annealed and PT2T:$PC_{61}BM$ as-cast and annealed. (c) Current−voltage characteristics for 1:1 bulk heterojunction blends of P3HT, P3HpT, PT2T, and PBTTT with $PC_{61}BM$. (d) Plot of the modulus of the BHJ blend vs the modulus of the neat polymer, which shows that the modulus of the blend depends linearly on the modulus of the neat polymer, independent of the details of the packing structure. Reproduced with permission from ref 214. Copyright 2015, Elsevier.

nevertheless able to use films with low levels of local order to make polarization-dependent organic photodetectors in which the active layer could be stretched by 100% without fracturing.[148] Birefringent absorption in these films was the result of strain-alignment of polymer chains. In addition to aligning of the main axis of the polymer chains along the strained direction, stretching can also produce changes in texture. Indeed, partial reorientation of P3HT chains from predominantly edge-on to partially face-on has been observed under both uniaxial[151] and biaxial tension.[149]

7.2. Interdigitation of Side Chains

In most semiconducting polymers, the lamellar stacking axis, along which the side chains are oriented, shows that the side chains are arranged end-to-end; that is, they do not interdigitate. In the case of decreased attachment density of the side chains, however, or under the right conditions of processing, it is possible for the side chains to interdigitate.[220−222] Polymers exhibiting interdigitation, e.g., PBTTT, often exhibit highly crystalline microstructures, with highly developed vibronic peaks by UV−vis, which are indicative of H-aggregates. The interdigitated microstructural motif is indicated by a shortening of the lamellar reflection by grazing-incidence X-ray scattering (GIXS). As Cates-Miller et al. have shown, interdigitation can be disrupted by the intercalation of fullerenes (and perhaps other molecules) between the side chains of the polymers, which decreases the scattering angle (i.e., indicates a larger distance) of the lamellar reflection.[117,212] While stereotypically noninterdigitated, the side chains of P3HT will interdigitate in samples with low degrees of polymerization ($i \leq 36$)[220] or if treated with the vapor of carbon disulfide.[223] The interdigitated structure of P3HT, called "form II", was remarked to have brittle mechanical properties, though these were not quantified.[220]

7.3. Intercalation of Fullerenes and Small Molecules

When semiconducting polymers with low attachment density of side chains are blended with fullerenes or small molecules, intercalation of these small molecules along the polymer backbone can occur.[212] Depending on the relative size of the small molecule and the free volume available between the side chains, this intercalation can either prevent polymer crystallization or produce bimolecular crystallites.[212] As an example, the polymers PT2T and PBTTT (Figure 21a), both of which allowed intercalation of the fullerenes, were inspected by UV−vis spectroscopy (Figure 21b).[214] The spectra of the neat polymers showed vibronic peaks indicative of aggregation; upon the addition of fullerene, the vibronic peaks completely disappeared in the PT2T spectrum indicating disruption of polymer ordering, yet remained in the PBTTT spectrum; the retention of these peaks hinted at bimolecular crystallization, which degrades the photovoltaic performance at low loadings of fullerenes because the bicontinuity of the blend is destroyed (Figure 21c).[214] These observations were attributed to differences in the molecular structures of the polymers. PT2T is a poly(terthiophene) with a similar structure to P3HT,[224] except every third thiophene is without a side-chain, and the 3-alkylthiophenes are tail-to-tail coupled rather than head-to-tail. This molecular structure created a large enough free volume between side-chains for fullerene to intercalate, however, the spacing was still relatively small and the cofacial π-stacking—and likely the lamellar stacking—was disrupted.[224] Conversely, PBTTT, which has a larger distance between side-chains due to the thienothiophene spacer, was able to accommodate intercalation of fullerenes without the disruption of aggregation.[225] When the tensile moduli of these polymers and their blends with fullerene were

DOI: 10.1021/acs.chemrev.7b00003
Chem. Rev. 2017, 117, 6467−6499

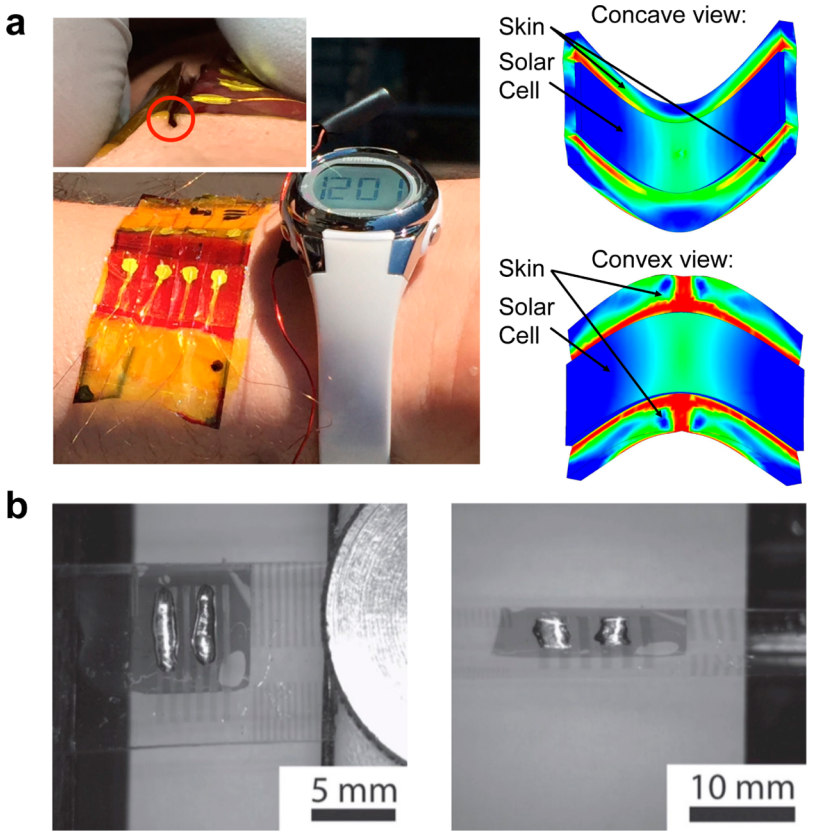

Figure 22. Examples of intrinsically deformable devices. (a) A skin-wearable solar cell capable of surviving 1000 cycles of compression, which produced bending radii of ~100 μm, as indicated in the finite-element model shown. Reproduced with permission from ref 145. Copyright 2015, Elsevier. (b) A stretchable organic thin-film transistor using carbon nanotube electrodes. Reproduced with permission from ref 39. Copyright 2014, Wiley-VCH Verlag, GmbH & Co. KGaA.

compared to P3HT and P3HpT, we found the surprising result that the moduli of the blends were linearly correlated with the moduli of the neat polymer (Figure 21d).[214] This observation suggested that—at least for polythiophenes—the tensile modulus of polymer:fullerene blends was dominated by the same molecular interactions that determined the tensile modulus in the neat polymers rather than the extent of molecular mixing.

8. INTRINSICALLY DEFORMABLE ORGANIC DEVICES

While the focus of this review is on chemical physical parameters that determine the ability of organic solids to store or absorb strain energy, the ultimate goal of researchers in the field of organic electronics is to construct useful devices (Figure 22).[226,5,227] This section describes examples of whole organic devices that have the characteristic that the active layer accommodates significant (≥10%) deformation intrinsically. This criterion is strict in that it requires each component—substrate, electrodes, and active materials—to accommodate strain. Examples of intrinsically deformable devices include solar cells (Figure 22a),[111,159,228] light-emitting devices,[9,146,229] thin-film transistors (Figure 22b),[39,145,230] and biosensors.[13,231] We find that in devices with the greatest performance, the choice of materials was made with regard to the molecular structures and solid-state packing structures that were known to produce the greatest deformability.

8.1. Solar Cells

The organic electronic device for which the greatest amount of effort has been spent to increase its deformability is the solar cell.[42] Truly deformable organic solar cells would be beneficial for three reasons. First, the ability of multilayer modules to survive the rigors of roll-to-roll coating would increase the attractiveness of solution-based printing.[12,23,40,108,232] Second, the use of mechanically robust active materials would reduce the burden on the substrate and encapsulant[37] to supply the mechanical stability, and it would thus be possible to reduce the thickness of these layers.[38] (The substrate and the encapsulant presently account for the greatest fraction of the cost and embodied energy of organic solar modules.[233,234]) Moreover, reduction in the weight of solar modules by using ultrathin substrates would reduce the cost of support racks and thus the so-called balance-of-system costs. Third, deformable organic semiconductors would increase the lifetime of devices in both portable applications[235] and in the outdoor environment,[11] where modules must be stable against the forces of the environment.

The first stretchable organic solar cell was not intrinsically stretchable; rather it used microscale wrinkles to accommodate strain.[159] This device was rendered stretchable by spin-coating the layers on a PDMS substrate prestrained by up to 30%. Upon release of the prestrain, the stiff active materials buckled. The active layer used (P3HT and $PC_{61}BM$) was stiff and brittle, and cracked readily when the device was stretched beyond the level of the prestrain.[159] Kaltenbrunner et al. used a similar approach to make stretchable solar cells on ultrathin poly(ethylene terephthalate) (PET) foil.[38] The first report of stretchable solar cells using intrinsically stretchable organic components (except for the cathode, which was the inorganic liquid eutectic gallium–indium) compared the evolution in photovoltaic

DOI: 10.1021/acs.chemrev.7b00003
Chem. Rev. 2017, 117, 6467–6499

properties of cells with active layers of both P3HT:$PC_{61}BM$ and DPPT-TT:$PC_{61}BM$.[158] The DPP-based polymer exhibited larger extensibilities in part because of the large, branched alkyl side chain.[158] The effect of side chains in stretchable solar cells was later found to be critical, and a direct comparison of P3HT and P3DDT containing bulk heterojunctions revealed highly stretchable behavior in uniaxially deformed cells.[34]

Biaxial stretchability for bonding to hemispherical substrates at room temperature was demonstrated using P3OT, owing to its low T_g.[147] This report was unique at the time in its use of an inverted architecture, which had PEDOT:PSS as a transparent anode (top contact in the inverted architecture) and PEDOT:PSS treated with poly(ethylenimine) (PEI) as the transparent cathode (bottom contact). The stretchability of solar cells could be further enhanced using a stretchable encapsulant, e.g., thermoplastic polyurethane, as was demonstrated by Sawyer et al. in the first "all-rubber" solar cell, which was composed of components that were entirely elastomeric (except for the $PC_{61}BM$).[37] In the absence of the encapsulant, strain is concentrated to thin areas and defects in the active film, and it thus cracks at strains smaller than would be observed for a mathematically uniform film. The ultimate extensibility of these devices was limited by the use of methanofullerenes as electron acceptors, which embrittle the films.[142] To avoid the embrittling effects of methanofullerenes on the mechanical properties of semiconducting polymers, all-polymer active layers can be employed. To this end, Kim and coworkers fabricated cells with active layers consisting entirely of polymers, which was the highest performing stretchable organic solar cell produced to date.[111] In order for these extraordinarily robust and compliant devices to have an impact in portable and outdoor applications, however, stretchable substrates and encapsulants must be developed that have impermeability to water vapor and oxygen.

8.2. Light-Emitting Devices

The arguments in favor of intrinsically highly deformable organic light-emitting devices (OLEDs) are largely similar as they are for organic solar cells: displays based on organic materials could be fabricated at low cost by printing, as could inexpensive panels for solid-state lighting. Rollable, foldable, portable, lightweight, and mechanically robust displays would be useful in consumer electronics devices, along with military and disaster relief applications. The first example of a stretchable organic light-emitting device was described by Someya and co-workers.[79] These authors used stretchable composite materials based on carbon nanotubes to provide electrical connections in a stretchable active matrix display. In this case, however, the emissive organic semiconductors were not deformable. The first intrinsically stretchable organic light-emitting device, and perhaps the first intrinsically stretchable organic electronic device of any kind, was an organic light-emitting electrochemical device produced by Pei and co-workers.[9] The authors demonstrated the ability to shape this device with heating. The electrodes that enabled this technology were based on silver nanowires in an early demonstration,[146] and later carbon nanotubes.[215] The blue emissive polymer used was PF-B, a polyfluorene copolymer. This structure has long alkyl side chains, which is consistent with the level of deformability possible, and was also mixed with the ionic conductor poly(ethylene oxide)dimethacrylate ether (PEO−DMA) and lithium trifluoromethanesulfonate (LiTf). It is likely that the ionic conductive polymer behaved as a plasticizer, though the authors did not investigate the mechanical properties of the emissive layer. The authors later showed a yellow emissive device using the poly(phenylenevinylene) (PPV) derivative "super yellow", which achieved impressive extensabilities of 120%.[236] An ultraflexible device was demonstrated by White et al. using the paradigm of ultrathin substrates previously demonstrated by the same laboratories for organic solar cells.[7]

8.3. Thin-Film Transistors

Perhaps the most fundamental organic electronic device is the thin-film transistor (OTFT),[52] because of its practical importance as well as its usefulness in establishing charge-transport characteristics of materials.[132] Several approaches have appeared in the literature whose goals have been to impart stretchability to OTFTs.[237] An advantage to mechanical deformability for OTFTs is the ability to pattern devices directly on flexible and stretchable substrates without the need for complex, patterned interconnects and relief features.[13] For example, the Bettinger laboratory used the buckled, wavy approach to generate the first stretchable OTFT,[238] while Chortos et al. showed that the cracks in the channel layer produced by stretching in P3HT devices were not sufficient to destroy charge transport.[39] Other composite approaches based on conjugated polymer nanofibers[239−241] have also been used, but the intrinsic deformability of the semiconductor is masked in cases where a stiff material is cast into a nanofiber. Goffri et al. reported a multicomponent design strategy in which the semiconducting polymer is mixed with a commodity semicrystalline polymer to obtain vertically stratified structures in a one step process. They found that the fraction of semiconducting polymer could be reduced to as low as 3 wt % without any degradation in device performance. It can be expected that the mechanical properties of this composite system would be dominated by the semicrystalline commodity polymer, however, no mechanical characterization was performed.[242]

Approaches toward intrinsically stretchable OTFTs have their roots in measurement of the effects of strain on charge-transport properties of flexible devices.[151] Early work by Someya elucidated the effect of mechanical strain on the charge-transport properties of small molecular semiconductors.[83] Among the authors findings were the importance of compressive strain on decreasing the intermolecular separation and hence increasing the charge-carrier mobility.[83] In a later study, Sokolov et al. introduced the metric of mobility factor, $F_M = \Delta\%\mu/\%\text{strain}$, which quantifies the relationship between mobility and strain.[243] In experiments on flexible transistors under tensile and compressive strain, the authors uncovered an important role of strain on the strain-evolved surface energy of the dielectric layer, which depending on the materials selected for the device produced a value of F_M that was either positive or negative.[243] The effects of strain could be mitigated by using an inorganic dielectric layer bearing a dense alkyl monolayer.

It has long been known that stretched films of conjugated polymers exhibit anisotropic charge transport, with the most facile direction being parallel to the stretched axis.[152] The microstructural rationale is alignment of chains,[152] which has been confirmed by X-ray diffraction,[149,151] by birefringent absorption by UV−vis,[148] and by molecular dynamics simulations.[130] The Bao laboratory used a method based on soft contact lamination and delamination to measure the hole mobility of conjugated polymers,[244] which, though not a device, will be a useful tool for the efficient determination of the effect of strain on the transport properties of organic semiconductors. One of the most successful examples of an intrinsically

DOI: 10.1021/acs.chemrev.7b00003
Chem. Rev. 2017, 117, 6467−6499

stretchable semiconductive polymer for TFT applications was that of Wu et al., who used an isoindigo-based donor−acceptor polymer bearing long, branched carbosilane side chains to achieve mobilities ≥1 $cm^2 V^{-1} s^{-1}$ even at strains as large as 60%.[107] Jeong and co-workers comprehensively reviewed approaches to generating active layers for deformable transistors.[237]

8.4. Biosensors

Integration of π-conjugated materials with biological systems, "organic bioelectronics",[99] requires seamless interfaces between devices and the biological milieu.[231] In the case of wearable devices, materials must accommodate the natural stretchability of the skin,[245] which extends by 30% or more, depending on the location and axis of strain.[246] Low stiffness, i.e., the combination of low thickness with low tensile modulus, would permit a strong chemical interface, which would be required for the detection of biological signals.[13] One of the advantages of stretchable thin-film and patch-like devices is imperceptibility by the user.[13] This attribute, sometimes called "mechanical invisibility", would lower the barriers to use and increase compliance of patients and the willingness of other users to adopt these wearable technologies.[3] Work on ultraflexible and stretchable devices using intrinsically deformable organic semiconductors is still in its early stages, but several proof-of-concept devices have been demonstrated.

Using ultrathin (1.4 μm) plastic foils, Kaltenbrunner et al. showed extraordinary bending stability of OTFTs for eventual use in "imperceptible" biological applications.[13] Schwartz et al. combined an organic transistor with a microstructured compressible gate dielectric in a flexible OTFT that was sufficiently sensitive to measure the pulse pressure waveform of the human radial artery.[247] Malliaras and co-workers have used the organic electrochemical transistor (OECT) for a variety of wearable devices for healthcare.[99] For example, PEDOT:PSS can be use to transduce electrical signals from the cardiac cycle (electrocardiography, ECG), eye movements (electrooculography, EOG), and neurological rhythms (electroencephalography, EEG).[98,199,248] Small electrical potentials drive ions in and out of the PEDOT:PSS channel to modulate the conductivity.[98] The mechanical interfaces in this type of device are unexplored, though typical formulations of PEDOT:PSS tend to be brittle.[104] While PEDOT:PSS is not a semiconductor, it is widely used for neural interfacing as exemplified by the work of Martin and co-workers.[198,249]

9. CONCLUSIONS AND OUTLOOK

Mechanical deformability is the property that enables essentially all advantages of organic electronic materials. Printed organic solar cells, light-emitting devices, thin-film transistors, and radio frequency identification tags must survive the rigors of roll-to-roll coating and also the mechanical insults of portable applications and the outdoor environment. Furthermore, organic bioelectronic devices must conform to the skin or the surfaces of internal organs to transduce biochemical signals; without a conformal mechanical interface, however, there can be no chemical interface. Achieving mechanical robustness in thin film devices is tantamount to minimizing the elastic modulus, increasing the toughness, elastic range, ductility, or other mechanical properties, depending on the application and the expected modes of deformation. These mechanical properties depend on molecular structure and the ways that these structures pack in solid films.

While molecular structure plays a role in determining the mechanical properties of a film, e.g., the size of side chains for a given attachment density is a good predictor of softness, the influence of molecular structure manifests strongly in its effect on structure in the solid state. Indeed, a recurring finding is the influence of how processing conditions influence mechanical properties. The conditions of spin coating can, for example, influence ordering and degree of crystallinity in a thin film. Self-aggregation in solution may produce kinetically trapped films upon solidification that exhibit a density of entanglements that is not ideal for applications intended to be robust. Interdigitation of side chains can produce stiffer and more brittle films. A complete understanding of the mechanical properties of π-conjugated materials must include expectations about how a given molecular structure will assemble in solution and then in the solid state.

The challenges of measuring the mechanical properties of delicate thin films of organic semiconductors have led to the development of metrological techniques with broad applicability to other types of thin solid films. For example, the film-on-elastomer and film-on-water methods can be readily applied to films of other technologically important polymers, such as optical coatings, photoresists, paints, and scratch-resistant layers. One aspect of organic semiconductors that is still poorly understood is time-dependent mechanical behavior. In order to understand the ways in which the microstructure of an organic semiconductor evolves over time when strained, i.e., creep, experiments should be designed specifically for thin films to anticipate these effects.

Organic semiconductor devices are already commercial in the form of large-area ultrahigh-definition display panels. Whether or not organic electronics meet their expectations in the areas of large-area solar panels or biosensors, it seems likely that at least some of these applications will be realized eventually. In the near term, we expect that a deeper knowledge of the mechanical properties of these materials will facilitate production of flexible devices on thin plastic foil, and enable their long-term reliability against mechanical and theromomechanical deformations. In the long term, work directed toward understanding and improving the thermomechanical properties of these materials may suggest ways in which other properties might be brought about that are reminiscent of biological materials, including biodegradability and self-repair. Thus, π-conjugated materials could more fully embody colloquial meanings of "organic" and "plastic", by which they are often referred.

AUTHOR INFORMATION

Corresponding Author

*E-mail: dlipomi@eng.ucsd.edu.

ORCID

Darren J. Lipomi: 0000-0002-5808-7765

Notes

The authors declare no competing financial interest.

Biographies

Samuel E. Root earned his undergraduate degree in chemical engineering from the University of Rochester in 2014. He is currently a Ph.D. student in chemical engineering under the supervision of Prof. Darren Lipomi at UC San Diego, where his research focuses on the theoretical aspects of the mechanical properties of organic semiconductors. He has developed computational molecular dynamics approaches to predicting the mechanical properties of polythiophenes and low-bandgap semiconducting polymers. In 2016, he received the Achievement Reward for College Scientists.

DOI: 10.1021/acs.chemrev.7b00003
Chem. Rev. 2017, 117, 6467−6499

Suchol Savagatrup received his B.S. in chemical engineering from the University of California, Berkeley in 2012, where he conducted research with Prof. Rachel Segalman in the Department of Chemical and Biomolecular Engineering and Dr. Adam Weber at Lawrence Berkeley National Laboratory. He completed his Ph.D. in 2016 at the University of California, San Diego, under the direction of Prof. Darren Lipomi where his work was funded by the NSF Graduate Research Fellowship Program. He is currently a postdoctoral scholar at the Massachusetts Institute of Technology.

Adam D. Printz earned his B.S. in finance from the University of Maryland and his Ph.D. in nanoengineering from the University of California, San Diego, in 2015, under the supervision of Prof. Darren Lipomi. His Ph.D. research focused on the microstructure of organic semiconductors and its effects on the mechanical properties of polymer and bulk heterojunction thin films. In 2016, he was the recipient of the Chancellor's Dissertation Medal, the highest award given to Ph.D. graduates in the Jacobs School of Engineering. Adam is now a postdoctoral scholar at Stanford University.

Daniel Rodriquez received his B.S. in nanoengineering from the University of California, San Diego in 2014. He is a U.S. Navy veteran who served five years and used the Post 9/11 GI Bill to fund his education. As an undergraduate he was a recipient of the Initiative for Maximizing Student Development fellowship. He is currently a Ph.D. student at the University of California, San Diego where he conducts research under Prof. Darren Lipomi on flexible organic electronics and is supported by the NSF Graduate Research Fellowship.

Darren J. Lipomi earned his undergraduate degree in chemistry from Boston University in 2005, and his Ph.D. at Harvard University in 2010, with Prof. George M. Whitesides. From 2010−2012, he was a postdoctoral fellow in the laboratory of Prof. Zhenan Bao at Stanford University. He began his independent position at UC San Diego in 2012 and is now an associate professor in the Department of Nano-Engineering. He is the recipient of the AFOSR Young Investigator Award and the NIH Director's New Innovator Award.

ACKNOWLEDGMENTS

This work was supported by a grant from the Air Force Office of Scientific Research Grant No. FA9550-16-1-0220. S.S. and D.A. were supported in part by the Graduate Research Fellowship Program of the National Science Foundation (DGE-1144086).

REFERENCES

(1) Kagan, C. R.; Fernandez, L. E.; Gogotsi, Y.; Hammond, P. T.; Hersam, M. C.; Nel, A. E.; Penner, R. M.; Willson, C. G.; Weiss, P. S. Nano Day: Celebrating the Next Decade of Nanoscience and Nanotechnology. *ACS Nano* **2016**, *10*, 9093−9103.
(2) Willson, C. G.; Roman, B. J. The Future of Lithography: Sematech Litho Forum 2008. *ACS Nano* **2008**, *2*, 1323−1328.
(3) Kim, D. H.; Lu, N. S.; Ma, R.; Kim, Y. S.; Kim, R. H.; Wang, S. D.; Wu, J.; Won, S. M.; Tao, H.; Islam, A.; et al. Epidermal Electronics. *Science* **2011**, *333*, 838−843.
(4) Bauer, S.; Bauer-Gogonea, S.; Graz, I.; Kaltenbrunner, M.; Keplinger, C.; Schwodiauer, R. 25th Anniversary Article: A Soft Future: From Robots and Sensor Skin to Energy Harvesters. *Adv. Mater.* **2014**, *26*, 149−162.
(5) Savagatrup, S.; Printz, A. D.; O'Connor, T. F.; Zaretski, A. V.; Lipomi, D. J. Molecularly Stretchable Electronics. *Chem. Mater.* **2014**, *26*, 3028−3041.
(6) Ying, M.; Bonifas, A. P.; Lu, N.; Su, Y. W.; Li, R.; Cheng, H. Y.; Ameen, A.; Huang, Y. G.; Rogers, J. A. Silicon Nanomembranes for Fingertip Electronics. *Nanotechnology* **2012**, *23*, 344004-1−344004-7.
(7) White, M. S.; Kaltenbrunner, M.; Glowacki, E. D.; Gutnichenko, K.; Kettlgruber, G.; Graz, I.; Aazou, S.; Ulbricht, C.; Egbe, D. A. M.; Miron, M. C.; et al. Ultrathin, Highly Flexible and Stretchable Pleds. *Nat. Photonics* **2013**, *7*, 811−816.
(8) Lee, J.; Wu, J. A.; Shi, M. X.; Yoon, J.; Park, S. I.; Li, M.; Liu, Z. J.; Huang, Y. G.; Rogers, J. A. Stretchable Gaas Photovoltaics with Designs That Enable High Areal Coverage. *Adv. Mater.* **2011**, *23*, 986−991.
(9) Yu, Z. B.; Niu, X. F.; Liu, Z.; Pei, Q. B. Intrinsically Stretchable Polymer Light-Emitting Devices Using Carbon Nanotube-Polymer Composite Electrodes. *Adv. Mater.* **2011**, *23*, 3989−3994.
(10) Kim, R. H.; Kim, D. H.; Xiao, J. L.; Kim, B. H.; Park, S. I.; Panilaitis, B.; Ghaffari, R.; Yao, J. M.; Li, M.; Liu, Z. J.; et al. Waterproof AlInGaP Optoelectronics on Stretchable Substrates with Applications in Biomedicine and Robotics. *Nat. Mater.* **2010**, *9*, 929−937.
(11) Krebs, F. C.; Espinosa, N.; Hosel, M.; Sondergaard, R. R.; Jorgensen, M. 25th Anniversary Article: Rise to Power - Opv-Based Solar Parks. *Adv. Mater.* **2014**, *26*, 29−39.
(12) Galagan, Y.; Coenen, E. W. C.; Zimmermann, B.; Slooff, L. H.; Verhees, W. J. H.; Veenstra, S. C.; Kroon, J. M.; Jorgensen, M.; Krebs, F. C.; Andriessen, R. Scaling up ITO-Free Solar Cells. *Adv. Energy Mater.* **2014**, *4*, 1300498.
(13) Kaltenbrunner, M.; Sekitani, T.; Reeder, J.; Yokota, T.; Kuribara, K.; Tokuhara, T.; Drack, M.; Schwodiauer, R.; Graz, I.; Bauer-Gogonea, S.; et al. An Ultra-Lightweight Design for Imperceptible Plastic Electronics. *Nature* **2013**, *499*, 458−463.
(14) Yang, Z. B.; Deng, J.; Sun, X. M.; Li, H. P.; Peng, H. S. Stretchable, Wearable Dye-Sensitized Solar Cells. *Adv. Mater.* **2014**, *26*, 2643−2647.
(15) Kim, D. H.; Viventi, J.; Amsden, J. J.; Xiao, J. L.; Vigeland, L.; Kim, Y. S.; Blanco, J. A.; Panilaitis, B.; Frechette, E. S.; Contreras, D.; et al. Dissolvable Films of Silk Fibroin for Ultrathin Conformal Bio-Integrated Electronics. *Nat. Mater.* **2010**, *9*, 511−517.
(16) Fu, K. K.; Wang, Z. Y.; Dai, J. Q.; Carter, M.; Hu, L. B. Transient Electronics: Materials and Devices. *Chem. Mater.* **2016**, *28*, 3527−3539.
(17) Kim, D. H.; Ahn, J. H.; Choi, W. M.; Kim, H. S.; Kim, T. H.; Song, J. Z.; Huang, Y. G. Y.; Liu, Z. J.; Lu, C.; Rogers, J. A. Stretchable and Foldable Silicon Integrated Circuits. *Science* **2008**, *320*, 507−511.
(18) Suo, Z.; Ma, E. Y.; Gleskova, H.; Wagner, S. Mechanics of Rollable and Foldable Film-on-Foil Electronics. *Appl. Phys. Lett.* **1999**, *74*, 1177−1179.
(19) Lipomi, D. J. Stretchable Figures of Merit in Deformable Electronics. *Adv. Mater.* **2016**, *28*, 4180−4183.
(20) Peet, J.; Heeger, A. J.; Bazan, G. C. "Plastic" Solar Cells: Self-Assembly of Bulk Heterojunction Nanomaterials by Spontaneous Phase Separation. *Acc. Chem. Res.* **2009**, *42*, 1700−1708.
(21) Krebs, F. C.; Tromholt, T.; Jorgensen, M. Upscaling of Polymer Solar Cell Fabrication Using Full Roll-to-Roll Processing. *Nanoscale* **2010**, *2*, 873−886.
(22) Krebs, F. C.; Gevorgyan, S. A.; Alstrup, J. A Roll-to-Roll Process to Flexible Polymer Solar Cells: Model Studies, Manufacture and Operational Stability Studies. *J. Mater. Chem.* **2009**, *19*, 5442−5451.
(23) Krebs, F. C. All Solution Roll-to-Roll Processed Polymer Solar Cells Free from Indium-Tin-Oxide and Vacuum Coating Steps. *Org. Electron.* **2009**, *10*, 761−768.
(24) Muller, C.; Goffri, S.; Breiby, D. W.; Andreasen, J. W.; Chanzy, H. D.; Janssen, R. A. J.; Nielsen, M. M.; Radano, C. P.; Sirringhaus, H.; Smith, P.; et al. Tough, Semiconducting Polyethylene-Poly(3-Hexylthiophene) Diblock Copolymers. *Adv. Funct. Mater.* **2007**, *17*, 2674−2679.
(25) Tummala, N. R.; Bruner, C.; Risko, C.; Bredas, J. L.; Dauskardt, R. H. Molecular-Scale Understanding of Cohesion and Fracture in P3HT:Fullerene Blends. *ACS Appl. Mater. Interfaces* **2015**, *7*, 9957−9964.
(26) Bruner, C.; Dauskardt, R. H. Role of Molecular Weight on the Mechanical Device Properties of Organic Polymer Solar Cells. *Macromolecules* **2014**, *47*, 1117−1121.
(27) Brand, V.; Bruner, C.; Dauskardt, R. H. Cohesion and Device Reliability in Organic Bulk Heterojunction Photovoltaic Cells. *Sol. Energy Mater. Sol. Cells* **2012**, *99*, 182−189.
(28) Savagatrup, S.; Zhao, X. K.; Chan, E.; Mei, J. G.; Lipomi, D. J. Effect of Broken Conjugation on the Stretchability of Semiconducting Polymers. *Macromol. Rapid Commun.* **2016**, *37*, 1623−1628.

DOI: 10.1021/acs.chemrev.7b00003
Chem. Rev. 2017, 117, 6467−6499

(29) Clark, J.; Silva, C.; Friend, R. H.; Spano, F. C. Role of Intermolecular Coupling in the Photophysics of Disordered Organic Semiconductors: Aggregate Emission in Regioregular Polythiophene. *Phys. Rev. Lett.* **2007**, *98*, 206406.
(30) Awartani, O.; Lemanski, B.; Ro, H. W.; Richter, L. J.; DeLongchamp, D. M.; O'Connor, B. T. Correlating Stiffness, Ductility, and Morphology of Polymer:Fullerene Films for Solar Cell Applications. *Adv. Energy Mater.* **2013**, *3*, 399−406.
(31) O'Connor, B.; Chan, E. P.; Chan, C.; Conrad, B. R.; Richter, L. J.; Kline, R. J.; Heeney, M.; McCulloch, I.; Soles, C. L.; DeLongchamp, D. M. Correlations between Mechanical and Electrical Properties of Polythiophenes. *ACS Nano* **2010**, *4*, 7538−7544.
(32) Postema, A. R.; Liou, K.; Wudl, F.; Smith, P. Highly Oriented, Low-Modulus Materials from Liquid Crystalline Polymers: The Ultimate Penalty for Solubilizing Alkyl Side Chains. *Macromolecules* **1990**, *23*, 1842−1845.
(33) Moulton, J.; Smith, P. Electrical and Mechanical Properties of Oriented Poly(3-Alkylthiophenes): 2. Effect of Side-Chain Length. *Polymer* **1992**, *33*, 2340−2347.
(34) Savagatrup, S.; Makaram, A. S.; Burke, D. J.; Lipomi, D. J. Mechanical Properties of Conjugated Polymers and Polymer-Fullerene Composites as a Function of Molecular Structure. *Adv. Funct. Mater.* **2014**, *24*, 1169−1181.
(35) Hiemenz, P. C.; Lodge, T. P. *Polymer Chemistry*, 2nd ed.; CRC Press: Boca Raton, FL, 2007.
(36) Koch, F. P. V.; Rivnay, J.; Foster, S.; Müller, C.; Downing, J. M.; Buchaca-Domingo, E.; Westacott, P.; Yu, L. Y.; Yuan, M. J.; Baklar, M.; et al. The Impact of Molecular Weight on Microstructure and Charge Transport in Semicrystalline Polymer Semiconductors–Poly(3-Hexylthiophene), a Model Study. *Prog. Polym. Sci.* **2013**, *38*, 1978−1989.
(37) Sawyer, E. J.; Zaretski, A. V.; Printz, A. D.; de los Santos, N. V.; Bautista-Gutierrez, A.; Lipomi, D. J. Large Increase in Stretchability of Organic Electronic Materials by Encapsulation. *Extreme Mech. Lett.* **2016**, *8*, 78−87.
(38) Kaltenbrunner, M.; White, M. S.; Glowacki, E. D.; Sekitani, T.; Someya, T.; Sariciftci, N. S.; Bauer, S. Ultrathin and Lightweight Organic Solar Cells with High Flexibility. *Nat. Commun.* **2012**, *3*, 770.
(39) Chortos, A.; Lim, J.; To, J. W. F.; Vosgueritchian, M.; Dusseault, T. J.; Kim, T. H.; Hwang, S. W.; Bao, Z. N. Highly Stretchable Transistors Using a Microcracked Organic Semiconductor. *Adv. Mater.* **2014**, *26*, 4253−4259.
(40) Dupont, S. R.; Oliver, M.; Krebs, F. C.; Dauskardt, R. H. Interlayer Adhesion in Roll-to-Roll Processed Flexible Inverted Polymer Solar Cells. *Sol. Energy Mater. Sol. Cells* **2012**, *97*, 171−175.
(41) Brand, V.; Levi, K.; McGehee, M. D.; Dauskardt, R. H. Film Stresses and Electrode Buckling in Organic Solar Cells. *Sol. Energy Mater. Sol. Cells* **2012**, *103*, 80−85.
(42) Savagatrup, S.; Printz, A. D.; O'Connor, T. F.; Zaretski, A. V.; Rodriquez, D.; Sawyer, E. J.; Rajan, K. M.; Acosta, R. I.; Root, S. E.; Lipomi, D. J. Mechanical Degradation and Stability of Organic Solar Cells: Molecular and Microstructural Determinants. *Energy Environ. Sci.* **2015**, *8*, 55−80.
(43) Onorato, J.; Pakhnyuk, V.; Luscombe, C. Structure and Design of Polymer for Durable, Stretchable Organic Electronics. *Polym. J.* **2017**, *49*, 41−60.
(44) Liu, F.; Gu, Y.; Shen, X. B.; Ferdous, S.; Wang, H. W.; Russell, T. P. Characterization of the Morphology of Solution-Processed Bulk Heterojunction Organic Photovoltaics. *Prog. Polym. Sci.* **2013**, *38*, 1990−2052.
(45) Treat, N. D.; Chabinyc, M. L. Phase Separation in Bulk Heterojunctions of Semiconducting Polymers and Fullerenes for Photovoltaics. *Annu. Rev. Phys. Chem.* **2014**, *65*, 59−81.
(46) Takacs, C. J.; Brady, M. A.; Treat, N. D.; Kramer, E. J.; Chabinyc, M. L. Quadrites and Crossed-Chain Crystal Structures in Polymer Semiconductors. *Nano Lett.* **2014**, *14*, 3096−3101.
(47) Treat, N. D.; Varotto, A.; Takacs, C. J.; Batara, N.; Al-Hashimi, M.; Heeney, M. J.; Heeger, A. J.; Wudl, F.; Hawker, C. J.; Chabinyc, M. L. Polymer-Fullerene Miscibility: A Metric for Screening New Materials for High-Performance Organic Solar Cells. *J. Am. Chem. Soc.* **2012**, *134*, 15869−15879.
(48) Cao, Y.; Smith, P. A.; Heeger, A. J. Mechanical and Electrical Properties of Highly Oriented Polyacetylene Films. *Synth. Met.* **1991**, *41*, 181−184.
(49) Cao, Y.; Smith, P.; Heeger, A. J. Mechanical and Electrical Properties of Polyacetylene Films Oriented by Tensile Drawing. *Polymer* **1991**, *32*, 1210−1218.
(50) Tokito, S.; Smith, P.; Heeger, A. J. Mechanical and Electrical Properties of Poly(2,5-Thienylene Vinylene) Fibers. *Synth. Met.* **1990**, *36*, 183−194.
(51) Fred Wudl, G. S. *Conducting Polymer Formed of Poly(2-Methoxy,5-(2′-Ethyl-Hexyloxy)-P-Phenylenevinylene)*. Office, U. S. P., Ed.; The Regents Of The University of California: Oakland, CA, 1993; Vol. *5189136*, p 6.
(52) Bao, Z. N.; Dodabalapur, A.; Lovinger, A. J. Soluble and Processable Regioregular Poly(3-Hexylthiophene) for Thin Film Field-Effect Transistor Applications with High Mobility. *Appl. Phys. Lett.* **1996**, *69*, 4108−4110.
(53) Burroughes, J. H.; Bradley, D. D. C.; Brown, A. R.; Marks, R. N.; Mackay, K.; Friend, R. H.; Burns, P. L.; Holmes, A. B. Light-Emitting Diodes Based on Conjugated Polymers. *Nature* **1990**, *347*, 539−541.
(54) Halls, J. J. M.; Walsh, C. A.; Greenham, N. C.; Marseglia, E. A.; Friend, R. H.; Moratti, S. C.; Holmes, A. B. Efficient Photodiodes from Interpenetrating Polymer Networks. *Nature* **1995**, *376*, 498−500.
(55) Yu, G.; Gao, J.; Hummelen, J. C.; Wudl, F.; Heeger, A. J. Polymer Photovoltaic Cells - Enhanced Efficiencies Via a Network of Internal Donor-Acceptor Heterojunctions. *Science* **1995**, *270*, 1789−1791.
(56) Sariciftci, N. S.; Smilowitz, L.; Heeger, A. J.; Wudl, F. Photoinduced Electron-Transfer from a Conducting Polymer to Buckminsterfullerene. *Science* **1992**, *258*, 1474−1476.
(57) Jones, J.; Lacour, S. P.; Wagner, S.; Suo, Z. G. Stretchable Wavy Metal Interconnects. *J. Vac. Sci. Technol., A* **2004**, *22*, 1723−1725.
(58) Lacour, S. P.; Wagner, S.; Huang, Z. Y.; Suo, Z. Stretchable Gold Conductors on Elastomeric Substrates. *Appl. Phys. Lett.* **2003**, *82*, 2404−2406.
(59) Khang, D. Y.; Xiao, J. L.; Kocabas, C.; MacLaren, S.; Banks, T.; Jiang, H. Q.; Huang, Y. Y. G.; Rogers, J. A. Molecular Scale Buckling Mechanics in Individual Aligned Single-Wall Carbon Nanotubes on Elastomeric Substrates. *Nano Lett.* **2008**, *8*, 124−130.
(60) Khang, D. Y.; Jiang, H. Q.; Huang, Y.; Rogers, J. A. A Stretchable Form of Single-Crystal Silicon for High-Performance Electronics on Rubber Substrates. *Science* **2006**, *311*, 208−212.
(61) Jung, I.; Shin, G.; Malyarchuk, V.; Ha, J. S.; Rogers, J. A.: Paraboloid Electronic Eye Cameras Using Deformable Arrays of Photodetectors in Hexagonal Mesh Layouts. *Appl. Phys. Lett.* **2010**, *96*, 02111010.1063/1.3290244
(62) Tseng, H. R.; Phan, H.; Luo, C.; Wang, M.; Perez, L. A.; Patel, S. N.; Ying, L.; Kramer, E. J.; Nguyen, T. Q.; Bazan, G. C.; et al. High-Mobility Field-Effect Transistors Fabricated with Macroscopic Aligned Semiconducting Polymers. *Adv. Mater.* **2014**, *26*, 2993−2998.
(63) Jorgensen, M.; Norrman, K.; Gevorgyan, S. A.; Tromholt, T.; Andreasen, B.; Krebs, F. C. Stability of Polymer Solar Cells. *Adv. Mater.* **2012**, *24*, 580−612.
(64) Rogers, J. A.; Someya, T.; Huang, Y. G. Materials and Mechanics for Stretchable Electronics. *Science* **2010**, *327*, 1603−1607.
(65) Lacour, S. P.; Chan, D.; Wagner, S.; Li, T.; Suo, Z. Mechanisms of Reversible Stretchability of Thin Metal Films on Elastomeric Substrates. *Appl. Phys. Lett.* **2006**, *88*, 204103.
(66) Gleskova, H.; Cheng, I. C.; Wagner, S.; Sturm, J. C.; Suo, Z. G. Mechanics of Thin-Film Transistors and Solar Cells on Flexible Substrates. *Sol. Energy* **2006**, *80*, 687−693.
(67) Lacour, S. P.; Jones, J.; Wagner, S.; Li, T.; Suo, Z. G. Stretchable Interconnects for Elastic Electronic Surfaces. *Proc. IEEE* **2005**, *93*, 1459−1467.
(68) Lacour, S. P.; Jones, J.; Suo, Z.; Wagner, S. Design and Performance of Thin Metal Film Interconnects for Skin-Like Electronic Circuits. *IEEE Electron Device Lett.* **2004**, *25*, 179−181.

DOI: 10.1021/acs.chemrev.7b00003
Chem. Rev. 2017, 117, 6467−6499

(69) Fan, J. A.; Yeo, W. H.; Su, Y. W.; Hattori, Y.; Lee, W.; Jung, S. Y.; Zhang, Y. H.; Liu, Z. J.; Cheng, H. Y.; Falgout, L.; et al. Fractal Design Concepts for Stretchable Electronics. *Nat. Commun.* **2014**, *5*, 3266.
(70) Xu, S.; Zhang, Y.; Cho, J. H.; Lee, J.; Huang, X.; Jia, L.; Fan, J. A.; Su, Y. W.; Su, J.; Zhang, H.; et al. Stretchable Batteries with Self-Similar Serpentine Interconnects and Integrated Wireless Recharging Systems. *Nat. Commun.* **2013**, *4*, 1543.
(71) Shin, G.; Jung, I.; Malyarchuk, V.; Song, J. Z.; Wang, S. D.; Ko, H. C.; Huang, Y. G.; Ha, J. S.; Rogers, J. A. Micromechanics and Advanced Designs for Curved Photodetector Arrays in Hemispherical Electronic-Eye Cameras. *Small* **2010**, *6*, 851−856.
(72) Ko, H. C.; Stoykovich, M. P.; Song, J. Z.; Malyarchuk, V.; Choi, W. M.; Yu, C. J.; Geddes, J. B.; Xiao, J. L.; Wang, S. D.; Huang, Y. G.; et al. A Hemispherical Electronic Eye Camera Based on Compressible Silicon Optoelectronics. *Nature* **2008**, *454*, 748−753.
(73) Viventi, J.; Kim, D. H.; Moss, J. D.; Kim, Y. S.; Blanco, J. A.; Annetta, N.; Hicks, A.; Xiao, J. L.; Huang, Y. G.; Callans, D. J.; et al. A Conformal, Bio-Interfaced Class of Silicon Electronics for Mapping Cardiac Electrophysiology. *Sci. Transl. Med.* **2010**, *2*, 24.
(74) Kim, D. H.; Lu, N.; Huang, Y. G.; Rogers, J. A. Materials for Stretchable Electronics in Bioinspired and Biointegrated Devices. *MRS Bull.* **2012**, *37*, 226−235.
(75) Hwang, S. W.; Tao, H.; Kim, D. H.; Cheng, H. Y.; Song, J. K.; Rill, E.; Brenckle, M. A.; Panilaitis, B.; Won, S. M.; Kim, Y. S.; et al. A Physically Transient Form of Silicon Electronics. *Science* **2012**, *337*, 1640−1644.
(76) Kim, D. H.; Rogers, J. A. Stretchable Electronics: Materials Strategies and Devices. *Adv. Mater.* **2008**, *20*, 4887−4892.
(77) Trung, T. Q.; Lee, N.-E. Recent Progress on Stretchable Electronic Devices with Instrinsically Stretchable Components. *Adv. Mater.* **2017**, *29*, 1603167.
(78) Sekitani, T.; Nakajima, H.; Maeda, H.; Fukushima, T.; Aida, T.; Hata, K.; Someya, T. Stretchable Active-Matrix Organic Light-Emitting Diode Display Using Printable Elastic Conductors. *Nat. Mater.* **2009**, *8*, 494−499.
(79) Sekitani, T.; Noguchi, Y.; Hata, K.; Fukushima, T.; Aida, T.; Someya, T. A Rubberlike Stretchable Active Matrix Using Elastic Conductors. *Science* **2008**, *321*, 1468−1472.
(80) Sekitani, T.; Takamiya, M.; Noguchi, Y.; Nakano, S.; Kato, Y.; Sakurai, T.; Someya, T. A Large-Area Wireless Power-Transmission Sheet Using Printed Organic Transistors and Plastic Mems Switches. *Nat. Mater.* **2007**, *6*, 413−417.
(81) Someya, T.; Kato, Y.; Sekitani, T.; Iba, S.; Noguchi, Y.; Murase, Y.; Kawaguchi, H.; Sakurai, T. Conformable, Flexible, Large-Area Networks of Pressure and Thermal Sensors with Organic Transistor Active Matrixes. *Proc. Natl. Acad. Sci. U. S. A.* **2005**, *102*, 12321−12325.
(82) Reeder, J.; Kaltenbrunner, M.; Ware, T.; Arreaga-Salas, D.; Avendano-Bolivar, A.; Yokota, T.; Inoue, Y.; Sekino, M.; Voit, W.; Sekitani, T.; et al. Mechanically Adaptive Organic Transistors for Implantable Electronics. *Adv. Mater.* **2014**, *26*, 4967−4973.
(83) Sekitani, T.; Iba, S.; Kato, Y.; Someya, T. Bending Effect of Organic Field-Effect Transistors with Polyimide Gate Dielectric Layers. *Jpn. J. Appl. Phys.* **2005**, *44*, 2841−2843.
(84) Wagner, S.; Bauer, S. Materials for Stretchable Electronics. *MRS Bull.* **2012**, *37*, 207−213.
(85) Kaltenbrunner, M.; Kettlgruber, G.; Siket, C.; Schwodiauer, R.; Bauer, S. Arrays of Ultracompliant Electrochemical Dry Gel Cells for Stretchable Electronics. *Adv. Mater.* **2010**, *22*, 2065−2067.
(86) Molberg, M.; Leterrier, Y.; Plummer, C. J. G.; Walder, C.; Löwe, C.; Opris, D. M.; Nüesch, F. A.; Bauer, S.; Månson, J.-A. E. Frequency Dependent Dielectric and Mechanical Behavior of Elastomers for Actuator Applications. *J. Appl. Phys.* **2009**, *106*, 054112.
(87) Keplinger, C.; Kaltenbrunner, M.; Arnold, N.; Bauer, S. Capacitive Extensometry for Transient Strain Analysis of Dielectric Elastomer Actuators. *Appl. Phys. Lett.* **2008**, *92*, 192903.
(88) Kaltenbrunner, M.; Adam, G.; Głowacki, E. D.; Drack, M.; Schwödiauer, R.; Leonat, L.; Apaydin, D. H.; Groiss, H.; Scharber, M. C.; White, M. S.; et al. Flexible High Power-Per-Weight Perovskite Solar Cells with Chromium Oxide-Metal Contacts for Improve Stability in Air. *Nat. Mater.* **2015**, *14*, 1032−1039.
(89) Moser, R.; Kettlgruber, G.; Siket, C. M.; Drack, M.; Graz, I. M.; Cakmak, U.; Major, Z.; Kaltenbrunner, M.; Bauer, S. From Playroom to Lab: Tough Stretchable Electronics Analyzed with a Tabletop Tensile Tester Made from Toy-Bricks. *Adv. Sci.* **2016**, *3*, 1500396.
(90) Lu, N. S.; Wang, X.; Suo, Z. G.; Vlassak, J. Metal Films on Polymer Substrates Stretched Beyond 50%. *Appl. Phys. Lett.* **2007**, *91*, 221909.
(91) Krebs, F. C.; Jorgensen, M.; Norrman, K.; Hagemann, O.; Alstrup, J.; Nielsen, T. D.; Fyenbo, J.; Larsen, K.; Kristensen, J. A Complete Process for Production of Flexible Large Area Polymer Solar Cells Entirely Using Screen Printing-First Public Demonstration. *Sol. Energy Mater. Sol. Cells* **2009**, *93*, 422−441.
(92) Voigt, M. M.; Mackenzie, R. C. I.; Yau, C. P.; Atienzar, P.; Dane, J.; Keivanidis, P. E.; Bradley, D. D. C.; Nelson, J. Gravure Printing for Three Subsequent Solar Cell Layers of Inverted Structures on Flexible Substrates. *Sol. Energy Mater. Sol. Cells* **2011**, *95*, 731−734.
(93) Krebs, F. C. Polymer Solar Cell Modules Prepared Using Roll-to-Roll Methods: Knife-over-Edge Coating, Slot-Die Coating and Screen Printing. *Sol. Energy Mater. Sol. Cells* **2009**, *93*, 465−475.
(94) Teichler, A.; Eckardt, R.; Hoeppener, S.; Friebe, C.; Perelaer, J.; Senes, A.; Morana, M.; Brabec, C. J.; Schubert, U. S. Combinatorial Screening of Polymer:Fullerene Blends for Organic Solar Cells by Inkjet Printing. *Adv. Energy Mater.* **2011**, *1*, 105−114.
(95) Fachetti, A. Pi-Conjugated Polymers for Organic Electronics and Photovoltaic Cell Applications. *Chem. Mater.* **2011**, *23*, 733−758.
(96) Amb, C. M.; Craig, M. R.; Koldemir, U.; Subbiah, J.; Choudhyry, K. R.; Gevorgyan, S. A.; Jorgensen, M.; Krebs, F. C.; So, F.; Reynolds, J. R. Aesthetically Pleasing Conjugated Polymer:Fullerene Blends for Blue-Green Solar Cells Via Roll-to-Roll Processing. *ACS Appl. Mater. Interfaces* **2012**, *4*, 1847−1853.
(97) Woo, C. H.; Beaujuge, P. M.; Holcombe, T. W.; Lee, O. P.; Fréchet, J. M. J. Incorporation of Furan into Low Band-Gap Polymers for Efficient Solar Cells. *J. Am. Chem. Soc.* **2010**, *132*, 15547−15549.
(98) Leleux, P.; Rivnay, J.; Lonjaret, T.; Badier, J. M.; Benar, C.; Herve, T.; Chauvel, P.; Malliaras, G. C. Organic Electrochemical Transistors for Clinical Applications. *Adv. Healthcare Mater.* **2015**, *4*, 142−147.
(99) Rivnay, J.; Owens, R. M.; Malliaras, G. C. The Rise of Organic Bioelectronics. *Chem. Mater.* **2014**, *26*, 679−685.
(100) Søndergaard, R. R.; Espinosa, N.; Jørgensen, M.; Krebs, F. C. Efficient Decommissioning and Recycling of Polymer Solar Cells: Justification for Use of Silver. *Energy Environ. Sci.* **2014**, *7*, 1006−1012.
(101) Shu, A. L.; Dai, A.; Wang, H.; Loo, Y. L.; Kahn, A. Electronic Structure and Carrier Transport at Laminated Polymer Homojunctions. *Org. Electron.* **2013**, *14*, 149−155.
(102) Oh, Y. J.; Rondeau-Gagné, S.; Chiu, Y. C.; Chortos, A.; Lissel, F.; Wang, G.-J. N.; Schroeder, B. C.; Kurosawa, T.; Lopez, J.; Katsumata, T.; et al. Intrinsically Stretchable and Healable Semiconducting Polymer for Organic Transistor. *Nature* **2016**, *539*, 411−415.
(103) Irimia-Vladu, M.; Sariciftci, N. S.; Bauer, S. Exotic Materials for Bio-Organic Electronics. *J. Mater. Chem.* **2011**, *21*, 1350−1361.
(104) Savagatrup, S.; Chan, E.; Renteria-Garcia, S.; Printz, A. D.; Zaretski, A. V.; O'Connor, T. F.; Rodriquez, D.; Valle, E.; Lipomi, D. J. Plasticization of Pedot:Pss by Common Additives for Mechanically Robust Organic Solar Cells and Wearable Sensors. *Adv. Funct. Mater.* **2015**, *25*, 427−436.
(105) Root, S. E.; Jackson, N. E.; Savagatrup, S.; Arya, G.; Lipomi, D. J. Modelling the Morphology and Thermomechanical Behaviour of Low-Bandgap Conjugated Polymers and Bulk Heterojunction Films *Energ. Energy Environ. Sci.* **2017**, *10*, 558−569.
(106) Schroeder, B. C.; Chiu, Y. C.; Gu, X. D.; Zhou, Y.; Xu, J.; Lopez, J.; Lu, C.; Toney, M. F.; Bao, Z. N. Non-Conjugated Flexible Linkers in Semiconducting Polymers: A Pathway to Improved Processability without Compromising Device Performance. *Adv. Electron. Mater.* **2016**, *2*, 1600104.
(107) Wu, H.-C.; Hung, C.-C.; Hong, C.-W.; Sun, H.-S.; Wang, J.-T.; Yamashita, G.; Higashihara, T.; Chen, W.-C. Isoindigo-Based Semiconducting Polymers Using Carbosilane Side Chains for High

DOI: 10.1021/acs.chemrev.7b00003
Chem. Rev. 2017, 117, 6467−6499

Performance Stretchable Field-Effect Transistors. *Macromolecules* **2016**, *49*, 8540−8548.
(108) Roth, B.; Savagatrup, S.; de los Santos, N. V.; Hagemann, O.; Carle, J. E.; Helgesen, M.; Livi, F.; Bundgaard, E.; Sondergaard, R.; Krebs, F. C.; et al. Mechanical Properties of a Library of Low-Bandgap Polymers. *Chem. Mater.* **2016**, *28*, 2363−2373.
(109) Tahk, D.; Lee, H. H.; Khang, D. Y. Elastic Moduli of Organic Electronic Materials by the Buckling Method. *Macromolecules* **2009**, *42*, 7079−7083.
(110) Printz, A. D.; Zaretski, A. V.; Savagatrup, S.; Chiang, A. S.-C.; Lipomi, D. J. Yield Point of Semiconducting Polymer Films on Stretchable Substrates Determined by Onset of Buckling. *ACS Appl. Mater. Interfaces* **2015**, *7*, 23257−23264.
(111) Kim, T.; Kim, J. H.; Kang, T. E.; Lee, C.; Kang, H.; Shin, M.; Wang, C.; Ma, B.; Jeong, U.; Kim, T. S.; et al. Flexible, Highly Efficient All-Polymer Solar Cells. *Nat. Commun.* **2015**, *6*, 8547.
(112) Chung, J. Y.; Nolte, A. J.; Stafford, C. M. Surface Wrinkling: A Versatile Platform for Measuring Thin-Film Properties. *Adv. Mater.* **2011**, *23*, 349−368.
(113) Stafford, C. M.; Harrison, C.; Beers, K. L.; Karim, A.; Amis, E. J.; Vanlandingham, M. R.; Kim, H. C.; Volksen, W.; Miller, R. D.; Simonyi, E. E. A Buckling-Based Metrology for Measuring the Elastic Moduli of Polymeric Thin Films. *Nat. Mater.* **2004**, *3*, 545−550.
(114) Kim, J. S.; Kim, J. H.; Lee, W.; Yu, H.; Kim, H. J.; Song, I.; Shin, M.; Oh, J. H.; Jeong, U.; Kim, T. S.; et al. Tuning Mechanical and Optoelectrical Properties of Poly(3-Hexylthiophene) through Systematic Regioregularity Control. *Macromolecules* **2015**, *48*, 4339−4346.
(115) Dupont, S. R.; Voroshazi, E.; Heremans, P.; Dauskardt, R. H. Adhesion Properties of Inverted Polymer Solarcells: Processing and Film Structure Parameters. *Org. Electron.* **2013**, *14*, 1262−1270.
(116) Dupont, S. R.; Novoa, F.; Voroshazi, E.; Dauskardt, R. H. Decohesion Kinetics of Pedot:Pss Conducting Polymer Films. *Adv. Funct. Mater.* **2014**, *24*, 1325−1332.
(117) Bruner, C.; Miller, N. C.; McGehee, M. D.; Dauskardt, R. H. Molecular Intercalation and Cohesion of Organic Bulk Heterojunction Photovoltaic Devices. *Adv. Funct. Mater.* **2013**, *23*, 2863−2871.
(118) Rodriquez, D.; Savagatrup, S.; Valle, E.; Proctor, C. M.; McDowell, C.; Bazan, G. C.; Nguyen, T. Q.; Lipomi, D. J. Mechanical Properties of Solution-Processed Small-Molecule Semiconductor Films. *ACS Appl. Mater. Interfaces* **2016**, *8*, 11649−11657.
(119) Müller, C. On the Glass Transition Temperature of Polymer Semiconductors and Its Impact on Polymer Solar Cell Stability. *Chem. Mater.* **2015**, *27*, 2740−2754.
(120) Tessarolo, M.; Guerrero, A.; Gedefaw, D.; Bolognesi, M.; Prosa, M.; Xu, X. F.; Mansour, M.; Wang, E.; Seri, M.; Andersson, M.; et al. Predicting Thermal Stability of Organic Solar Cells through and Easy and Fast Capacitance Measurement. *Sol. Energy Mater. Sol. Cells* **2015**, *141*, 240−247.
(121) Sung, M. J.; Luzio, A.; Park, W. T.; Kim, R. H.; Gann, E.; Maddalena, F.; Pace, G.; Xu, Y.; Natali, D.; de Falco, C.; et al. High-Mobility Napthalene Diimide and Selenophene-Vinylene-Selenophene-Based Conjugated Polymer: N-Channel Organic Field-Effect Transistors and Structure-Property Relationship. *Adv. Funct. Mater.* **2016**, *26*, 4984−4997.
(122) Lan, L. Y.; Chen, Z. M.; Ying, L.; Huang, F.; Cao, Y. Acenaphtho[1,2-B]Quinoxaline Diimides Derivative as a Potential Small Molecule Non-Fullerene Acceptor for Organic Solar Cells. *Org. Electron.* **2016**, *30*, 176−181.
(123) Patel, S. N.; Su, G. M.; Luo, C.; Wang, M.; Perez, L. A.; Fischer, D. A.; Predergast, D.; Bazan, G. C.; Heeger, A. J.; Chabinyc, M. L.; et al. Nexafs Spectroscopy Reveals the Molecular Orientation in Blade-Coated Pyridal[2,1,3]Thiadiazole-Containing Conjugated Polymer Thin Films. *Macromolecules* **2015**, *48*, 6606−6616.
(124) Hufnagel, M.; Thelakkat, M. Simultaneous Morphological Stability and High Charge Carrier Mobilities in Donor-Acceptor Block Cpolymer/Pcbm Blends. *J. Polym. Sci., Part B: Polym. Phys.* **2016**, *54*, 1125−1136.
(125) Cho, E. C.; Chang-Jian, C. W.; Hsiao, Y. S.; Lee, K. C.; Huang, J. H. Influence of the Bridging Atom on the Electrochromic Performance of a Cyclopentadithiophene Polymer. *Sol. Energy Mater. Sol. Cells* **2016**, *150*, 43−50.
(126) Ishida, H.; Rotter, G. Dynamic Mechanical Analysis of the Glass Transition: Curve Resolving Applied to Polymers. *Macromolecules* **1992**, *25*, 2170−2176.
(127) Beaucage, G.; Composto, R.; Stein, R. S. Ellipsometric Study of the Glass Transition and Thermal Expansion Coefficients of Thin Polymer Films. *J. Polym. Sci., Part B: Polym. Phys.* **1993**, *31*, 319−326.
(128) Kahle, O.; Wielsch, U.; Metzner, H.; Bauer, J.; Uhlig, C.; Zawatzki, C. Glass Transition Temperature and Thermal Expansion Behaviour of Polymer Films Investigated by Variable Temperature Spectroscopic Ellipsometry. *Thin Solid Films* **1998**, *313*−*314*, 803−807.
(129) Müller, C.; Andersson, L. M.; Peña-Rodriguez, O.; Garriga, M.; Inganäs, O.; Campoy-Quiles, M. Determination of Thermal Transition Depth Profiles in Polymer Semiconductor Films with Ellipsometry. *Macromolecules* **2013**, *46*, 7325−7331.
(130) Root, S. E.; Savagatrup, S.; Pais, C. J.; Arya, G.; Lipomi, D. J. Predicting the Mechanical Properties of Organic Semiconductors Using Coarse-Grained Molecular Dynamics Simulations. *Macromolecules* **2016**, *49*, 2886−2894.
(131) Rivnay, J.; Mannsfeld, S. C. B.; Miller, C. E.; Salleo, A.; Toney, M. F. Quantitative Determination of Organic Semiconductor Microstructure from the Molecular to Device Scale. *Chem. Rev.* **2012**, *112*, 5488−5519.
(132) Salleo, A.; Kline, R. J.; DeLongchamp, D. M.; Chabinyc, M. L. Microstructural Characterization and Charge Transport in Thin Films of Conjugated Polymers. *Adv. Mater.* **2010**, *22*, 3812−3838.
(133) Savagatrup, S.; Printz, A. D.; Wu, H. S.; Rajan, K. M.; Sawyer, E. J.; Zaretski, A. V.; Bettinger, C. J.; Lipomi, D. J. Viability of Stretchable Poly(3-Heptylthiophene) (P3hpt) for Organic Solar Cells and Field-Effect Transistors. *Synth. Met.* **2015**, *203*, 208−214.
(134) Savagatrup, S.; Printz, A. D.; Rodriquez, D.; Lipomi, D. J. Best of Both Worlds: Conjugated Polymers Exhibiting Good Photovoltaic Performance and High Tensile Elasticity. *Macromolecules* **2014**, *47*, 1981−1992.
(135) Stafford, C. M.; Vogt, B. D.; Harrison, C.; Julthongpiput, D.; Huang, R. Elastic Moduli of Ultrathin Amorphous Polymer Films. *Macromolecules* **2006**, *39*, 5095−5099.
(136) Oliver, W. C.; Pharr, G. M. An Improved Technique for Determining Hardness and Elastic Modulus Using Load and Displacement Sensing Indentation Experiments. *J. Mater. Res.* **1992**, *7*, 1564−1583.
(137) Zeng, K. Y.; Chen, Z. K.; Shen, L.; Liu, B. Study of Mechanical Properties of Light-Emitting Polymer Films by Nano-Indentation Technique. *Thin Solid Films* **2005**, *477*, 111−118.
(138) Vanlandingham, M. R.; Villarrubia, J. S.; Guthrie, W. F.; Meyers, G. F. Nanoindentation of Polymers: An Overview. *Macromol. Symp.* **2001**, *167*, 15−43.
(139) Rodriquez, D.; Kim, J.-H.; Root, S. E.; Fei, Z. P.; Boufflet, P.; Heeney, M.; Kim, T.-S.; Lipomi, D. J. Comparison of Methods for Determining the Mechanical Properties of Semiconducting Polymer Films for Stretchable Electronics. *ACS Appl. Mater. Interfaces* **2017**, DOI: 10.1021/acsami.6b16115.
(140) Bowden, N.; Brittain, S.; Evans, A. G.; Hutchinson, J. W.; Whitesides, G. M. Spontaneous Formation of Ordered Structures in Thin Films of Metals Supported on an Elastomeric Polymer. *Nature* **1998**, *393*, 146−149.
(141) Ro, H. W.; Akgun, B.; O'Connor, B. T.; Hammond, M.; Kline, R. J.; Snyder, C. R.; Satija, S. K.; Ayzner, A. L.; Toney, M. F.; Soles, C. L.; et al. Poly(3-Hexylthiophene) and [6,6]-Phenyl-C61-Butyric Acid Methyl Ester Mixing in Organic Solar Cells. *Macromolecules* **2012**, *45*, 6587−6599.
(142) Savagatrup, S.; Rodriquez, D.; Printz, A. D.; Sieval, A.; Hummelen, J. C.; Lipomi, D. J. [70]Pcbm and Incompletely Separated Grades of Methanofullerenes Produce Bulk Heterojunctions with Increased Robustness for Ultra-Flexible and Stretchable Electronics. *Chem. Mater.* **2015**, *27*, 3902−3911.
(143) Meitl, M. A.; Zhu, Z. T.; Kumar, V.; Lee, K. J.; Feng, X.; Huang, Y. Y.; Adesida, I.; Nuzzo, R. G.; Rogers, J. A. Transfer Printing by Kinetic

DOI: 10.1021/acs.chemrev.7b00003
Chem. Rev. 2017, 117, 6467−6499

Control of Adhesion to an Elastomeric Stamp. *Nat. Mater.* **2006**, *5*, 33−38.
(144) Venkatanarayanan, R. I.; Krishnan, S.; Sreeram, A.; Yuya, P. A.; Patel, N. G.; Tandia, A.; McLaughlin, J. B. Simulated Dilatometry and Static Deformation Prediction of Glass Transition and Mechanical Properties of Polyacetylene and Poly(Para-Phenylene Vinylene). *Macromol. Theory Simul.* **2016**, *25*, 238−253.
(145) O'Connor, T. F.; Zaretski, A. V.; Savagatrup, S.; Printz, A. D.; Wilkes, C. D.; Diaz, M. I.; Lipomi, D. J. Wearable Organic Solar Cells with High Cyclic Bending Stability: Materials Selection Criteria. *Sol. Energy Mater. Sol. Cells* **2016**, *144*, 438.
(146) Yu, Z. B.; Zhang, Q. W.; Li, L.; Chen, Q.; Niu, X. F.; Liu, J.; Pei, Q. B. Highly Flexible Silver Nanowire Electrodes for Shape-Memory Polymer Light-Emitting Diodes. *Adv. Mater.* **2011**, *23*, 664−668.
(147) O'Connor, T. F.; Zaretski, A. V.; Shiravi, B. A.; Savagatrup, S.; Printz, A. D.; Diaz, M. I.; Lipomi, D. J. Stretching and Conformal Bonding of Organic Solar Cells to Hemispherical Substrates. *Energy Environ. Sci.* **2014**, *7*, 370−378.
(148) Awartani, O.; Kudenov, M. W.; O'Connor, B. T. Organic Photovoltaic Cells with Controlled Polarization Sensitivity. *Appl. Phys. Lett.* **2014**, *104*, 093306.
(149) Gargi, D.; Kline, R. J.; DeLongchamp, D. M.; Fischer, D. A.; Toney, M. F.; O'Connor, B. T. Charge Transport in Highly Face-on Poly(3-Hexylthiophene) Films. *J. Phys. Chem. C* **2013**, *117*, 17421−17428.
(150) Awartani, O.; Zhao, B. X.; Currie, T.; Kline, R. J.; Zikry, M. A.; O'Connor, B. T. Anisotropic Elastic Modulus of Oriented Regioregular Poly(3-Hexylthiophene) Films. *Macromolecules* **2016**, *49*, 327−333.
(151) O'Connor, B.; Kline, R. J.; Conrad, B. R.; Richter, L. J.; Gundlach, D.; Toney, M. F.; DeLongchamp, D. M. Anisotropic Structure and Charge Transport in Highly Strain-Aligned Regioregular Poly(3-Hexylthiophene). *Adv. Funct. Mater.* **2011**, *21*, 3697−3705.
(152) Yasuda, T.; Han, L. Y.; Tsutsui, T. Fabrication of Stretch-Oriented Regioregular Poly(3-Hexylthiophene) Film and Its Application to Organic Field-Effect Transistors. *J. Photopolym. Sci. Technol.* **2009**, *22*, 713−717.
(153) Israelachvili, J. N. *Intermolecular and Surface Forces*, 3rd ed.; Elsevier: Waltham, MA, 2011.
(154) Ward, I. M.; Sweeney, J. *Mechanical Properties of Solid Polymers*, 3rd ed.; Wiley: New York, 2012.
(155) Seitz, J. T. The Estimation of Mechanical-Properties of Polymers from Molecular Structure. *J. Appl. Polym. Sci.* **1993**, *49*, 1331−1351.
(156) Creton, C.; Brown, H. R.; Shull, K. R. Molecular Weight Effects in Chain Pullout. *Macromolecules* **1994**, *27*, 3174−3183.
(157) Washiyama, J.; Kramer, E. J.; Creton, C. F.; Hui, C. Y. Chain Pullout Fracture of Polymer Interfaces. *Macromolecules* **1994**, *27*, 2019−2024.
(158) Lipomi, D. J.; Chong, H.; Vosgueritchian, M.; Mei, J. G.; Bao, Z. N. Toward Mechanically Robust and Intrinsically Stretchable Organic Solar Cells: Evolution of Photovoltaic Properties with Tensile Strain. *Sol. Energy Mater. Sol. Cells* **2012**, *107*, 355−365.
(159) Lipomi, D. J.; Tee, B. C.-K.; Vosgueritchian, M.; Bao, Z. N. Stretchable Organic Solar Cells. *Adv. Mater.* **2011**, *23*, 1771−1775.
(160) Graz, I. M.; Cotton, D. P. J.; Lacour, S. P. Extended Cyclic Uniaxial Loading of Stretchable Gold Thin-Films on Elastomeric Substrates. *Appl. Phys. Lett.* **2009**, *98*, 071902.
(161) Printz, A. D.; Chiang, A. S.-C.; Savagatrup, S.; Lipomi, D. J. Fatigue in Organic Semiconductors: Spectroscopic Evolution of Microstructure Due to Cyclic Loading in Poly(3-Heptylthiophene). *Synth. Met.* **2016**, *217*, 144−151.
(162) Chen, S. A.; Ni, J. M. Structure/Properties of Conjugated Conductive Polymers. 1. Neutral Poly(3-Alkylthiophene)S. *Macromolecules* **1992**, *25*, 6081−6089.
(163) Pankaj, S.; Hempel, E.; Beiner, M. Side-Chain Dynamics and Crystallization in a Series of Regiorandom Poly(3-Alkythiophenes). *Macromolecules* **2009**, *42*, 716−724.
(164) Smith, Z. C.; Wright, Z. M.; Aronold, A. M.; Sauvé, G.; McCullough, R. D.; Sydlik, S. A. Increased Toughness and Excellent Electronic Properties in Regioregular Random Copolymers of 3-Alkylthiophenes and Thiophene. *Adv. Electron. Mater.* **2017**, *3*, 1600316.
(165) Pankaj, S.; Beiner, M. Confined Dynamics and Crystallization in Self-Assembled Alkyl Nanodomains. *J. Phys. Chem. B* **2010**, *114*, 15459−15465.
(166) van de Leur, B.; de Ruiter, B.; Breen, J. Dielectrical and Dynamic Mechanical Properties of Three Poly(3-N-Alkaylthiophene)S. *Synth. Met.* **1993**, *57*, 4956−4961.
(167) Barard, S.; Heeney, M.; Chen, L.; Cölle, M.; Shkunov, M.; McCulloch, I.; Stingelin, N.; Philips, M.; Kreouzis, T. Separate Charge Transport Pathways Determined by the Time of Flight Method in Bimodal Polytriarylamine. *J. Appl. Phys.* **2009**, *105*, 013701.
(168) Jin, Y. J.; Bae, J. E.; Cho, K. S.; Lee, W. E.; Hwang, D. Y.; Kwak, G. Room Temperature Fluorescent Conjugated Polymer Gums. *Adv. Funct. Mater.* **2014**, *24*, 1928−1937.
(169) Keplinger, C.; Sun, J. Y.; Foo, C. C.; Rothemund, P.; Whitesides, G. M.; Suo, Z. Stretchable, Transparent, Ionic Conductors. *Science* **2013**, *341*, 984−987.
(170) Tummala, N. R.; Risko, C.; Bruner, C.; Dauskardt, R. H.; Brédas, J. L. Entanglements in P3HT and Their Influence on Thin-Film Mechanical Properties: Insights from Molecular Dynamics Simulations. *J. Polym. Sci., Part B: Polym. Phys.* **2015**, *53*, 934−942.
(171) Towns, J.; Cockerill, T.; Dahan, M.; Foster, I.; Gaither, K.; Grimshaw, A.; Hazlewood, V.; Lathrop, S.; Lifka, D.; Peterson, G. D.; et al. Xsede: Accelerating Scientific Discovery. *Comput. Sci. Eng.* **2014**, *16*, 62−74.
(172) Peter, C.; Kremer, K. Multiscale Simulation of Soft Matter Systems − from the Atomistic to the Coarse-Grained Level and Back. *Soft Matter* **2009**, *5*, 4357−4366.
(173) Martin, M. G.; Siepmann, J. I. Transferable Potentials for Phase Equilibria. 1. United-Atom Description of N-Alkanes. *J. Phys. Chem. B* **1998**, *102*, 2569−2577.
(174) Agrawal, V.; Arya, G.; Oswald, J. Simultaneous Iterative Boltzmann Inversion for Coarse-Graining of Polyurea. *Macromolecules* **2014**, *47*, 3378−3389.
(175) Lee, C. K.; Pao, C. W.; Chu, C. W. Multiscale Molecular Simulations of the Nanoscale Morphologies of P3HT:Pcbm Blends for Bulk Heterojunction Organic Photovoltaic Cells. *Energy Environ. Sci.* **2011**, *4*, 4124−4132.
(176) Huang, D. M.; Faller, R.; Do, K.; Moule, A. J. Coarse-Grained Computer Simulations of Polymer/Fullerene Bulk Heterojunctions for Organic Photovoltaic Applications. *J. Chem. Theory Comput.* **2010**, *6*, 526−537.
(177) Jones, M. L.; Huang, D. M.; Chakrabarti, B.; Groves, C. Relating Molecular Morphology to Charge Mobility in Semicrystalline Conjugated Polymers. *J. Phys. Chem. C* **2016**, *120*, 4240−4250.
(178) Kröger, M. Shortest Multiple Disconnected Path for the Analysis of Entanglements in Two- and Three-Dimensional Polymeric Systems. *Comput. Phys. Commun.* **2005**, *168*, 209−232.
(179) Jackson, N. E.; Kohlstedt, K. L.; Savoie, B. M.; Olvera de la Cruz, M.; Schatz, G. C.; Chen, L. X.; Ratner, M. A. Conformational Order in Aggregates of Conjugated Polymers. *J. Am. Chem. Soc.* **2015**, *137*, 6254−6262.
(180) Liu, J. S.; Lowe, R. S.; McCullough, R. D. Employing Maldi-Ms on Poly(Alkylthiophenes): Analysis of Molecular Weights, Molecular Weight Distributions, End-Group Structures, and End-Group Modifications. *Macromolecules* **1999**, *32*, 5777−5785.
(181) Koch, F. P. V.; Smith, P.; Heeney, M. "Fibonacci's Route" to Regioregular Oligo(3-Hexylthiophene)S. *J. Am. Chem. Soc.* **2013**, *135*, 13695−13698.
(182) Everaers, R.; Sukumaran, S. K.; Grest, G. S.; Svaneborg, C.; Sivasubramanian, A.; Kremer, K. Rheology and Microscopic Topology of Entangled Polymeric Liquids. *Science* **2004**, *303*, 823−826.
(183) Sukumaran, S. K.; Grest, G. S.; Kremer, K.; Everaers, R. Identifying the Primitive Path Mesh in Entangled Polymer Liquids. *J. Polym. Sci., Part B: Polym. Phys.* **2005**, *43*, 917−933.
(184) Hoy, R. S.; Foteinopoulou, K.; Kröger, M. Topological Analysis of Polymeric Melts: Chain-Length Effects and Fast-Converging Estimators for Entanglement Length. *Phys. Rev. E* **2009**, *80*, 031803.

DOI: 10.1021/acs.chemrev.7b00003
Chem. Rev. 2017, 117, 6467−6499

(185) Shanbhag, S.; Kröger, M. Primitive Path Networks Generated by Annealing and Geometrical Methods: Insights into Differences. *Macromolecules* **2007**, *40*, 2897−2903.
(186) Mei, J. G.; Bao, Z. N. Side Chain Engineering in Solution Processible Conjugated Polymers. *Chem. Mater.* **2014**, *26*, 604−615.
(187) Bundgaard, E.; Livi, F.; Hagemann, O.; Carlé, J. E.; Helgesen, M.; Heckler, I. M.; Zawacka, N. K.; Angmo, D.; Larsen-Olsen, T. T.; dos Reis Benatto, G. A.; et al. Matrix Organization and Merit Factor Evaluation as a Method to Address the Challenge of Finding a Polymer Material for Roll Coated Polymer Solar Cells. *Adv. Energy Mater.* **2015**, *5*, 1402186.
(188) McCullough, R. D. The Chemistry of Conducting Polythiophenes. *Adv. Mater.* **1998**, *10*, 93−116.
(189) McCullough, R. D.; Tristramnagle, S.; Williams, S. P.; Lowe, R. D.; Jayaraman, M. Self-Orienting Head-to-Tail Poly(3-Alkylthiophenes) - New Insights on Structure-Property Relationships in Conducting Polymers. *J. Am. Chem. Soc.* **1993**, *115*, 4910−4911.
(190) Chen, T. A.; Rieke, R. D. The First Regioregular Head-to-Tail Poly(3-Hexylthiophene-2,5-Diyl) and a Regiorandom Isopolymer: Nickel Versus Palladium Catalysis of 2(5)-Bromo-5(2)-(Bromozincio)-3-Hexylthiophene Polymerization. *J. Am. Chem. Soc.* **1992**, *114*, 10087−10088.
(191) Lu, C.; Lee, W. Y.; Gu, X. D.; Xu, J.; Chou, H. H.; Yan, H. P.; Chiu, Y. C.; He, M. Q.; Matthews, J. R.; Niu, W. J.; et al. Effects of Molecular Structure and Packing Order on the Stretchability of Semicrystalline Conjugated Poly(Tetrathienoacene-Diketopyrrolopyrrole) Polymers. *Adv. Electron. Mater.* **2017**, *3*, 1600311.
(192) Zhao, Y.; Zhao, X. K.; Zang, Y. P.; Di, C.-A.; Diao, Y.; Mei, J. G. Conjugation-Break Spacers in Semiconducting Polymers: Impact on Polymer Processability and Charge Transport Properties. *Macromolecules* **2015**, *48*, 2048−2053.
(193) Peet, J.; Kim, J. Y.; Coates, N. E.; Ma, W. L.; Moses, D.; Heeger, A. J.; Bazan, G. C. Efficiency Enhancement in Low-Bandgap Polymer Solar Cells by Processing with Alkane Dithiols. *Nat. Mater.* **2007**, *6*, 497−500.
(194) Graham, K. R.; Mei, J. G.; Stalder, R.; Shim, J. W.; Cheun, H.; Steffy, F.; So, F.; Kippelen, B.; Reynolds, J. R. Polydimethylsiloxane as a Molecular Additive for Enhanced Performance of Molecular Bulk Heterojunction Organic Solar Cells. *ACS Appl. Mater. Interfaces* **2011**, *3*, 1210−1215.
(195) Na, S. I.; Wang, G.; Kim, S. S.; Kim, T. W.; Oh, S. H.; Yu, B. K.; Lee, T.; Kim, D. Y. Evolution of Nanomorphology and Anisotropic Conductivity in Solvent-Modified Pedot:Pss Films for Polymeric Anodes of Polymer Solar Cells. *J. Mater. Chem.* **2009**, *19*, 9045−9053.
(196) Lang, U.; Rust, P.; Schoberle, B.; Dual, J. Piezoresistive Properties of Pedot:Pss. *Microelectron. Eng.* **2009**, *86*, 330−334.
(197) Lang, U.; Naujoks, N.; Dual, J. Mechanical Characterization of Pedot:Pss Thin Films. *Synth. Met.* **2009**, *159*, 473−479.
(198) Bhagwat, N.; Kiick, K. L.; Martin, D. C. Electrochemical Deposition and Characterization of Carboxylic Acid Functionalized Pedot Copolymers. *J. Mater. Res.* **2014**, *29*, 2835−2844.
(199) Stavrindou, E.; Winther-Jensen, O.; Shekibi, B. S.; Armel, V.; Rivnay, J.; Ismailova, E.; Sanaur, S.; Malliaras, G. C.; Winther-Jensen, B. Engineering Hydrophilic Conducting Composites with Enhanced Ion Mobility. *Phys. Chem. Chem. Phys.* **2014**, *16*, 2275−2279.
(200) Elschner, A.; Kirchmeyer, S.; Lovenich, W.; Merker, U.; Reuter, K. *Pedot: Principles and Applications of an Intrinsically Conductive Polymer*; CRC: New York, 2011.
(201) Hansen, T. S.; West, K.; Hassager, O.; Larsen, N. B. Highly Stretchable and Conductive Polymer Material Made from Poly(3,4-Ethylenedioxythiophene) and Polyurethane Elastomers. *Adv. Funct. Mater.* **2007**, *17*, 3069−3072.
(202) Hansen, T. S.; Hassager, O.; Larsen, N. B.; Clark, N. B. Micropatterning of a Stretchable Conductive Polymer Using Inkjet Printing and Agarose Stamping. *Synth. Met.* **2007**, *157*, 961−967.
(203) Kim, Y. H.; Sachse, C.; Machala, M. L.; May, C.; Muller-Meskamp, L.; Leo, K. Highly Conductive Pedot:Pss Electrode with Optimized Solvent and Thermal Post-Treatment for Ito-Free Organic Solar Cells. *Adv. Funct. Mater.* **2011**, *21*, 1076−1081.
(204) Crispin, X.; Jakobsson, F. L. E.; Crispin, A.; Grim, P. C. M.; Andersson, P.; Volodin, A.; van Haesendonck, C.; Van der Auweraer, M.; Salaneck, W. R.; Berggren, M. The Origin of the High Conductivity of Poly(3,4-Ethylenedioxythiophene)-Poly(Styrenesulfonate) (Pedot-Pss) Plastic Electrodes. *Chem. Mater.* **2006**, *18*, 4354−4360.
(205) Vosgueritchian, M.; Lipomi, D. J.; Bao, Z. N. Highly Conductive and Transparent Pedot:Pss Films with a Fluorosurfactant for Stretchable and Flexible Transparent Electrodes. *Adv. Funct. Mater.* **2012**, *22*, 421−428.
(206) Simmons, G. W. H. *Single Crystal Elastic Constants and Calculated Aggregate Properties: A Handbook*; The MIT Press: Cambridge, MA, 1971.
(207) Cun, H.; Wang, Y.; Du, S.; Zhang, L.; Zhang, L.; Yang, B.; He, X.; Wang, Y.; Zhu, X.; Yuan, Q.; et al. Tuning Structural and Mechanical Properties of Two-Dimensional Molecular Crystals: The Roles of Carbon Side Chains. *Nano Lett.* **2012**, *12*, 1229−1234.
(208) Treat, N. D.; Brady, M. A.; Smith, G.; Toney, M. F.; Kramer, E. J.; Hawker, C. J.; Chabinyc, M. L. Interdiffusion of Pcbm and P3HT Reveals Miscibility in a Photovoltaically Active Blend. *Adv. Energy Mater.* **2011**, *1*, 82−89.
(209) Brady, M. A.; Su, G. M.; Chabinyc, M. L. Recent Progress in the Morphology of Bulk Heterojunction Photovoltaics. *Soft Matter* **2011**, *7*, 11065−11077.
(210) Hoppe, H.; Sariciftci, N. S. Morphology of Polymer/Fullerene Bulk Heterojunction Solar Cells. *J. Mater. Chem.* **2006**, *16*, 45−61.
(211) Coakley, K. M.; McGehee, M. D. Conjugated Polymer Photovoltaic Cells. *Chem. Mater.* **2004**, *16*, 4533−4542.
(212) Miller, N. C.; Cho, E. K.; Gysel, R.; Risko, C.; Coropceanu, V.; Miller, C. E.; Sweetnam, S.; Sellinger, A.; Heeney, M.; McCulloch, I.; et al. Factors Governing Intercalation of Fullerenes and Other Small Molecules between the Side Chains of Semiconducting Polymers Used in Solar Cells. *Adv. Energy Mater.* **2012**, *2*, 1208−1217.
(213) Miller, N. C.; Gysel, R.; Beiley, Z.; Miller, C. E.; Toney, M. F.; Heeney, M.; McCulloch, I.; McGehee, M. D. Tuning the Properties of Polymer Bulk Heterojunction Solar Cells by Adjusting Fulleren Size to Control Intercalation. *Nano Lett.* **2009**, *9*, 4153−4157.
(214) Printz, A. D.; Savagatrup, S.; Rodriquez, D.; O'Connor, T. F.; Lipomi, D. J. Role of Molecular Mixing on the Compliance and Ductility of Polymer:Fullerene Bulk Heterojunction Films. *Sol. Energy Mater. Sol. Cells* **2015**, *134*, 64−72.
(215) Du, J. H.; Pei, S. F.; Ma, L. P.; Cheng, H. M. 25th Anniversary Article: Carbon Nanotube- and Graphene-Based Transparent Conductive Films for Optoelectronic Devices. *Adv. Mater.* **2014**, *26*, 1958−1991.
(216) Müller, C.; Ferenczi, T. A. M.; Campoy-Quiles, M.; Frost, J. M.; Bradley, D. D. C.; Smith, P.; Stingelin-Stutzmann, N.; Nelson, J. Binary Organic Photovoltaic Blends: A Simple Rationale for Optimum Compositions. *Adv. Mater.* **2008**, *20*, 3510−3515.
(217) Sonar, P.; Lim, J. P. F.; Chan, K. L. Organic Non-Fullerene Acceptors for Organic Photovoltaics. *Energy Environ. Sci.* **2011**, *4*, 1558−1574.
(218) Holliday, S.; Ashraf, R. S.; Wadsworth, A.; Baran, D.; Yousaf, S. A.; Nielsen, C. B.; Tan, C.-H.; Dimitrov, S. D.; Shang, Z. G.; Gasparini, N.; et al. High-Efficiency and Air-Stable P3HT-Based Polymer Solar Cells with a New Non-Fullerene Acceptor. *Nat. Commun.* **2016**, *7*, 11585.
(219) Sun, T.; Scott, J. I.; Wang, M.; Kline, R. J.; Bazan, G. C.; O'Connor, B. T. Plastic Deformation of Polymer Blends as a Means to Achieve Stretchable Organic Transistors. *Adv. Electron. Mater.* **2017**, *3*, 1600388.
(220) Koch, F. P. V.; Heeney, M.; Smith, P. Thermal and Structural Characteristics of Oligo(3-Hexylthiophene)S (3ht)N, N = 4−36. *J. Am. Chem. Soc.* **2013**, *135*, 13699−13709.
(221) McCulloch, I.; Heeney, M.; Bailey, C.; Genevicius, K.; MacDonald, I.; Shkunov, M.; Sparrowe, D.; Tierney, S.; Wagner, R.; Zhang, W. M.; et al. Liquid-Crystalline Semiconducting Polymers with High Charge-Carrier Mobility. *Nat. Mater.* **2006**, *5*, 328−333.
(222) Keg, P.; Lohani, A.; Fichou, D.; Lam, Y. M.; Wu, Y. L.; Ong, B. S.; Mhaisalkar, S. G. Direct Observation of Alkyl Chain Interdigitation in

DOI: 10.1021/acs.chemrev.7b00003
Chem. Rev. 2017, 117, 6467−6499

Conjugated Polyquarterthiophene Self-Organized on Graphite Surfaces. *Macromol. Rapid Commun.* **2008**, *29*, 1197−1202.
(223) Liu, J. G.; Sun, Y.; Gao, X.; Xing, R.; Zheng, L. D.; Wu, S. P.; Geng, Y. H.; Han, Y. C. Oriented Poly(3-Hexylthiophene) Nanofibril with the Π-Π Stacking Growth Direction by Solvent Directional Evaporation. *Langmuir* **2011**, *27*, 4212−4219.
(224) Koppe, M.; Scharber, M.; Brabec, C. J.; Duffy, W.; Heeney, M.; McCulloch, I. Polyterthiophenes as Donors for Polymer Solar Cells. *Adv. Funct. Mater.* **2007**, *17*, 1371−1376.
(225) Mayer, A. C.; Toney, M. F.; Scully, S. R.; Rivnay, J.; Brabec, C. J.; Scharber, M.; Koppe, M.; Heeney, M.; McCulloch, I.; McGehee, M. D. Bimolecular Crystals of Fullerenes in Conjugated Polymers and the Implications of Molecular Mixing for Solar Cells. *Adv. Funct. Mater.* **2009**, *19*, 1173−1179.
(226) Qian, Y.; Zhang, X. W.; Xie, L. H.; Qi, D. P.; Chandran, B. K.; Chen, X. D.; Huang, W. Stretchable Organic Semiconductor Devices. *Adv. Mater.* **2016**, *28*, 9243−9265.
(227) O'Connor, T. F.; Savagatrup, S.; Lipomi, D. J. Soft Power: Stretchable and Ultra-Flexible Energy Sources for Wearable and Implantable Devices. In *Stretchable Bioelectronics for Medical Devices and Systems*; Rogers, J. A., Kim, D.-H., Ghaffari, R., Eds.; Springer: Berlin, 2016.
(228) Lipomi, D. J.; Bao, Z. N. Stretchable, Elastic Materials and Devices for Solar Energy Conversion. *Energy Environ. Sci.* **2011**, *4*, 3314−3328.
(229) Li, J. P.; Liang, J.; Li, L.; Ren, F. B.; Hu, W.; Li, J.; Qi, S. H.; Pei, Q. B. Healable Capacitive Touch Screen Sensors Based on Transparent Composite Electrodes Comprising Silver Nanowires and a Furan/Maleimide Diels-Alder Cycloaddition Polymer. *ACS Nano* **2014**, *8*, 12874−12882.
(230) Liang, J.; Li, L.; Chen, D.; Hajagos, T.; Ren, Z.; Chou, S.-Y.; Hu, W.; Pei, Q. B. Intrinsically Stretchable and Transparent Thin-Film Transistors Based on Printable Silver Nanowires, Carbon Nanotubes and an Elastomeric Dielectric. *Nat. Commun.* **2015**, *6*, 7647.
(231) O'Connor, T. F.; Rajan, K. M.; Printz, A. D.; Lipomi, D. J. Toward Organic Electronics with Properties Inspired by Biological Tissue. *J. Mater. Chem. B* **2015**, *3*, 4947−4952.
(232) Carle, J. E.; Helgesen, M.; Madsen, M. V.; Bundgaard, E.; Krebs, F. C. Upscaling from Single Cells to Modules − Fabrication of Vacuum- and Ito-Free Polymer Solar Cells on Flexible Substrates with Long Lifetime. *J. Mater. Chem. C* **2014**, *2*, 1290−1297.
(233) Anctil, A.; Babbitt, C. W.; Raffaelle, R. P.; Landi, B. J. Cumulative Energy Demand for Small Molecule and Polymer Photovoltaics. *Prog. Photovoltaics* **2013**, *21*, 1541−1554.
(234) Anctil, A.; Babbitt, C. W.; Raffaelle, R. P.; Landi, B. J. Material and Energy Intensity of Fullerene Production. *Environ. Sci. Technol.* **2011**, *45*, 2353−2359.
(235) Krebs, F. C.; Nielsen, T. D.; Fyenbo, J.; Wadstrom, M.; Pedersen, M. S. Manufacture, Integration and Demonstration of Polymer Solar Cells in a Lamp for the "Lighting Africa" Initiative. *Energy Environ. Sci.* **2010**, *3*, 512−525.
(236) Liang, J. J.; Li, L.; Niu, X. F.; Yu, Z. B.; Pei, Q. B. Elastomeric Polymer Light-Emitting Devices and Displays. *Nat. Photonics* **2013**, *7*, 817−824.
(237) Lee, Y. J.; Shin, M. K.; Thiyagarajan, K.; Jeong, U. Approaches to Stretchable Polymer Active Channels for Deformable Transistors. *Macromolecules* **2016**, *49*, 433−444.
(238) Wu, H. S.; Kustra, S.; Gates, E. M.; Bettinger, C. J. Topographic Substrates as Strain Relief Features in Stretchable Organic Thin Film Transistors. *Org. Electron.* **2013**, *14*, 1636−1642.
(239) Choi, D.; Kim, H. C.; Persson, N.; Chu, P.-H.; Chang, M.; Kang, J.-H.; Graham, S.; Reichmanis, E. Elastomer−Polymer Semiconductor Blends for High-Performance Stretchable Charge Transport Networks. *Chem. Mater.* **2016**, *28*, 1196−1204.
(240) Shin, M.; Song, J. H.; Lim, G. H.; Lim, B.; Park, J. J.; Jeong, U. Highly Stretchable Polymer Transistors Consisting Entirely of Stretchable Device Components. *Adv. Mater.* **2014**, *26*, 3706−3711.
(241) Xu, J.; Wang, S.; Wang, G.-J. N.; Zhu, C.; Luo, S.; Jin, L.; Gu, X.; Chen, S.; Feig, V. R.; To, J. W. F.; et al. Highly Stretchable Polymer Semiconductor Films through the Nanoconfinement Effect. *Science* **2017**, *355*, 59−64.
(242) Goffri, S.; Müller, C.; Stingelin-Stutzmann, N.; Breibry, D. W.; Radano, C. P.; Andreasen, J. W.; Thompson, R.; Janssen, R. A. J.; Nielsen, M. M.; Smith, P.; et al. Multicomponent Semiconducting Polymer Systems with Low Crystallization-Induced Percolation Threshold. *Nat. Mater.* **2006**, *5*, 950−956.
(243) Sokolov, A. N.; Cao, Y.; Johnson, O. B.; Bao, Z. N. Mechanistic Considerations of Bending Strain Effects within Organic Semiconductors on Polymer Dielectrics. *Adv. Funct. Mater.* **2012**, *22*, 175−183.
(244) Wu, H. C.; Benight, S. J.; Chortos, A.; Lee, W. Y.; Mei, J. G.; To, J. W. F.; Lu, C.; He, M. Q.; Tok, J. B.-H.; Chen, W. C.; et al. A Rapid and Facile Soft Contact Lamination Method: Evaluation of Polymer Semiconductors for Stretchable Transistors. *Chem. Mater.* **2014**, *26*, 4544−4551.
(245) Yang, W.; Sherman, V. R.; Gludovatz, B.; Schaible, E.; Stewart, P.; Ritchie, R. O.; Meyers, M. A. On the Tear Resistance of Skin. *Nat. Commun.* **2015**, *6*, 6649.
(246) Annaidh, A. N.; Ottenio, M.; Bruyer, K.; Destrade, M.; Gilchrist, M. D. Mechaical Properties of Excised Human Skin. *IFMBE Proc.* **2010**, *31*, 1000−1003.
(247) Schwartz, G.; Tee, B. C.-K.; Mei, J. G.; Appleton, A. L.; Kim, D. H.; Wang, H. L.; Bao, Z. N. Flexible Polymer Transistors with High Pressure Sensitivity for Application in Electronic Skin and Health Monitoring. *Nat. Commun.* **2013**, *4*, 1859.
(248) Leleux, P.; Badier, J. M.; Rivnay, J.; Benar, C.; Herve, T.; Chauvel, P.; Malliaras, G. C. Conducting Polymer Electrodes for Electroencephalography. *Adv. Healthcare Mater.* **2014**, *3*, 490−493.
(249) Abidian, M. R.; Corey, J. M.; Kipke, D. R.; Martin, D. C. Conducting-Polymer Nanotubes Improve Electrical Properties, Mechanical Adhesion, Neural Attachment, and Neurite Outgrowth of Neural Electrodes. *Small* **2010**, *6*, 421−249.

DOI: 10.1021/acs.chemrev.7b00003
Chem. Rev. 2017, 117, 6467−6499